Deltares

Implications of the KNMI'23 climate scenarios for the discharge of the Rhine and Meuse

Implications of the KNMI'23 climate scenarios for the discharge of the Rhine and Meuse

Author(s)
Joost Buitink
Athanasios Tsiokanos
Tjitske Geertsema
Corine ten Velden
Laurene Bouaziz
Frederiek Sperna Weiland

Implications of the KNMI'23 climate scenarios for the discharge of the Rhine and Meuse

Client	Rijkswaterstaat Water, Verkeer en Leefomgeving
Contact	de heer R. Schielen
Reference	-
Keywords	Climate change, KNMI'23, Rhine, Meuse

Document control	
Version	1.1
Date	07-12-2023
Project nr.	11209265-002
Document ID	11209265-002-ZWS-0003
Pages	85
Classification	
Status	final

Author(s)

	Joost Buitink	
	Athanasios Tsiokanos	
	Tjitske Geertsema	
	Corine ten Velden	
	Laurene Bouaziz	
	Frederiek Sperna Weiland	

1 Summary

This report summarizes the main implications of the latest generation of climate change scenarios on the discharge of the rivers Rhine and Meuse. The main objectives of this report are:

- The analysis and presentation of the effects of climate change on the river discharges of the Rhine and Meuse derived from the recently released KNMI'23 climate scenarios;
- The comparison of the discharge projections for these rivers based on the new KNMI'23 climate scenarios with the prevailing projections based on the KNMI'14 climate scenarios;
- Introduction of the KNMI'23 derived discharge time-series that are available for use in further impact assessments and research.

1.1 Methods

Recently KNMI has developed the new Dutch national climate scenarios. These so called KNMI'23 climate scenarios are based on climate simulations run with the Global Circulation Model (GCM) EC-EARTH that were downscaled using the higher resolution Regional Climate Model (RCM) RACMO. KNMI ensured that the spread in climate projections over the Netherlands and its transboundary river basins obtained with the combination of ECEARTH-RACMO realistically represented the climate signal spread obtained from a much larger ensemble of GCMs over the same area.

This climate assessment considers three future emission scenarios; development towards high emissions (H; SSP5-8.5), moderate emissions (M; SSP2-4.5) and low emissions (L; SSP1-2.6). Climate scenario datasets were constructed for the reference period 1991-2020 and future time-horizons: 2050, 2100, 2150 and 2033 (which corresponds to the 1.5 degrees temperature increase of the Paris agreement). For each future time-horizon a surrounding 30-year period is considered (i.e., 2050 = 2036-2065). To ensure that natural climate variability is well captured, KNMI provided for each period of 30-years an ensemble of 8 time-series.

Finally, for each scenario and time-horizon combination KNMI constructed both a wet (n) and a dry (d) scenario variant, these wet or dry conditions are valid for several climate statistics such as winter, summer and year-round wet or dry conditions. Table 1-1 provides an overview of all scenario-time horizon combinations considered. In the low emission scenario (L) the variation in climate conditions between 2050, 2100 and 2150 is neglectable and they are all represented by a single simulation for the future time-horizon 2100.

Table 1-1: Overview of future scenarios considered.

Time horizon	Low	Moderate	High
2033	2033L (Paris)		
2050	2100Ln / 2100Ld	2050Mn / 2050Md	2050Hn / 2050Hd
2100		2100Mn / 2100Md	2100Hn / 2100Hd
2150		2150Mn / 2150Md	2150Hn / 2150Hd

The river discharges for the reference climate (i.e., 1991-2020) and future discharge scenarios have been simulated with the hydrological wflow_sbm model. The wflow_sbm models for the Rhine and Meuse have been developed in the past years in a collaboration between Deltares and Rijkswaterstaat. The wflow_sbm model is a spatially distributed gridded hydrological model (van Verseveld et al., 2022). With its distributed nature wflow_sbm can benefit from the high-resolution spatial datasets that become increasingly available. These datasets represent land cover, vegetation (e.g., Leaf Area Index), glacier extents and soil properties within wflow_sbm. The wflow models have been optimized with local data such as for example target water levels and dimensions for the Swiss lakes using historical weather observations, e.g. precipitation, temperature, as input. In the past years the models have been calibrated against station discharge observations. The wflow_sbm model for the Meuse performs very well. Yet, simulations for the Rhine deviate from observed discharges for the reference climate period. The model simulates relatively high discharges in winter and too low discharges in summer. This is probably caused by a precipitation deficit in the meteorological data that is visible mainly in the Alps and a switch in potential evaporation method applied after the calibration.

For some applications, accurate simulation of absolute discharge values is essential, i.e., when working with threshold-based discharge analysis or for further impact modelling. Therefore, current and future climate discharges have been bias-corrected for the Rhine. The differences in relative climate signal between the corrected and non-corrected time-series are minimal.

Since biases in simulated discharges for the historical period are small for the Meuse. No bias-correction was conducted for the Meuse.

The analysis of future discharge changes focuses on the river gauging stations near the Dutch border. In addition, several gauging stations upstream were considered to explain the behavior of the projected changes. The analysis includes changes in the river regime and a selection of hydrologic statistics, i.e., the average annual minimum 7-day discharge, the average annual maximum discharge and the annual average discharge based on the ensemble of eight 30-year time-series for each climate scenario.

1.2 Results

According to all KNMI’23 scenarios, the discharges of the rivers Rhine and Meuse will show a general increase of discharges in winter and spring and a decrease of discharge in (late) summer. This is in line with the results of the former KNMI’14 scenarios and earlier climate effect studies for the Rhine and the Meuse.

The further away in time, the more the KNMI ’23 projections deviate from each other. By 2150 the high-end scenario (Hn) projects a temperature increases up to 5 or even 7 degrees Celsius for both the basins of the Meuse and Rhine. Rising temperatures in winter will result in a reduction of water stored as snow. In the lower mountain ranges snow accumulation will only seldomly occur. This results in a reduction of snow melt driven discharge peaks in the Rhine and a decrease of (late) summer discharge due to the absence of melt water from glaciers. According to the wet high and moderate scenarios annual average precipitation increases over the Rhine basin.

All scenarios project increases in annual maximum discharge. Annual average Rhine discharge will decrease according to the low-end and dry scenario groups but will increase according to the high scenarios.

The *7-day minimum discharge* at Lobith is consistently projected to decrease with decreases of 20% by 2050 and nearly 35% by 2150 according to Hd.

Projections in temperature and precipitation for the Meuse are in line with the projections for the Rhine. Towards the end of the century nearly all scenarios except the most extreme wet, project decreases in average Meuse river discharge. The 7-day minimum discharge is consistently projected to decrease throughout time for all scenarios, with decreases up to ~-30%. By 2050, changes in the annual maximum discharge are uncertain and small, but by 2150 increases are more likely and the Hn scenario even projects an increase of ~35%.

The comparison of the KNMI'23 based discharge projections with those based on KNMI'14 focusses on the differences between median projected change per scenario. Additionally, the KNMI '23 scenarios are extended with projections for 2150. Overall, the direction of projected changes remains the same, however the magnitudes do change. There are a few results that stand out:

Meuse:

- For the Meuse the largest projected reduction in minimum 7-day discharge is smaller in the KNMI'23 scenarios than it used to be in the KNMI'14 scenarios (-30% vs -50%);
- The dry KNMI'23 scenarios (Ld and Md) project decreases in annual maximum discharge, whereas KNMI14 projected increases for all scenarios;

Rhine:

- The KNMI'23 scenarios for 2150 for the Rhine are rather similar to the KNMI'14 projections for the Rhine for 2085 for annual average discharge and annual maximum discharge. This suggests that the future extremes we are currently preparing for, may occur later in time.
- By 2100 the spread in KNMI'23 projected discharge changes for 7-day minimum and average discharge is smaller than the spread of the KNMI'14 projected changes for 2085.
- The projections in 7-day minimum discharge are more or less in line. Several KNMI'14 scenarios projected small increases in 7-day minimum discharge by 2050, these are not present in the KNMI'23 scenarios. By 2150 the largest projected decrease (more than -30%) is only slightly larger than the KNMI'14 scenarios already projected for 2085 (more than -25%). This indicates that the decrease will slow down and there is limited need for further adaptation.

It should be noted that the outcomes of the comparison between the KNMI'14 and KNMI'23 results might also be influenced by changes in the data handling and hydrological model set up. These changes include improvements in the climate models and down-scaling methods, inclusion of climate data bias-correction and the shift from the HBV lumped hydrological model to the distributed hydrological wflow_sbm model that will likely provide a more realistic representation of physical processes and the influence of climate change thereon. In addition, the future time-horizons vary, i.e., the KNMI'23 time-horizons are further away in time and the reference period differs (1961- 1995 for KNMI'14 vs 1991 – 2020 for KNMI'23). The comparison can therefore only focus on trends in changes.

Changes in discharge extremes

In 2024 a second report will be released summarizing the main findings of the assessment of the impacts of the KNMI'23 scenarios on discharge extremes for high return periods. These extreme discharge projections will be relevant for the design of the flood defenses in The Netherlands.

In this report the flood statistics, in Dutch also called 'werklijnen' will be presented that will be proposed as input for the Assessment and Design Toolbox (in Dutch: BOI) used for the flood protection design.

Contents

2 Introduction

2.1 Background

In October 2023 the Royal Dutch Netherlands Meteorological Institute (KNMI) released the new generation of national climate scenarios for the Netherlands, the KNMI'23 scenarios. Rijkswaterstaat Water Verkeer en Leefomgeving (RWS WVL) requested Deltares and KNMI to assess the implications of the KNMI'23 climate scenarios for the discharge of the Dutch rivers Rhine and Meuse. Over the past two years these discharge scenarios have been developed and all results have been jointly evaluated. The outcomes are presented in the current report which is relevant for those involved in water policy such as Delta Programma Zoetwater, Klimaatbestendige netwerken and Integrated River Management as well as flood and water management such as Rijkswaterstaat.

The latest riverine climate impact assessment was conducted in 2015 (Deltares, 2015; Hegnauer, 2020) and was based on the KNMI'14 climate scenarios. An update that offers insights into possible deviation from the current KNMI'14 projections is highly relevant for effective water management and timely climate adaptation in the Netherlands. Therefore, next to the presentation of the new discharge scenarios, this report focuses on a comparison between discharge statistics for the Rhine and the Maas derived from the KNMI'14 and KNMI'23 based climate scenarios.

The discharge time-series presented in the current report are specifically provided for drought related assessments and can be used for analysis of low or average flow conditions. The data and report for the analysis of high discharge extremes (return periods of 5 years or less frequent) will be provided in 2024 with an accompanying report. The report only focuses on the Rhine and Meuse, discharge projections for the Vecht will become available at a later stage. Finally, this report focusses on the changes in discharge statistics and does not elaborate on possible consequences for water management. The data presented in this report can be used to address this in follow-on reports.

The underlying ensemble of 8 daily discharge time-series of 30-years for the current and future climate scenarios for the Rhine and Meuse are available for further assessments and analysis.

The data can be obtained from:

https://waterinfo-extra.rws.nl/projecten/@287051/knmi-23-afvoerscenario-rijn-maas/

2.2 Objectives

The main objectives of this study are:

- The analysis and presentation of the effects of climate change on the river discharges of the Rhine and Meuse derived from the recently released KNMI'23 climate scenarios;
- The comparison of the discharge projections for these rivers based on the new KNMI'23 climate scenarios with the prevailing projections based on the KNMI'14 climate scenarios;
- Generating discharge time-series that are available for use in further impact assessments and research.

3 Methods: KNMI'23 climate scenarios

KNMI carried out climate scenario simulations and exported the resulting precipitation, temperature, and radiation for the river basins of the Rhine and Meuse to enable the current assessment of future changes in river discharges. These climate scenarios are consistent with the scenarios which were made for the Netherlands (KNMI, 23). The range of projected changes corresponds with the spread in the set of internationally used global climate models. This will be explained in detail below.

3.1 Selected future socio-economic pathways

The future climate projections are based on Shared Socioeconomic Pathways (SSPs), which are scenarios of projected socioeconomic global changes given in Figure 3-1. The lower SSP numbers represent more sustainable developments whereas SSP5 represents a continuation of former practices leading to the highest greenhouse gas emissions and most severe impacts of climate change.

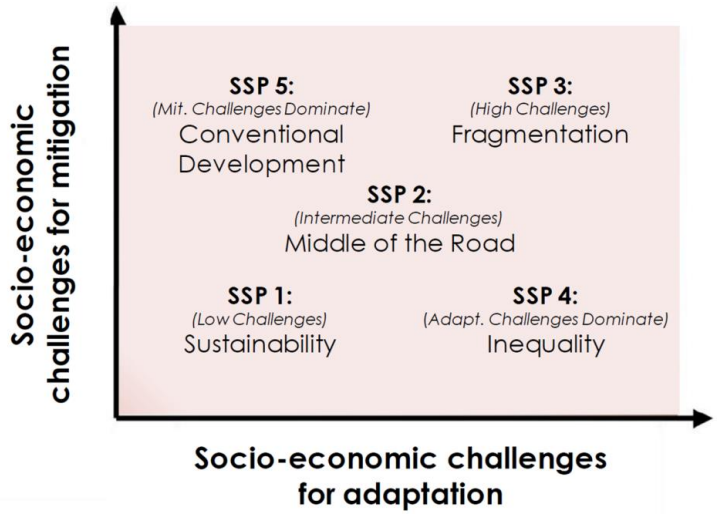

Figure 3-1: Shared Socioeconomic Pathways mapped in the challenges to mitigation/adaptation space (copied from O'Neill et al., 2017).

The full scenario names are identified by a name of the form SSPx-y, where SSPx is the socioeconomic pathway used to model the scenario (as displayed in Figure 3-1) and y is the approximate level of so-called 'radiative forcing' (downward-directed radiant energy upon the Earth's surface) resulting from the socio-economic scenario in 2100. The higher the greenhouse gas concentrations in the atmosphere the higher the radiative forcing and the larger the temperature increase (IPCC, 2021). For the KNMI'23 scenarios the pathways SSP1-2.6 (**L** - low), SSP2-4.5 (**M** - moderate) and SSP5-8.5 (**H** - high) are selected.

3.2 Division in dry and wet scenario groups

For the construction of the KNMI23 scenarios, KNMI started off from a set of 33 GCMs that were selected based on current and future climate data availability. The spread in the climate response resulting from this 33 member GCM ensemble is large. It was decided to represent this uncertainty with two relevant and distinct scenarios. This resulted in 11 GCMs that are relatively dry in winter, summer and on an annual base ('dry-trending' group) and 11 GCMs that are relatively wet ('wet-trending group'; see Figure 3-2; source: KNMI, 2023)).

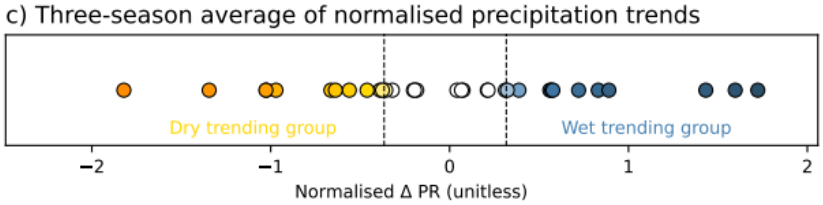

Figure 3-2: CMIP6 model projections of normalised precipitation change (delta PR) in NL+ the Rhine and Meuse basins for SSP5-8.5 in 2100. Shown are the change values averaged over summer (JJA), Winter (DJF) and annual. Vertical dashed lines show the separation of the 33 models into three groups of 11 models. Colours indicate the wetness (from orange = dry to dark blue =wet) [Source: KNMI,2023].

3.3 Dynamical downscaling

Regional climate impact analyses such as this assessment for the basins of the Rhine and Meuse require a higher spatial resolution than can be obtained from GCMs. Therefore, an RCM is used to dynamically downscale the data. An RCM requires data from a steering GCM at its boundaries. Unfortunately, not all 33 GCMs provide the relevant variables and running an RCM with data from all GCMs would be computationally too demanding.

To solve this issue, KNMI applied a resampling technique aimed at reconstructing the regional climate response in the wet- and dry-trending groups of 11 GCMs. They ran an ensemble of 16 members for the GCM EC-Earth for periods of 30 years (Döscher et al., 2022). All of these simulations start with different initial conditions and together they represent internal climate variability. The EC-Earth simulations were dynamically down-scaled to a resolution of 12x12 km with RACMO v2.3 (van Meijgaard et al., 2012) and all variables required for the subsequent hydrological modelling were stored.

3.4 Resampling procedure to obtain the most representative regional climate change signal

From the set of 16 RACMO members, KNMI resampled 8 members. These 8 members were selected and constructed in such a way that they form the best possible representation of the regional climate change signal in the dry-trending and wet-trending GCM groups. For this selection, KNMI applied 18 constraints for similarity in change signal related to precipitation (seasonal, annual, 10-day max above the Netherlands (NL) and above the Netherlands and Rhine and Meuse basins (NL+RM)), temperature (seasonal and annual) and the water balance (cumulative difference between potential evaporation and precipitation for May and September starting on the 1st of April). Based on these criteria, specific years - or groups of years - are taken from the 16 members and combined into 8 time-series of 30-years (see Figure 3-3: a) Schematic image of the original 16-member EC-Earth3 p5 ensemble dataset, b) schematic image of a resampled dataset (SSP5-8.5 2100, dry-trending group, future period). Displayed numbers and colours refer to the ensemble member of the original ensemble dataset [Source: KNMI, 2023].

Each of the 8 time-series of 30-years is representative for the climate in either the reference period (1991-2020) or the 30-year period surrounding one of the future time-horizons (2050, 2100, 2150). By having 8 time-slices instead of 1, a user has additional information on internal climate variability for the given 30-year time-period. Although together they provide 240 years of data, they cannot be treated as a continuous time-series of 240 years.

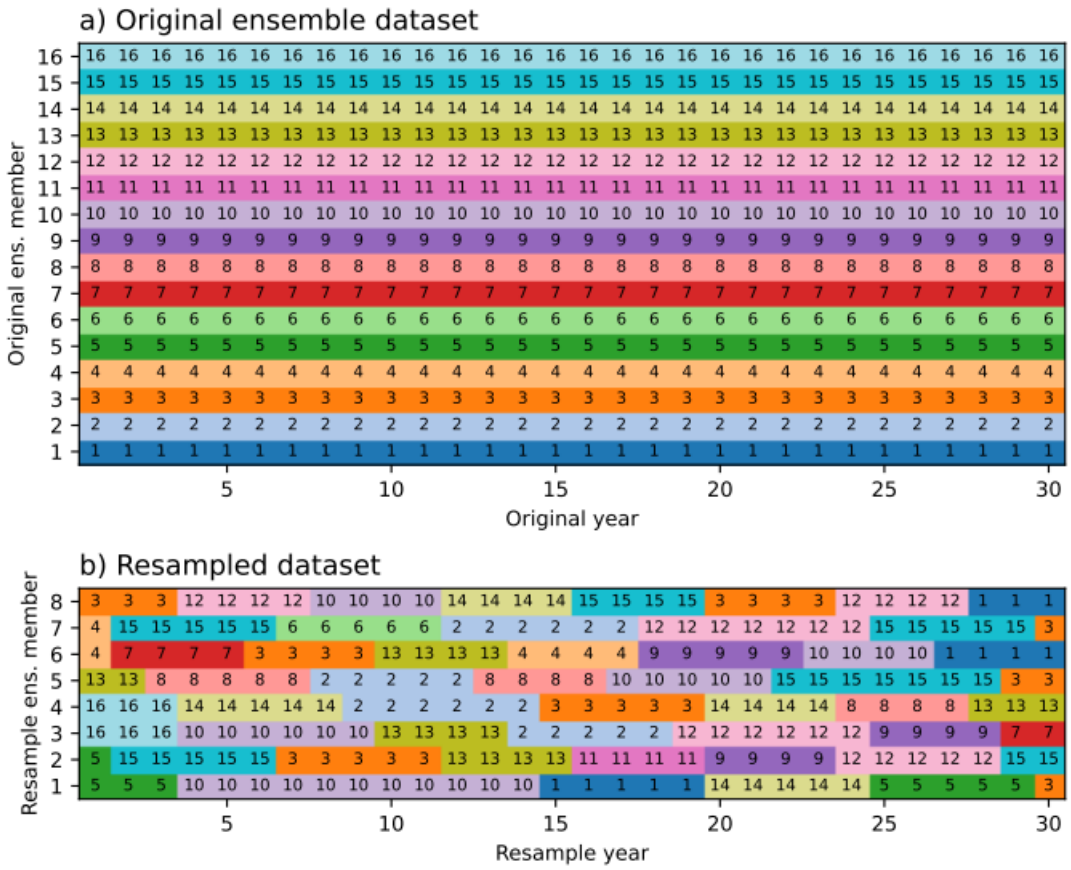

Figure 3-3: a) Schematic image of the original 16-member EC-Earth3 p5 ensemble dataset, b) schematic image of a resampled dataset (SSP5-8.5 2100, dry-trending group, future period). Displayed numbers and colours refer to the ensemble member of the original ensemble dataset [Source: KNMI, 2023]

3.5 Bias-correction climate data

To overcome differences between the observed meteorological conditions and climate simulations from RACMO, the RACMO output data (temperature, precipitation, and radiation) for the current and future climate were bias corrected using the quantile mapping method (Cannon et al., 2015). With this method specific attention is given to a good correction of both the average and extremes values. The methods and detailed explanations of the different scenarios is explained in the report by KNMI (KNMI, 2023).

3.6 Overview of scenarios considered

The resulting 8 time-series of 30 years form the KNMI'23 scenario input for the discharge simulations. Future changes in river discharge are assessed for the "scenario – time-horizon" combinations listed in Table 3-1. The climate scenarios are derived for the future time-horizons 2050, 2100 and 2150 and the year 2033 that corresponds to the 1.5 degrees warming set in the Paris agreement.

For the L scenario only the future time-horizon 2100 is considered, because under this scenario the climate shows little variation over time. For all scenario combinations both the wet (n = nat (in Dutch)) and dry (d = droog (in Dutch)) scenario variant are evaluated. By 2033 the difference between the wet and dry scenario is that small that only the wet scenario is presented.

Table 3-1: Overview of the different scenarios and their names

Time horizon	Low (SSP1-2.6)	Moderate (SSP2-4.5)	High (SSP5-8.5)
2033 (Paris)	2033L (Paris)		
2050	2100Ln / 2100Ld	2050Mn / 2050Md	2050Hn / 2050Hd
2100		2100Mn / 2100Md	2100Hn / 2100Hd
2150		2150Mn / 2150Md	2150Hn / 2150Hd

All changes are presented relative to the reference period 1991-2020. As reference climate, the control climate of the 2050Md scenario was chosen. However, all 15 scenarios have their own control climate that represents the climate of 1991-2020. Yet, considering all these individual reference climates would result in 15 x 8 x 30 years of wflow simulations for the historical period which is too long and will also be too long for impact models in follow-up work. The control climate of 2050 Md scenario was selected as the reference climate because it had the best statistical match on several climate variables with the characteristics of all control climates combined (van den Brink, 2023). The reference climate also consists of 8 ensemble members, each consisting of 30 years of data.

4 Methods: Generation of future discharge projections for the Rhine and Meuse

4.1 The river basins and main locations of interest

4.1.1 Rhine

The Rhine is one of the main river basins in Western Europe and is intensively used for agriculture, industry, and navigation (Kwadijk and Rotmans, 1995). The basin area up till Lobith is 185 000 km^2 and has about 58 million inhabitants of which 10.5 million live in flood-prone areas (ICPR, 2001). The river originates in the Swiss Alps, it discharges along the boundary between France and Germany, continues through Germany before it enters the Netherlands at Lobith (Te Linde et al., 2011). On its course downstream its regime changes from snowmelt to a combined rain-snowmelt driven regime. At Lobith the average discharge is ~2230 m^3/s. The maximum measured discharge was observed in 1926 and reached up to 12 600 m^3/s (Pinter et al., 2006).

This report focusses on the climate projections for Lobith at the German-Dutch border where the Rhine enters the Netherlands (Figure 4-1). Next to Lobith, we also included the analysis for Maxau, where the Rhine dominantly has a snow-melt regime, and for Cochem where the discharge regime is dominated by rainfall with a strong seasonality.

4.1.2 Meuse

The Meuse basin extends over an area of 33 000 km^2 in France, Belgium, Luxembourg, Germany, and the Netherlands (Deltares, 2020; Ward et., 2008). The Meuse is a rain-fed river with relatively short response times. River discharge has a strong seasonality with low discharges in summer and high discharges in winter due to the variability in evaporation rates. Precipitation is relatively uniformly distributed throughout the year. Snow is not a major component of the water balance, but snow melt can have a large influence during some events (de Boer-Euser, 2017). Annual average river discharge at the Dutch border is approximately 350 m^3/s.

This report focusses on the climate projections for the Belgian-Dutch border where the Meuse enters the Netherlands (Figure 4-2). The hydrological model simulates the natural flow and doesn't include any abstractions such as the Albert Kanaal. Therefore, the simulated outflow at the border cannot directly be linked to a real gauging station. The simulated discharges and the change signal therein are a proxy for the discharge at Eijsden. In the remainder of the report where we refer to changes in the Meuse without an exact location, we refer to the Meuse in the wflow_sbm model at the Belgian-Dutch border. Next to this, also the analysis for Chooz located at the French-Belgium border and Chaudfontaine the most downstream station in the Vesdre catchment located in the eastern part of the Belgian Meuse are included.

4.2 Hydrological Modelling

4.2.1 Wflow_sbm

Deltares started working on a distributed hydrological model for the Rhine and Meuse, wflow_sbm (Van Verseveld et al., 2022) in 2015. The developments were initiated in collaboration with Rijkswaterstaat. This hydrological model is used to convert the climate projections into discharge projections, simulations are conducted with the Rhine and Meuse wflow_sbm models. These models have been developed and optimized during the past years in collaboration between Deltares and RWS (Deltares, 2020, 2021, 2022, 2023).

The wflow_sbm model is a spatially distributed gridded hydrological model (van Verseveld et al., 2022). With its distributed nature wflow_sbm can benefit from the high-resolution spatial datasets that become increasingly available, often at a global scale. These datasets represent land cover, vegetation (e.g., Leaf Area Index), glacier extents and soil properties within wflow_sbm. In Chapter 5 and Annex A we will further discuss the transition from the former HBV model to the current wflow_sbm model.

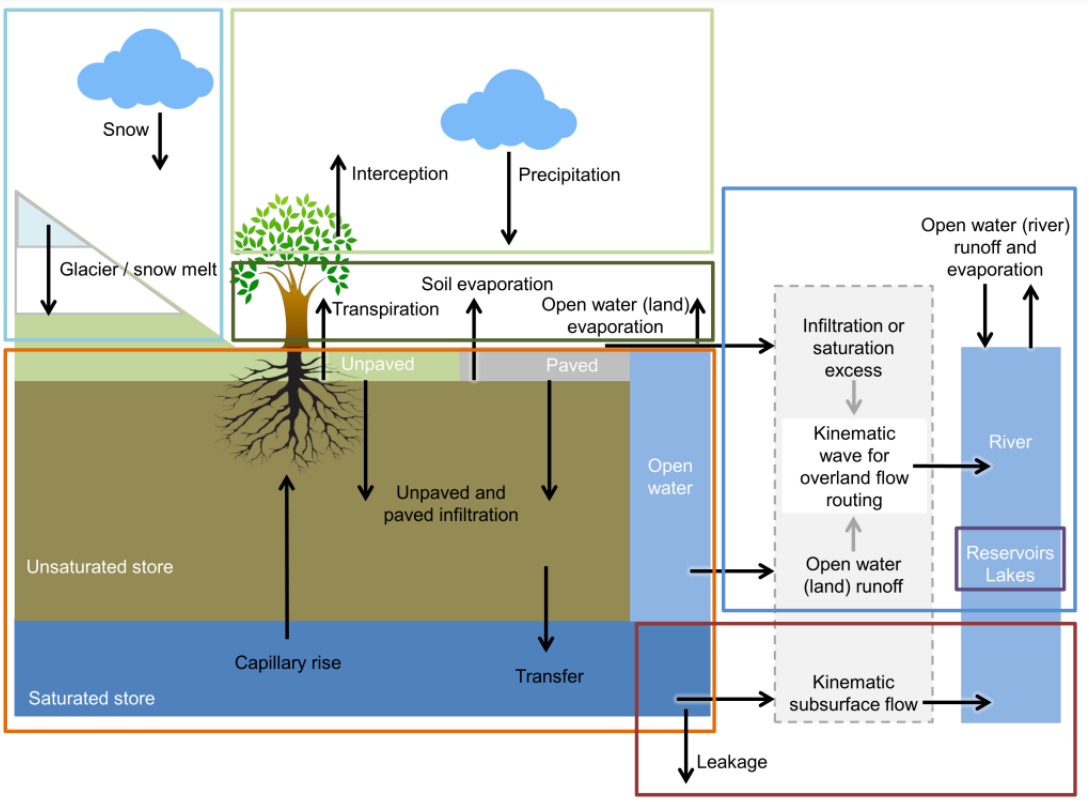

Figure 4-1: An overview of the different processes and fluxes in the wflow_sbm model [source: van Verseveld et al., 2022].

Figure 4-1 presents the different processes and fluxes in the wflow_sbm model. The model includes the following routines: Interception (green), Snow and glaciers (light blue), Soil module and evapotranspiration (orange), Lateral subsurface flow (brown), Surface routing (dark blue) and Reservoirs and lakes (black).

Precipitation enters each grid cell through the interception routine. Throughfall and stemflow from the interception routine are transferred to the optional snow (based on the HBV-96 hydrologic model concept (Bergström, 1992)) and glacier routines based on the degree-day method.

The soil in every grid cell is considered as a single bucket, divided into a saturated and unsaturated store. The remaining throughfall infiltrates into the soil or becomes direct runoff based on the river fraction or open water (excluding rivers) fraction. Soil infiltration is determined separately for the paved and nonpaved areas. Infiltration excess occurs when the infiltration capacity is smaller than the available infiltration rate, and this amount of water is also added to the runoff routing scheme for overland flow.

Potential evaporation is supplied to the model as external input. Within the model actual evapotranspiration is calculated. Part of the water evaporates through soil evaporation and open water evaporation. Besides transpiration, capillary rise and leakage result in a flux from the saturated store to the unsaturated store and results in recharge in an infinite bucket. The kinematic-wave approach is used to route subsurface flow laterally. Saturation excess water is added to the runoff routing scheme for overland flow. For overland and river routing the kinematic, local inertia equation or floodplain approach can be selected. To improve the simulation of lake levels over time, lake target levels can be set based on operational levels.

4.2.2 Automized model implementation and overall performance

In line with the need to improve the transparency, reproducibility, and ease of setting up hydrologic models the wflow plugin (HydroMT-Wflow, Eilander et al., 2022) of the HydroMT Python package (Eilander and Boisgontier, 2022) is developed. It can be used to set up wflow_sbm models for any catchment based on globally available datasets. Point scale (pedo)transfer-functions (PTFs) from literature are used to derive model parameters at the highest available resolution of the data and scaled with suitable upscaling operators (Imhoff et al., 2020) to the desired model resolution.

Wflow_sbm model implementations developed with the Python tool HydroMT-Wflow based on globally available datasets and parameterized through the use of point-scale (pedo)transfer functions generally result in a satisfactory (0.4 - >= Kling-Gupta Efficiency (KGE) < 0.7) to good (KGE ≥ 0.7) performance a-priori (without further tuning; Gupta et al., 2009). With the limited parameter calibration, we can assume the model is not overfitted to match the river discharge observations and will thus more likely perform better under changing climate conditions than HBV used to do. The model has been applied recently in a peer-revied published climate change study for 9 river basins in different climate zones in Europe (Sperna Weiland et al., 2021) and performs well under wet and dry conditions.

The wflow_sbm model has also been applied in many applied-research studies for ECMWF/ESA, World Bank, AXA, and the model is part of several forecasting systems like the Delft-FEWS forecasting systems for the Sava, Lempa and Australian Bureau of Meteorology. These applications world wide cover a wide spectrum of different climate conditions, which provides additional evidence that the model performance is robust under various, and also changing, climate conditions.

4.2.3 Parameter estimation

Most wflow_sbm parameters are based on physical characteristics or processes and can thus be derived from global soil and land cover maps, an overview is given below:

- CORINE land use cover (European Environment Agency) was used to estimate rooting depth and interception parameters.
- Soilgrids 1.0 dataset (Hengl et al., 2017) was used to estimate porosity, residual water content and soil thickness.
- MODIS MCD15A3H (Mynemi et al., 2016) was used for monthly Leaf Area Index.
- Brakensiek pedotransfer function was used to estimate the saturated hydraulic conductivity.

The wflow_sbm models for both the Rhine and the Meuse are explained in more detail in Deltares (2022, 2023), including descriptions of the additional calibration and inclusion of a (simple) hydraulic routing that takes the floodplains into account.

4.2.4 Wflow_sbm Rhine

The wflow_sbm model for the Rhine until Lobith (Figure 4-2) has a resolution of 0.00833° (or approximately 600 m x 925 m) and runs from the Swiss Alps until the Dutch border at Lobith. The Rhine model is described in detail in Deltares (2021, 2022, 2023).

Reservoirs are automatically taken from the GRanD database (Lehner et al., 2011). In addition, local data is used to ensure realistic performance of the reservoirs. Lakes are automatically implemented from the hydroLAKES database (Messager et al., 2016). This lake data is in the model enriched with local data and rules for the lake regulation of the large lakes in Switzerland in the Rhine model.

Glacier extents and volume are taken from the Randolph Glacier Inventory dataset (Pfeffer et al., 2014). The glaciers in wflow_sbm are modelled via a mass-balance approach based on a degree-day approach. They can thus retreat when temperatures rise. We do not simulate the growth in extent (e.g., covering “new” regions) of glaciers.

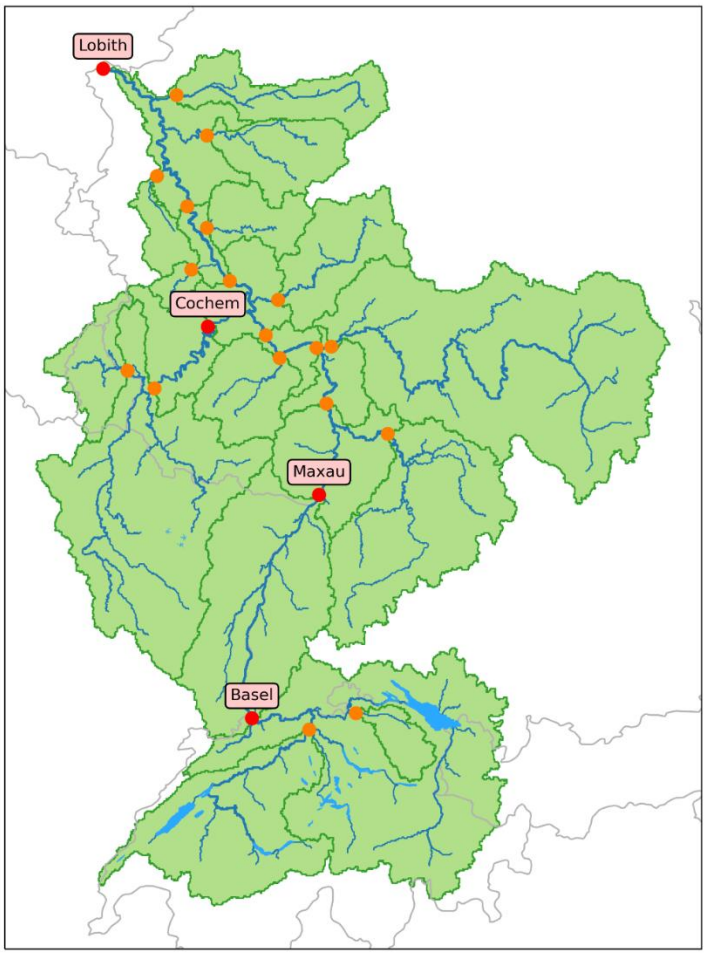

Figure 4-2: Extent of the Rhine model with stations that were analysed in this study. Orange dots present the stations for which simulated discharge time-series can be retrieved. The red dots present the stations for which the results are discussed in the report. The lakes are shown in light blue.

4.2.5 Wflow_sbm Meuse

The wflow_sbm model for the Meuse (Figure 4-3) is a spatially distributed gridded model with a resolution of 0.00833° (or approximately 600 m x 925 m). The model has been validated in previous studies upstream of Borgharen at the the Belgian-Dutch border (Deltares, 2021, 2022, 2023). The model does not include any man-made structures or abstractions for waterways (such as the Albert Kanaal). Nor does it include the contributions of tributaries such as the Geul, as these merge with the Meuse downstream of the Dutch border.

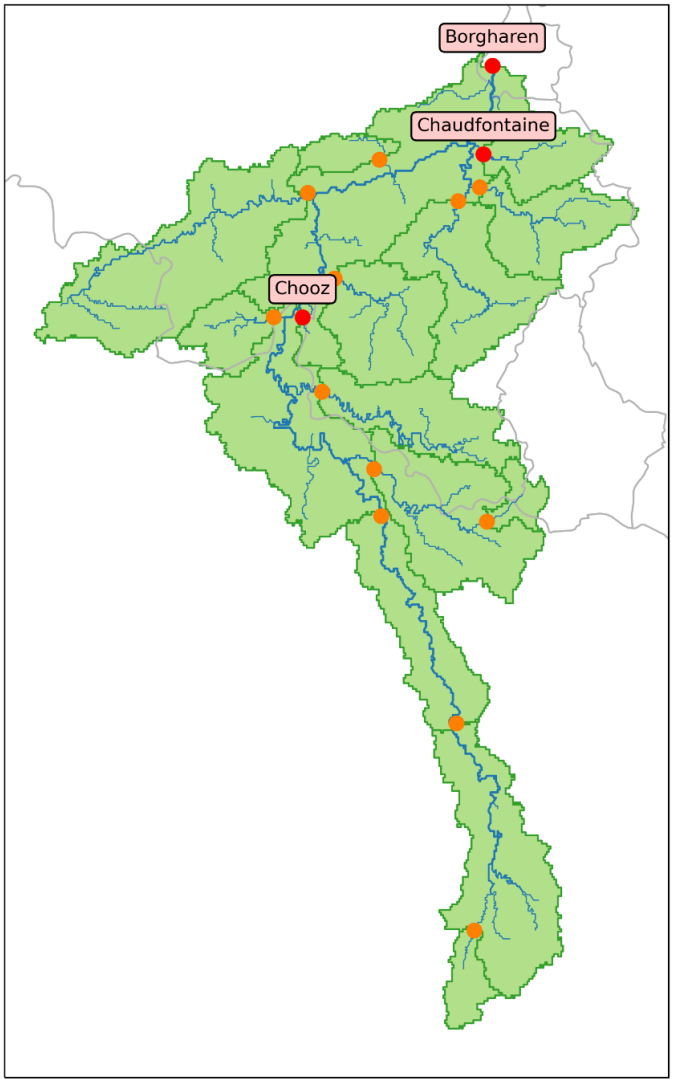

Figure 4-3: Extent of the Meuse model with stations that were analysed in this study. Orange dots present the stations for which simulated discharge time-series can be retrieved. The red dots present the stations for which the results are discussed in the report.

4.2.6 Initial conditions for future scenarios

As shown in Table 3-1, the different scenarios cover different time horizons. As each time-horizon is represented by a 30-year period around its time-horizon we do not have continuous climate time-series. However, it is important to start the hydrological simulations with conditions that are representative for the start of that 30-year period.

This is especially important for long-term water storages, such as glaciers, persistent snowpacks, groundwater and deeper soil layers, which are expected to gradually decrease over time as a result of increasing temperatures and drying conditions. It should be noted that we do not aim to produce transient continuous time-series, but rather provide time-series that are representative for the climate in the future time-horizons and that start with the correct initial conditions.

To start the hydrological model with representative conditions for the time-horizon of (for example) 2150, we would need a continuous timeseries until the start of the 30-year period of this time horizon (2136-2165 for 2150). These continuous time-series of precipitation, temperature and potential evaporation are not available from RACMO and we need to fill the gaps between each time horizon. We decided to virtually extend each time horizon block, such that we can cover the gaps in between each time horizon. Figure 4-4 shows how the different time horizons are extended to retrieve a continuous time series until the start of the last time horizon of each scenario. Please note that this only applies to the climate scenarios for the future time horizons. For the reference climate scenario, we used initial conditions that are representative for the start of 1991. The 8 blocks of 30 years in the reference climate are all starting from these initial conditions.

For the future time horizons, and to explain this figure, we take the Hn and Hd scenario as example. The initialization process of the future climate simulations starts with initial conditions obtained by simulating the historical period using observed meteorological data. The observation based meteorological dataset covers the period 1991-2018. We use this data (in contrast to the provided reference climate) as this observational dataset contains the most accurate meteorological conditions representative for this period. As a result, this will lead to the most accurate hydrological conditions for this historical period, and thus as an accurate starting point to estimate the initial conditions and long-term water storages.

The first future time horizon is the 30-year block around 2050, which covers the period 2036 to 2065. To create a continuous time series, such that we can create realistic initial conditions and have an accurate estimate of the long-term water storages, we need to fill the period from 2019 until 2036. This block of 17 years is split into two equal parts, and a period of 2 years for warming up the model: Fill 1, Fill 2, and Warmup. For the first fill block (Fill 1) we are using the last 7 years from the previous simulated time series (the historical period in this case).

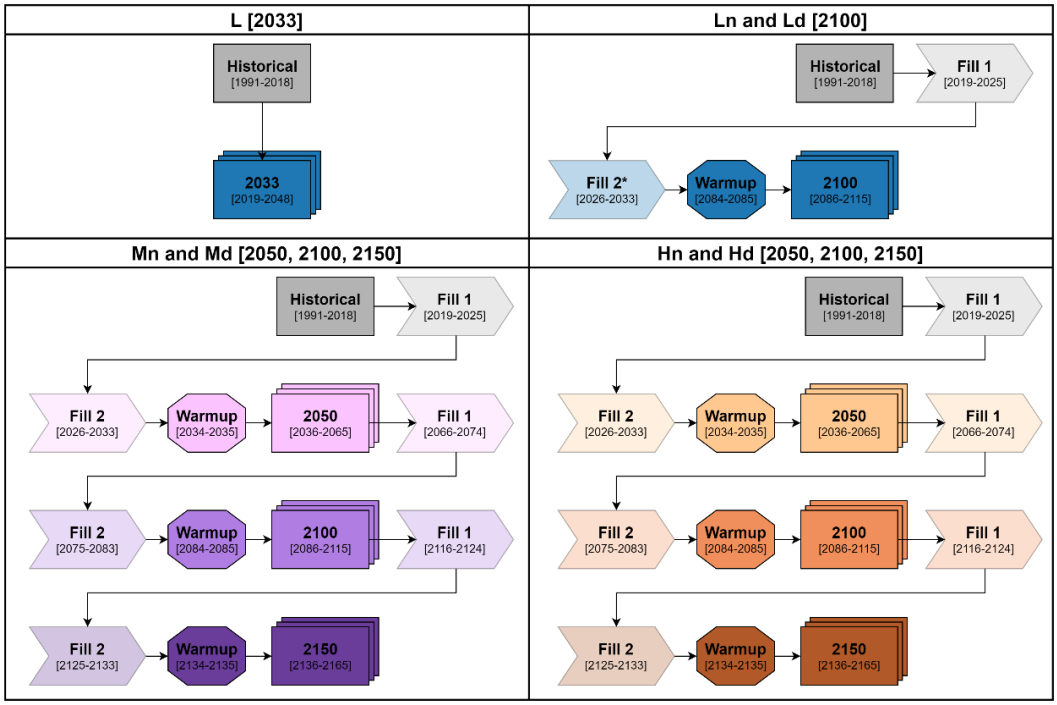

Figure 4-4: Dependencies between the different time horizons, and which states are used for each scenario. The stacked squares represent the 8 blocks of 30 years for each time horizon, which combined make the 240 years of data per scenario and time horizon.

For the second fill block (Fill 2), we are using the first 8 years from the next time horizon (the 2050 block in this case). However, in these 8 years, there is already a (small) climate signal present. To prevent this signal to slightly interfere with the initial conditions, we decided to do a simulation of 2 years that has the smallest climate signal present (i.e., the first years of the 30-year block). This 2-year simulation (called the “Warmup” in the figure above) are done to retrieve the initial conditions that will be used in the 8 blocks of 30 years. For these “Warmup” runs, we use the third and fourth year of the time horizon (2050 in this case). Although the first and second year should have an even smaller climate signal, we decided to not use these years, as these years would be repeated in the actual simulations (2050 in this case, after the warmup). If these two years would be extreme conditions, they would occur twice: in the warmup and in the actual simulation. This could potentially exacerbate the hydrological response. It should be noted that, despite that our approach largely minimizes this risk, there remains a small possibility that this approach introduces artificial persistency in extreme years.

As mentioned before, each time horizon consists of 8 ensembles of the 30-year period. Each of these ensemble members are started from the same hydrological warmup conditions. The conditions of the first ensemble member are used to continue this method with filling and warmup until the last time horizon is reached.

Please note that all L scenarios have small deviations from this setup. For 2033L, the representative years of the 30-year block is directly followed after the historical period, so we decided to directly use the model conditions after the historical period to initialize each ensemble member of this scenario. This way, we have an accurate match between the representative period of the scenario and the simulated years. For 2100Ln and 2100Ld, the only time horizon considered is 2100 because of the limited climate change signal (KNMI, 2023). This would mean we would have to fill the period from 2019-2085, i.e., to the start of the 30-year period surrounding 2100.

As there is only a very limited climate signal present in this scenario, we decided to treat the filling as if the time horizon was placed at 30 years around 2050. This way, we reduce the amount of gap filling we need to do (and the potentially added uncertainty). Here we do neglect possible changes in glacier conditions between 2050 and 2100 for the L scenario in order to reduce computation time.

4.3 Bias-correction of discharge results

Figure 4-5 shows a mismatch between the discharges simulated with wflow_sbm and the measured discharges for the Rhine. Therefore, a bias correction seemed to be necessary. In the following sections we first reflect on the causes of the bias in the simulated discharge (section 4.3.1). We than explain the type of correction applied (section 4.3.2). Finally, we present some results of the hydrological response after discharge bias-correction (section 4.3.3).

For the Meuse the simulated discharge resembles the observed values well and no bias-correction is needed (see Annex B).

4.3.1 Biases in the wflow_sbm simulations for the Rhine

If we compare the simulated discharges at Lobith based on HYRAS meteorological data with the discharge observations, a deviation between the two becomes apparent (see Figure 4-5). This figure shows higher discharge values during the winter-half-year, and lower discharge values during the summer-half-year. The simulated 7-day minimum discharges values underestimate the observed values. A result that was also presented in Deltares (2022).

Figure 4-5 (bottom panel left) also presents that despite this, the return periods, up to 30 years, of the annual maximum discharge match the observed discharge relatively well.

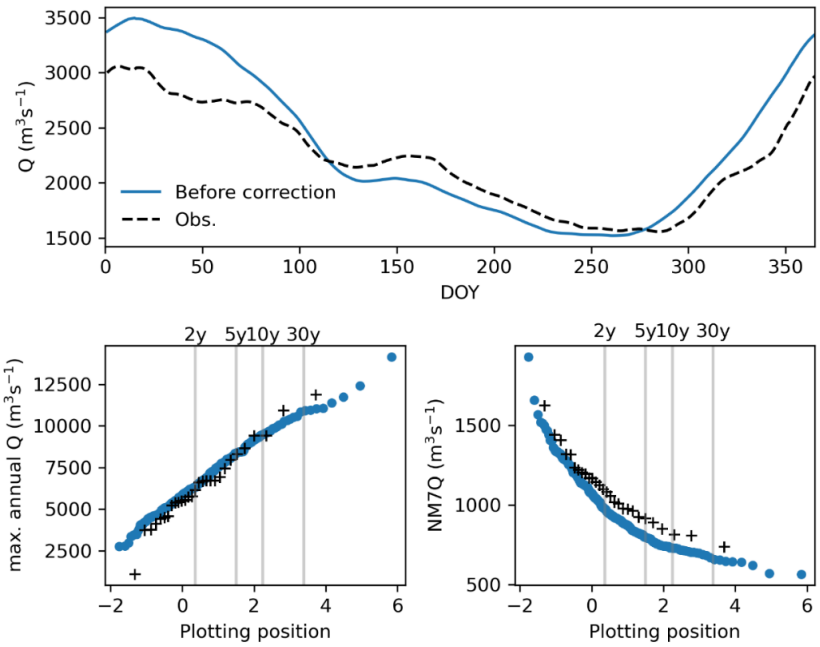

Figure 4-5: Comparing the simulated discharge of the reference climate (blue dots) with the observed discharge values at Lobith (black crosses), including the return periods of the annual maxima and the 7-day minima discharges. The upper panel shows the annual discharge regime is shown, the bottom left graph provides the Gumbel plot for maximum discharges, the bottom right graph presents the Gumbel plot for the 7-day minimum flow.

There are two important reasons for the deviation between simulated and observed discharge that will be explained in detail in section 4.3.2:

1 ***the reference meteorological dataset*** that is used for the bias-correction of the climate datasets probably underestimates precipitation over the Alps.

2 the method used to calculate the ***potential evaporation*** estimates probably too low potential evaporation in winter.

4.3.2 The meteorological reference data

The HYRAS dataset exists of daily high-resolution (5 km × 5 km) grids of average, minimum, and maximum temperature and relative humidity for Germany and its catchment areas (Razafimaharo et al., 2020). In total more than 1300 stations are considered for the construction. Station data is interpolated to the grid following inverse distance weighting. Overall, it can be set that the HYRAS dataset was constructed with great care, and it is a well acknowledge meteorological dataset for the Rhine basin. Yet, biases in the observed station data are also present in the gridded product after interpolation. The HYRAS dataset is used for the bias-correction of the climate datasets. Consequently, biases that are present in the HYRAS datasets are also imposed on the climate datasets.

To understand the influence of the precipitation data on the simulated discharges, we also performed simulations using precipitation from the ERA5 dataset instead of the HYRAS dataset. The ERA5 dataset is a re-analysis dataset, constructed with a numerical weather model that assimilates (satellite) observed data for the best possible representation of the historical meteorological conditions. The dataset is constructed by the European Centre for Medium-range Weather Forecasting (ECMWF; Hersbach et al., 2020). Although this dataset is far from perfect, and has a much coarser resolution, the influence of snow under-catch in the station observations and the lack of data for higher elevations mountains is not present in this dataset. Therefore, this dataset does provide a reasonable reference to compare the HYRAS dataset with.

In Deltares (2022) we found that the wflow_sbm simulations for the Rhine basin using the HYRAS dataset result in an underestimation of the spring-summer discharges at Lobith. In this report, this underestimation of discharges is for the vast majority traced back to a severe underestimation of discharges at Basel (see Figure 4-6: Average monthly discharge at Basel (left) and Lobith (right), simulated using the HYRAS and ERA5 precipitation.. The results from these simulations showed that the discharge at Basel and Lobith when using ERA5 does not lead to underestimations of the discharge during spring and summer. The with ERA5 simulated discharge for Basel is much closer to the observed values during these periods (see Figure 4-6) and low summer flows are better represented in the ERA5 based wflow simulation.

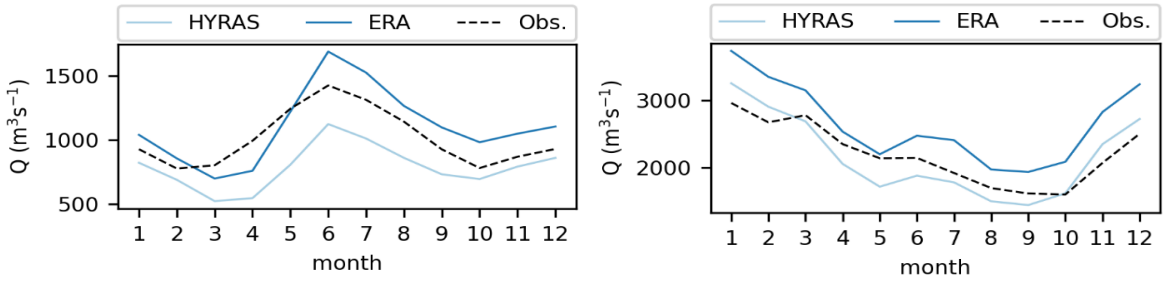

Figure 4-6: Average monthly discharge at Basel (left) and Lobith (right), simulated using the HYRAS and ERA5 precipitation.

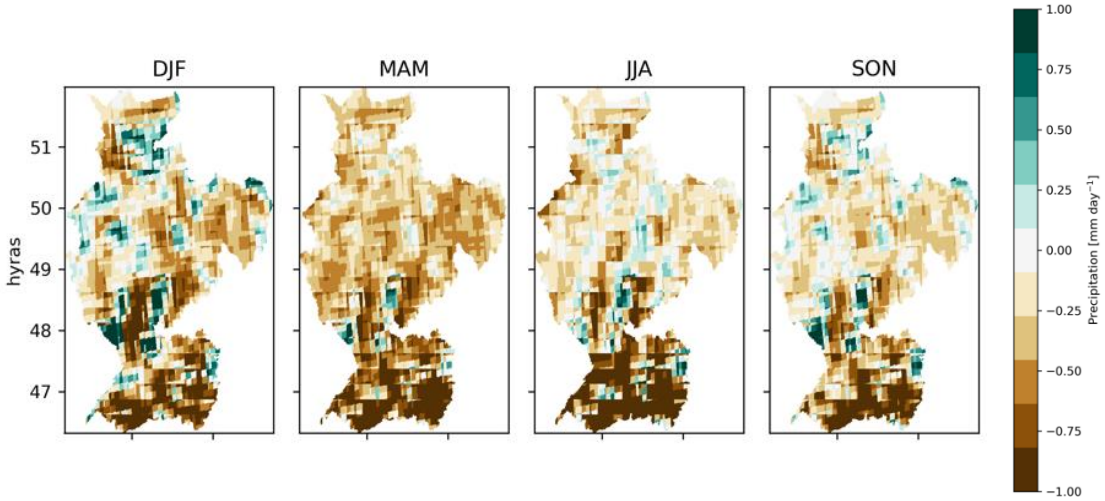

Figure 4-7: Differences in seasonal precipitation amounts (mm/day) when comparing HYRAS to ERA5 (where positive values indicate higher precipitation in HYRAS and vice versa).

It should also be noted that the discharge at Lobith simulated with ERA5 is consistently too high. This suggests that on an annual basis the precipitation in ERA5 might be too high. Comparing the precipitation maps per season, we see that the HYRAS precipitation is substantially lower than the ERA5 precipitation, with the largest deficit in the Swiss Alps (see Figure 4-7). This precipitation deficit in HYRAS causes the bias in simulated summer discharges.

4.3.3 The potential evaporation method

In the upper panel of Figure 4-5 we found an overestimation of the average winter discharges for Lobith. This is largely a result of the switch in potential evaporation method used for wflow_sbm calculations after calibration of the wflow_sbm model. This will be explained in this sub-section.

Over the past years the wflow_sbm model was calibrated and optimized using the de Bruin equation for calculating potential evaporation, which is the method that Deltares uses most frequently as input for wflow_sbm. However, for this climate assessment KNMI calculated the potential evaporation with the Makkink equation. This is done for reasons of consistency, as KNMI also applies Makkink for the preparation of the climate scenario data for the Netherlands, and also due to data availability, as all required variables needed to be bias-corrected based on the data present in the E-OBS dataset.

Switching a forcing dataset after model calibration, has negative effects on model performance. The parameters resulting from the calibration are (at least partly) tuned to compensate for errors/uncertainties in the forcing dataset. These uncertainties are different in the new forcing dataset, hence there is often a loss in model performance.

The Makkink and de Bruin equations follow slightly different approaches and input fields, yielding different PET timeseries as well. The difference in potential evaporation calculated by the two methods is visualized in Figure 4-8. The figure presents potential evaporation averaged over the full Rhine basin.

As can be seen there are substantial differences in the potential evaporation, with the main differences during the winter period. In this part of the year, the potential evaporation calculated using Makkink is substantially lower (~-35%). When switching from de Bruin to Makkink, substantially less water is evaporated during the winter months (where water is typically in abundance, and the actual evaporation is often not water-limited), which leads to the higher discharge values. This response in discharge is clearly visible in Figure 4-9, where we compared the simulations based on the two different potential evaporation methods.

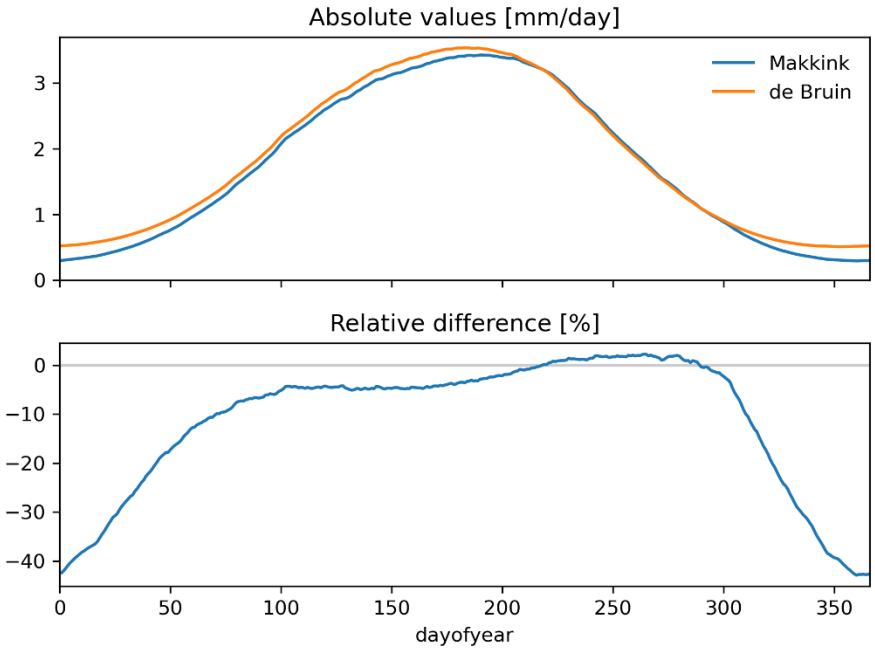

Figure 4-8: Potential evaporation timeseries as averages over the full Rhine basin, averaged per day-of-year, and with a rolling window of 30 days. Averages are calculated over the period 1980-2019.

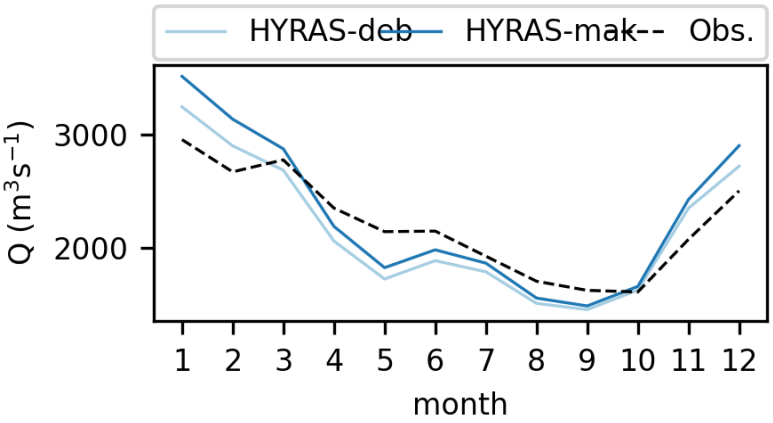

Figure 4-9: Discharge regime simulated with wflow_sbm forced Makkink potential evaporation (HYRAS-mak; dark blue) and de Bruin potential evaporation (HYRAS-deb; light blue), together with the observed regime (Obs.; dashed black).

As the wflow_sbm model was calibrated based on de Bruin, it is not a surprise that we see a decrease in model performance when switching to Makkink. The optimal parameter set resulting from the calibration performed in Deltares (2022), is searching for a balance between a parameter set that (partly) tries to compensate for the lack of precipitation in the Swiss Alps (as explained in Section 4.3.2), which likely results in the slight overestimation of discharge during the winter period. Now that we switched to Makkink, and reduce the evaporation during the winter period, this overestimation is exaggerated.

4.3.4 Decision on the use of bias-corrected discharges

Despite the fact that KNMI applied a quantile mapping bias-correction on the climate time-series, it did not result in simulated discharge values that directly match the observed values. This is because (1) errors in the HYRAS dataset are transferred to the corrected climate time-series and (2) the switch in potential evaporation method caused a decrease in model performance. This suggest that a correction of the simulated discharges for the Rhine may be needed. The main reason to use the bias-corrected discharge time-series is when there is a clear need for the correct representation of absolute discharges. This is in general the case:

- When making the connection to other models to simulate impacts on related processes such as sedimentation, navigation, water management, water distribution and compound flooding, or;
- When working with discharge threshold-based analysis such as for example performed by Deelprogramma Zoetwater.

It should be noted that the bias-correction method may introduce some noise, i.e., slight change in climate change signal. In Annex C the influence of the bias-correction on the climate change signal is evaluated. For mean discharges there is nearly any change in the climate change signal calculated from the corrected and uncorrected discharge time-series. For the high and low discharge indicators we do some difference. This could be a reason to work with the uncorrected time-series when only the change signal is important.

4.3.5 The bias-correction method explained

For the bias-correction of the simulated discharges we apply a quantile mapping approach (Cannon et al., 2015), similar to the method used by KNMI to correct the forcing timeseries.

Empirical quantile mapping is essentially transferring the probability distribution function (pdf) of simulated historical climate discharge time-series to the pdf of observed discharge time-series for a given station by defining a transfer function (Figure 4-10).

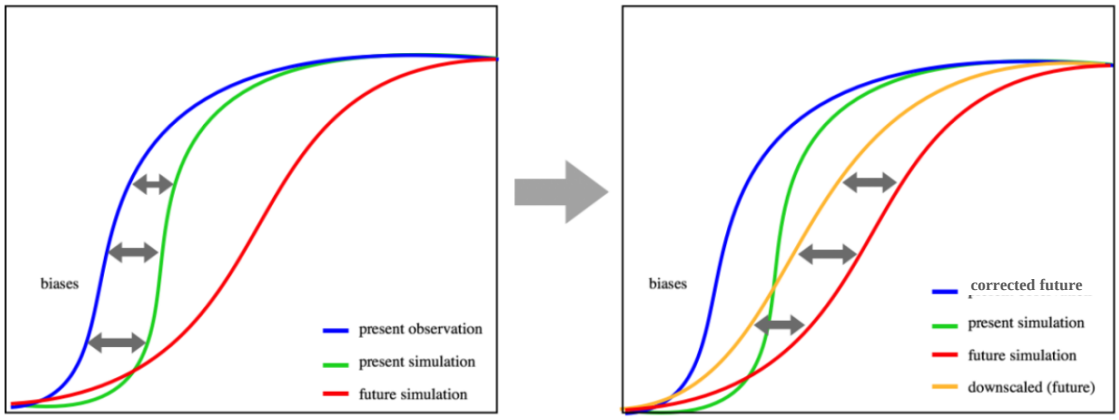

Figure 4-10: Illustration of quantile mapping approach (source: NASA). First the biases are calculated for each percentile in the cumulative distribution function of the current climate simulation (green to blue – grey arrows represent biases). Then the calculated biases are applied to each corresponding percentile in the cdf of the future simulation to correct the biases of each percentile.

The transfer function, derived for the correction of the historical climate discharges, is then used to also correct the future simulated discharge time-series for the given station for all scenarios (Cannon et al., 2015). By applying quantile mapping, biases in both the current and future climate time-series are thus corrected.

The method performs best when applied to sub-annual or finer time scales, because of seasonal discharge variations (Zhao et al., 2017). This means that the optimal correction factor might also change throughout the year. To account for this pattern, we define correction factor for each day-of-year (DOY), ranging from 1 to 366. Below follows a stepwise description of the approach.

1) We simulate the uncorrected current and future climate discharges with wflow using the KNMI'23 precipitation, temperature, and potential evaporation as input.

2) We group the 8 times 30-year time-series of simulated discharges and observed discharges per day-of -year. For example, we take for the 15th of March all values for the 15th of March that are present in the dataset for the given scenario and given time-horizon; i.e., 8 times 30 values. However, to infer a probability density function (pdf) from these series, we want to include as much data as possible to reduce noise. To account for this, we take a window of 30 days (before and after the selected DOY), the ensure a more realistic and smoother pdf.

3) We calculate correction factors for each percentile in the range from 0.1 to 0.9 (with a total of 25 steps). This results in 25 correction factors per DOY to transfer the pdf based on the simulated values to the pdf based on the observed values. The correction factors are defined as multiplicative values, to prevent the correction to accidentally result into negative discharge values.

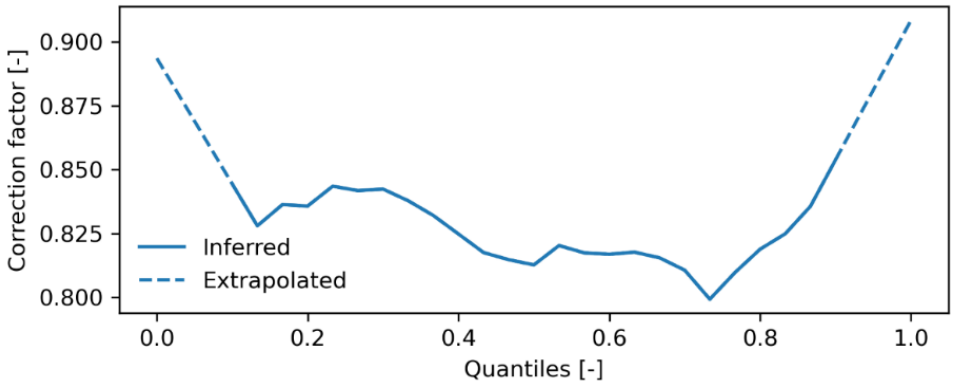

Figure 4-11: Example showing the extrapolation of correction factors at the low and high tails of the quantile values, shown for a single DOY (in this case for the first day of the year).

4) It is important to stress that the tails of a pdf distribution contain the most relevant hydrological values: the extreme maxima and minima values. Values such as the annual maximum or the 7-day minimum discharge, are typically well in the tail ends of these distributions (>0.95 and < 0.05, respectively). However, the derived pdf at these tail ends is relatively uncertain, as they only contain a handful of data points. This uncertainty might lead into unrealistic correction factors, that disturb and impose an incorrect signal on the resulting extreme values. To prevent this from happening, while still correcting these values, we extrapolated the slope in the correction factors of the most outside percentile values to these tail ends of the distribution (see Figure 4-11). This approach is followed based on advice of KNMI who applied the same method for the climate datasets.

5) We apply the correction factors both to the current and future climate wflow_sbm simulated discharges to arrive at the corrected discharge time-series.

4.3.6 Bias-corrected discharge projections for Lobith

Figure 4-12 shows that the values after the discharge bias-correction (orange lines) follow the observed values much better, both in terms of the discharge regime throughout the year, as for the 7-day minimum discharges. There is a slight decrease in performance for the annual maximum values, but this might also be related to the limited length of the observed discharge time series.

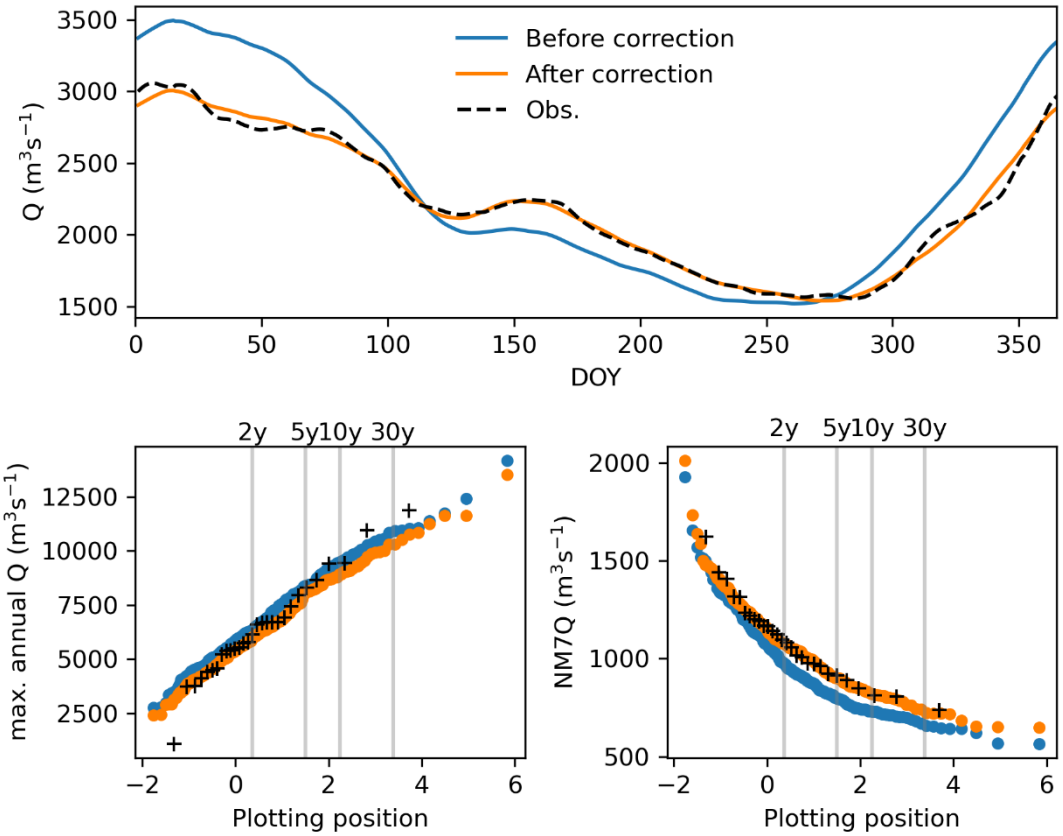

Figure 4-12: Comparing the simulated discharge of the reference climate with the observed values at Lobith, including the return periods of the annual maxima and the 7-day minima discharges for the observed (+) , the non-corrected (blue) and corrected (orange) simulations. Top panel presents the annual average discharge regime, bottom left the Gumbel plot for annual discharge maxima and bottom right the Gumbel plot for 7-day minimum flow.

In Annex C we also present the influence of the bias-correction on the simulated time-series. Overall, the statistics of the corrected time-series are closer to those of the observations, especially for low discharges. The graphs presented were also made to check whether the bias-correction does not introduce any unexpected irregularities or other unwanted side-effects. The graphs confirm that this is not the case. Still, the corrected time-series do not perfectly match the observations as the method focusses on the correction of monthly discharge percentiles to allow it to be applied to historic and future climate datasets as well.

5 Methods: Main differences in experiment set-up between KNMI'14 and KNMI'23

Since the release of the KNMI'14 scenarios and the accompanying discharge scenarios, progress has been made including improvements in climate and atmospheric modelling, improved scenario definition and improved hydrological modelling. Table 5-1 provides an overview of the differences in modelling chain for the KNMI'23 and KNMI'14 discharge scenarios. The main differences that need additional explanation are addressed in this chapter.

Table 5-1: Overview of the differences in the modelling chain between the KNMI'14 scenarios and the here presented KNMI'23 discharge scenarios.

Component	KNMI'14	KNMI'23
Climate scenarios		
IPCC generation	AR5	AR6
Climate model	GCM (available simulations for AR5)	RCM (EC-EARTH – RACMO)
Length of individual scenarios	66 years	8 ensembles of 30 years representing internal climate variability
Time-series correction	Time-series transformation	Bias-correction (quantile mapping)
Future time horizons	2050, 2085	2050, 2100, 2150
Reference period used for the climate change signal	1961-1995	1991-2020 (based on RACMO simulations, with 8 ensembles)
Reference time-series	1950-2006 (based on meteorological observations)	1991 – 2020 (8 x 30-year timeseries of RACMO output)
Number of scenarios	4 per time horizon + additional dry scenario (WHdry)	6 per time horizon
Discharge scenarios		
Hydrological model	HBV – lumped	Wflow_sbm – distributed
Initial conditions hydrological model	Same for all future horizons	Created continuous time series

AR5 – AR6

The KNMI'23 scenarios are developed based upon the latest generation of IPCC scenarios that were released in 2021 for the IPCC 6th assessment report (AR6: IPCC, 2021). The IPCC AR6 report is written based upon simulations from the state-of-the-art climate models that all have been improved since the 5th assessment (AR5) report. With the currently available datasets we can project until 2150 instead of 2085.

GCM – RCM

For the KNMI'14 scenarios, KNMI used the data from a large set of GCMs and statistically downscaled those for the Rhine and Meuse. For the KNMI'23 scenarios it was decided to apply a similar method over the Netherlands and its transboundary basins. For the Netherlands a larger set of KNMI'23 climate variables (including wind etc.) is needed from the climate models than for the hydrological modelling of the Meuse and Rhine.

Not all these variables are available from the open access GCM datasets. Therefore, and to reach a higher spatial resolution, it was decided to run the KNMI RCM RACMO (see chapter 3.1.3).

Scenarios
The 4 main KNMI'14 scenarios were based on temperature rise (moderate (G) or warm (W)) and change in air circulation pattern (low (L) and high (H)). At a later stage one additional scenario was added, the WH_{dry} scenario, because the most extreme scenario (WH) could not represent the wettest maximum flow conditions while also covering the driest summer low flow conditions. They more or less represented the spread between the Representative Concentration Pathways RCP4.5 and RCP8.5.

The 4 main KNMI'23 scenarios are based on the future CO_2 emissions (low or high) and a drying (d) or wetting (n) climate. They present the spread between SSP1-2.6 and SSP5-8.5. For the current discharge projections also a moderate emission scenario (SSP2-4.5) is considered.

Time-series transformation – bias-correction
Instead of generating future time-series following time-series transformation with the Advanced Delta Change method (Ruiter, 2012) where the climate change signal is applied to transfer the observed time-series into future time-series. KNMI now uses a quantile mapping approach (see also 3.1.4) to bias-correct the climate data. Herewith, changes in persistency (like multi-year droughts), frequency and intensity, that can have a large impact on especially the severity of floods and droughts, are also present in the future climate datasets. The pros and cons of bias-correction vs time-series transformation are presented in Annex E.

Hydrological modelling
The KNMI'14 discharge scenarios are derived with the lumped hydrological model HBV (Bergstrom, 1992) developed by the Swedish Meteorological and hydrological Institute (SMHI). However, a lumped hydrological model cannot fully account for the large spatial heterogeneity within the sub-basins. In addition, due to its lumped nature, it can only to a limited extend benefit from the newly available gridded high-resolution data products for elevation, soil type and meteorology. And finally, the HBV code is closed and over the past years Deltares noticed that not having the ability to improve, or sometimes even fully understand, the way hydrological processes have been implemented hampered the work. Similar to the Netherlands the German Bundesanstalt für Gewässerkunde is exploring the application of a grid-based hydrological model instead of using HBV.

Deltares started working on a distributed hydrological model for the Rhine and Meuse, wflow_sbm (Van Verseveld et al., 2022) in 2015. The developments were initiated in collaboration with Rijkswaterstaat as part of the 4-year lasting European H2020 project IMPREX (Imhoff et al., 2020). In their PhD trajectories Bart van Osnabrugge and Laurene Bouaziz (Bouaziz, 2021) worked on the improved modelling of the hydrology of respectively the Rhine and the Meuse. After that further improvements were made both by calibrating the hydrological model, implementing reservoir operation schemes (Imhoff et al., 2022) and by improving the implementation of the hydrological processes in the wflow_sbm code. At the end of 2022 a wflow_sbm version has been delivered that has been approved by RWS for further use in this climate change assessment. Deltares (2022) describes in detail the improvements of wflow over HBV. Annex A presents a comparison between HBV and wflow_sbm simulations. Overall wflow_sbm outperformed HBV, especially for the Meuse where the wflow_sbm model performs best for all performance tests (KGE, NSE, logNSE etc.).

6 Results: KNMI’23 discharge projections

Statistics considered

In the previous chapters we introduced the KNMI’23 climate scenarios and the methods that have been applied to translate the climate changes into discharge changes for the rivers Rhine and Meuse. In this chapter we present the future changes in river discharges that result from the KNMI’23 scenarios. We focus on the Meuse at the Dutch border and the Rhine at Lobith. For the Rhine we chose to show the results for the bias-corrected discharges. In addition, we analyse and explain the changes by considering the projected behaviour at upstream gauging stations and the changes in the driving meteorological variables. We provide a series of statistics to describe these changes. All these statistics are based on the RACMO simulations.

- River regime plots
- Average annual discharge
- Average annual 7-day-average minimum discharge
- Average annual maximum discharge

The results for each river start with the interpretation of climate projections for precipitation, temperature and potential evaporation that induce the presented discharge changes. The number of statistics is limited, yet the daily discharge time-series can be downloaded and are available for further analysis.

Analysis of the results

To better understand and capture the hydrological response to the new climate scenarios, we created boxplots that clearly capture the signal of the change relative to the reference climate, while also giving an indication of the spread/variability inside a single scenario (see the first boxplot in Figure 6-1). Here, the yearly basin-average temperatures (8 x 30 years, resulting in 240 values) make up a single boxplot. The whiskers of the boxplot represent the 5-95% data range, the box represents the 25-75% data range, and the horizontal line represents the median value.

For some of the variables, we also showed the relative changes in percentages. These are calculated as follows: the results from a climate scenario are compared against the results from the simulation with the reference scenario. Both results contain 240 different values (yearly basin-average temperatures in the example above), which are both sorted from low to high values. Next, the relative difference for each pair of points is calculated, resulting in 240 new values, which can be used to create a similar boxplot, following the same definitions for the whiskers and the box.

6.1 Meuse

6.1.1 Climate projections

For the Meuse all scenarios project increases in temperature (see Figure 6-1: Annual average temperature over the Meuse basin up till the Dutch border (degrees Celsius) for the current (Ref = grey) and future climate (future time-horizons on the x-axis). Blue boxes present the low climate change scenarios (Ln = wet and Ld = dry), purple boxes present the moderate scenario (Mn = wet and Md = dry) and brown boxes present the high scenario (Hn = wet and Hd = dry).Figure 6-1). According to the Hd scenario median temperature may increase up to 6 degrees Celsius by 2150. The Ld/Ln scenarios project smaller changes, increases of less than 1 degree.

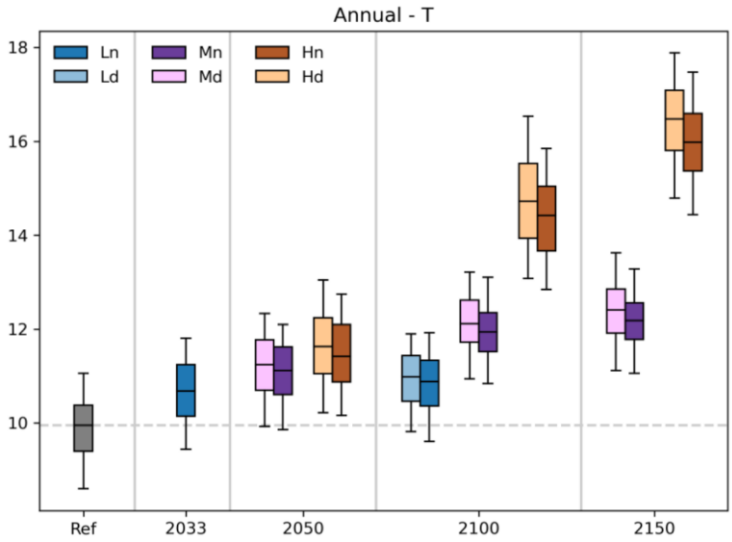

Figure 6-1: Annual average temperature over the Meuse basin up till the Dutch border (degrees Celsius) for the current (Ref = grey) and future climate (future time-horizons on the x-axis). Blue boxes present the low climate change scenarios (Ln = wet and Ld = dry), purple boxes present the moderate scenario (Mn = wet and Md = dry) and brown boxes present the high scenario (Hn = wet and Hd = dry).

The increases in temperature lead to increases in potential evaporation (EP, see Figure 6-2). The scenarios with the largest temperature increase (Hn and Hd) also show the largest increase in potential evaporation. The potential evaporation increases from ~640 mm/year for the reference scenario to ~820 mm/year for the most extreme scenario (2150Hd).

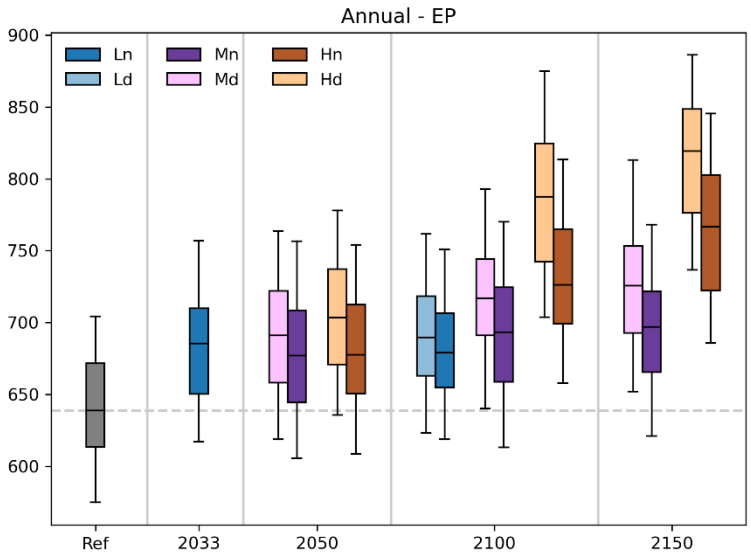

Figure 6-2: Annual average potential evaporation (EP) over the Meuse basin up till the Dutch border (mm per year) for the current (Ref = grey) and future climate (future time-horizons on the x-axis). Blue boxes present the low climate change scenarios (Ln = wet and Ld = dry), purple boxes present the moderate scenario (Mn = wet and Md = dry) and brown boxes present the high scenario (Hn = wet and Hd = dry).

When evaluating the full set of precipitation projections for the Meuse (see Figure 6-3) the number of median projected increases (represented by the central line of the boxplots) equals the number of projected decreases. All wet scenario versions project increases but the size of the increase is in general smaller than the projected decreases obtained for the dry scenarios. Overall, the signal (median change in precipitation) is small and the variability between and within scenarios is large. We therefore also looked at the changes in summer (Figure 6-4) and winter (Figure 6-5) precipitation. Precipitation over the Meuse basin in the winter will likely increase whereas summer precipitation will likely decrease. The median of the projected summer precipitation changes is negative (i.e., a reduction) for both the wet and dry scenarios.

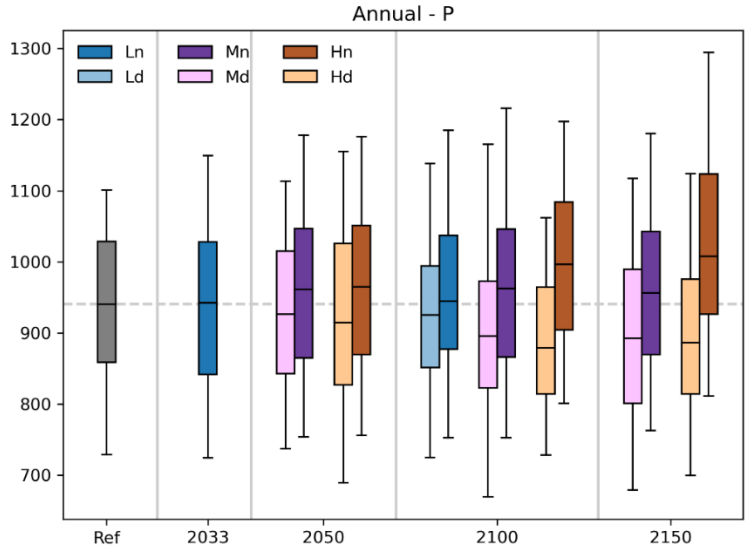

Figure 6-3: Annual average precipitation over the Meuse basin up till the Dutch border (mm per year) for the current (Ref = grey) and future climate (future time-horizons on the x-axis). Blue boxes present the low climate change scenarios (Ln = wet and Ld = dry), purple boxes present the moderate scenario (Mn = wet and Md = dry) and brown boxes present the high scenario (Hn = wet and Hd = dry).

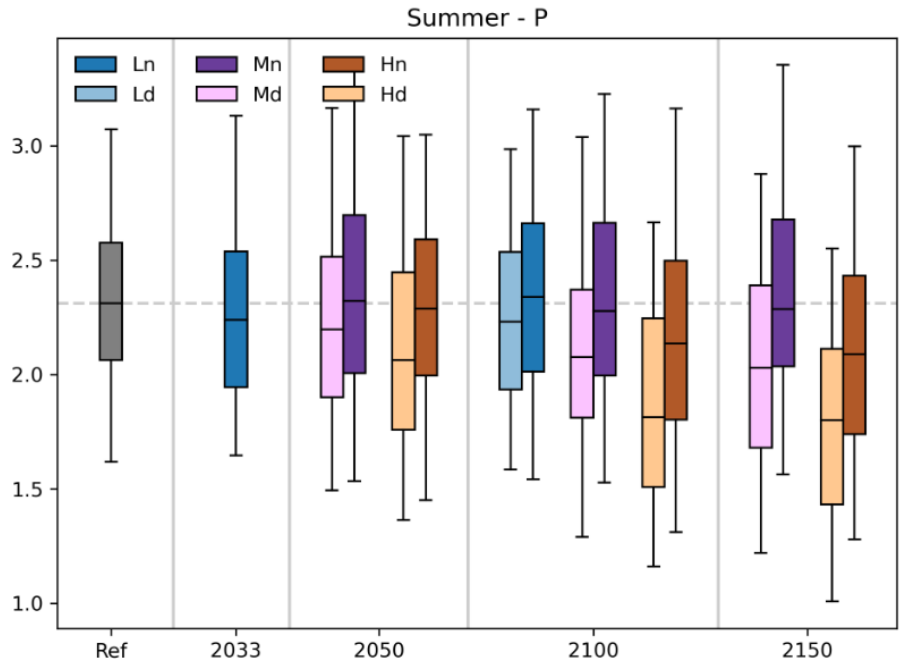

Figure 6-4: Change in average daily summer precipitation over the Meuse basin up till the Dutch border (mm per day) for the current (Ref = grey) and future climate (future time-horizons on the x-axis). Blue boxes present the low climate change scenarios (Ln = wet and Ld = dry), purple boxes present the moderate scenario (Mn = wet and Md = dry) and brown boxes present the high-end scenario (Hn = wet and Hd = dry).

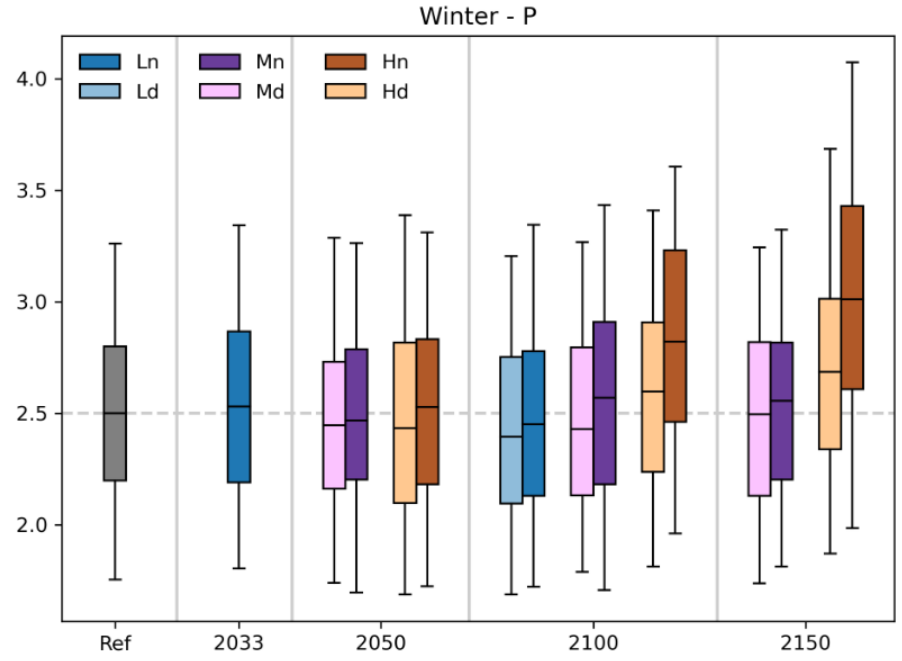

Figure 6-5: Change in average daily winter precipitation over the Meuse basin up till the Dutch border (mm per day) for the current (Ref = grey) and future climate (future time-horizons on the x-axis). Blue boxes present the low climate change scenarios (Ln = wet and Ld = dry), purple boxes present the moderate scenario (Mn = wet and Md = dry) and brown boxes present the high scenario (Hn = wet and Hd = dry).

6.1.2 Discharge projections

Figure 6-6 displays the *annual discharge regime* for the current climate and Paris scenario (on top) and the other scenarios for 2050, 2100, 2150 (top to bottom). The values in the graph are the long-term average discharge values for the given day-of-the year (DOY) to avoid an irregular pattern caused by short extremes the graphs are smoothened by applying a moving average window of 30 days. For the Meuse we see future increases in discharge for the winter period and lower discharges in the late summer period. The latter is a result of increased evapotranspiration and consequent drying of the soils. By 2033 changes are neglectable and even by 2050 the discharge regime remains quite similar compared to the current climate conditions. By 2150 the Hn scenario projects large increases, especially for the winter, this is caused by increased rainfall. The changes in summer discharge seem to be small, although the future discharges come closer to the criteria for droughts and resulting water use restrictions in the Netherlands.

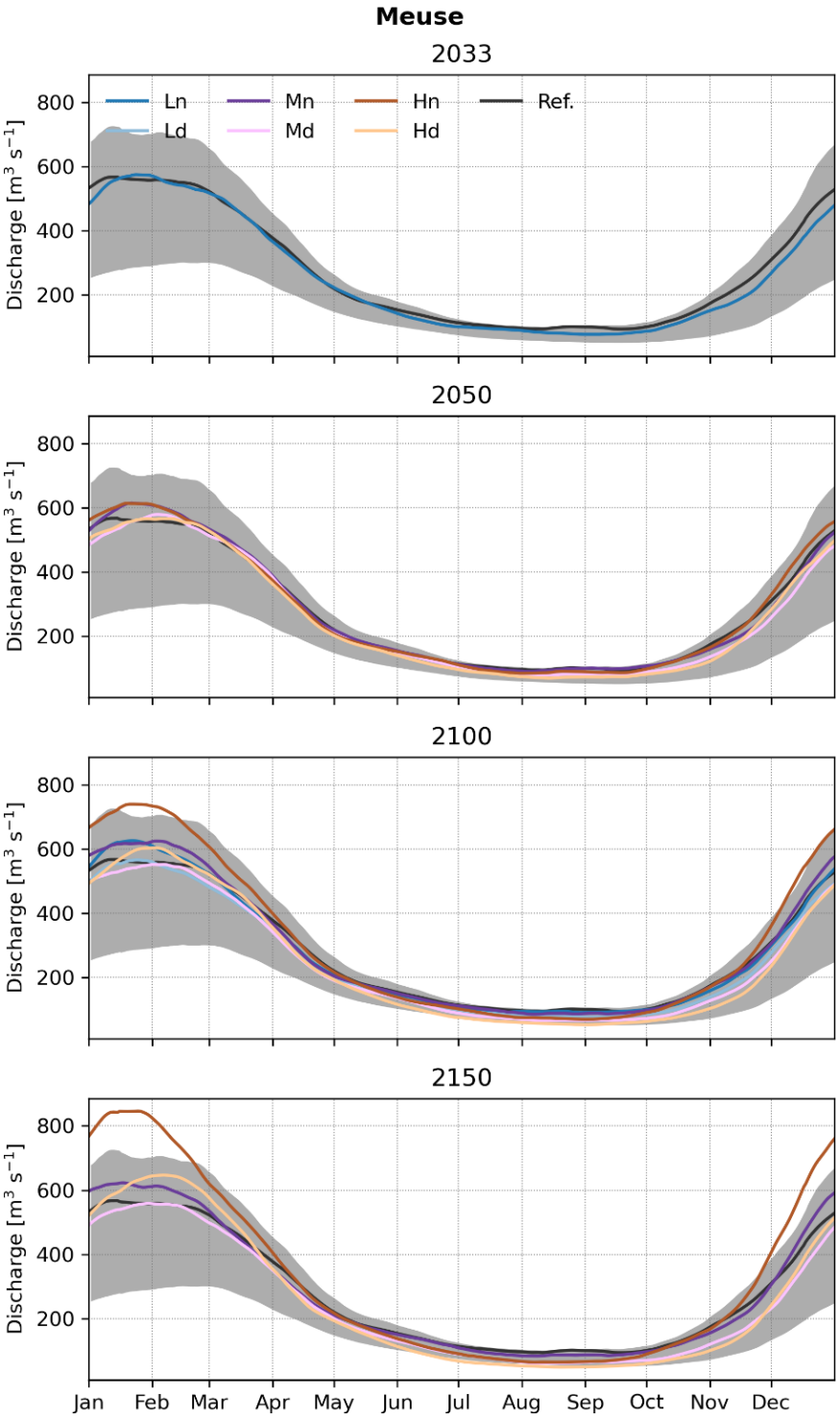

Figure 6-6: Long-term average Meuse discharge at the Dutch border for the given day-of-year (DOY) derived from the 30-year time windows, considering a moving average window of 30 days. Blue lines present the low climate change scenarios (Ln = wet and Ld = dry), purple lines present the moderate scenario (Mn = wet and Md = dry) and brown lines present the high scenarios (Hn = wet and Hd = dry). The top panel contains the results for the current climate including the interannual variation (grey bands, representing the 25% to 75% range), the reference climate simulation (black line) and the Paris scenario (blue line). The next panels contain the 3 future time-horizons of interest: 2050, 2100 and 2150.

For the upstream location Chooz (Figure 6-7), we see similar changes as at the border. For Chaudfontaine (Figure 6-8), located along the Vesdre increases in winter discharges are not that large, decreases in (late) summer discharge are more pronounced. The maps in Figure 6-9 show that also the increases in winter precipitation are smaller for the area upstream of Chaudfontaine.

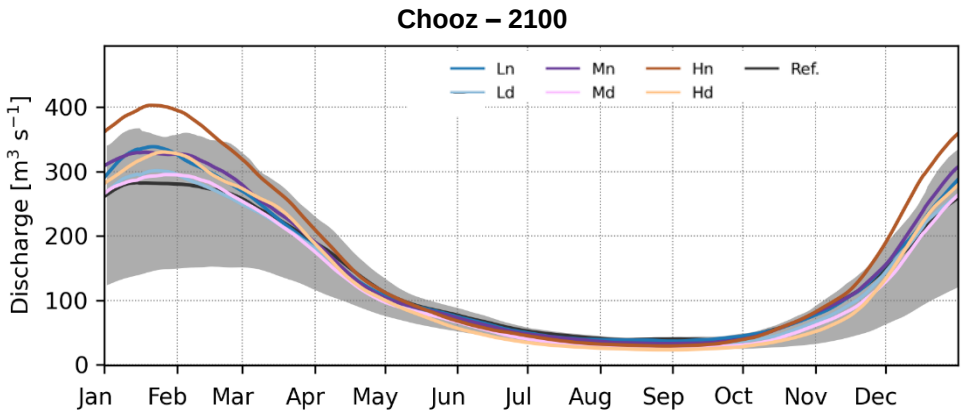

Figure 6-7: Similar to Figure 6-6 panel 3 but than for long-term average discharge of the Meuse at Chooz for the given day-of-year for 2100.

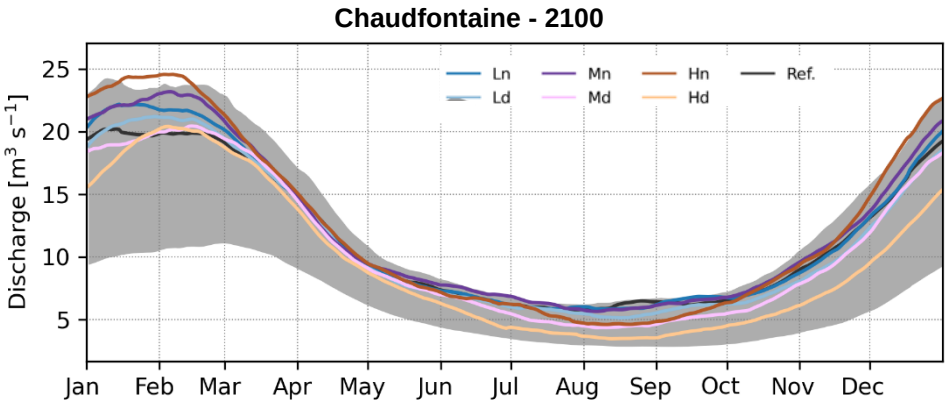

Figure 6-8: Similar to Figure 6-6 panel 3 but than for long-term average discharge of the Vesdre at Chaudfontaine for the given day-of-year for 2100.

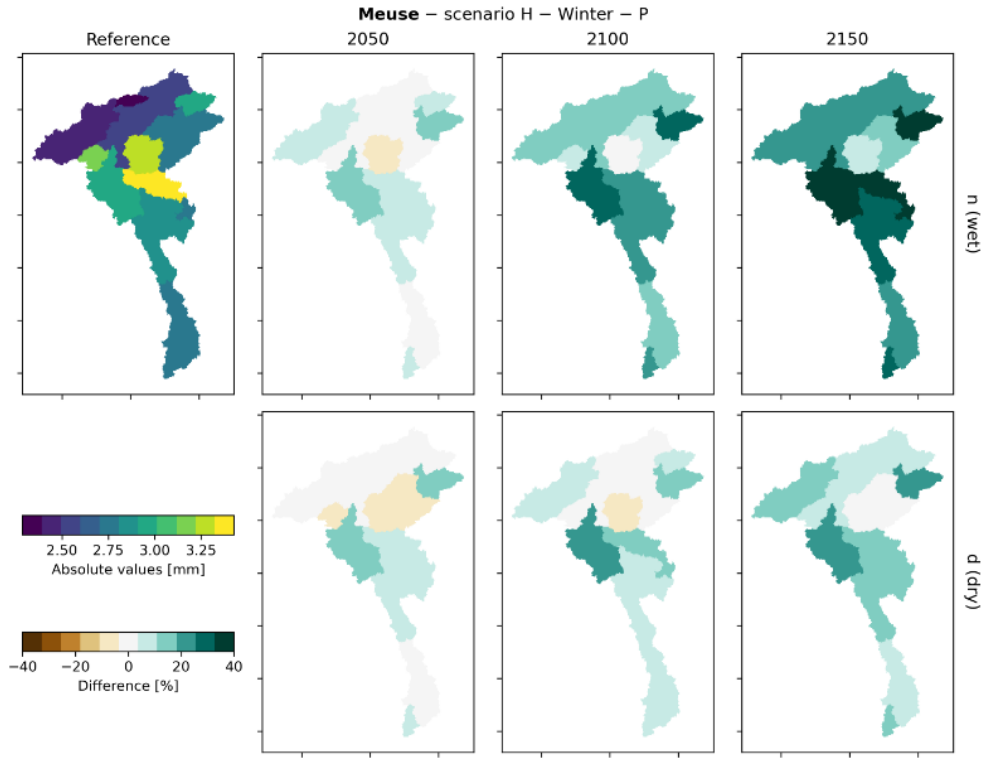

Figure 6-9: Historical average daily winter precipitation (top-left; absolute values) and projected changes in winter rainfall amounts for the Meuse basin for the time-horizons 2050, 2100, 2150 (from left to right) for the wet (top) and dry (bottom) variants of the High scenario.

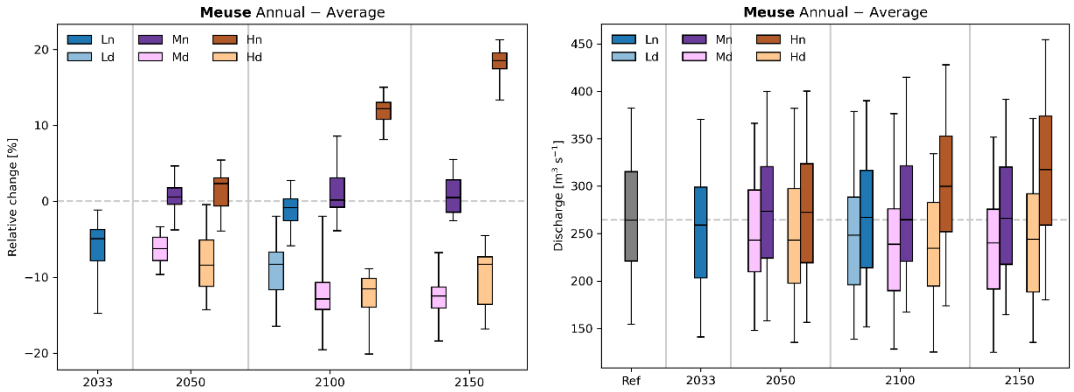

Figure 6-10: Change in annual average discharge at the Dutch border for the future climate (future time-horizons on the x-axis). Left panel shows the relative changes, right panel the absolute values. Blue boxes present the low climate change scenarios (Ln = wet and Ld = dry), purple boxes present the moderate scenarios (Mn = wet and Md = dry) and brown boxes present the high scenarios (Hn = wet and Hd = dry).

For the Meuse, only the most extreme scenario projects envisages an increases in future *annual average discharge* (Figure 6-10). This is mainly caused by the increase in precipitation shown in Figure 6-3. The difference between the Hd and Hn scenarios increases with time. Hd projects increases up to 20%, whereas Hn projects decreases of approximately 10%. For the Hn scenario we also see large increases in precipitation. Increases in precipitation for the Hd scenario are small and potential evaporation will increase. This results in the projected decreases.

For the Meuse we looked at the differences in change signals for *summer and winter discharge* as well. Average summer discharge will very likely decrease (Figure 6-11). This is directly related to the projected decreases in summer precipitation which are especially large for the Hd scenario (Figure 6-4). The projections from the dry scenarios vary a lot more than for the wet scenarios.

The projected change in summer discharge for the L scenario in 2033 is already similar to the projections for the Md/Mn scenarios by 2050. The projected change in annual precipitation is also rather similar for the L and Md/Mn scenarios (Figure 6-3) and also projected potential evaporation change is similar for the Meuse basin for these scenarios (Figure 6-2).

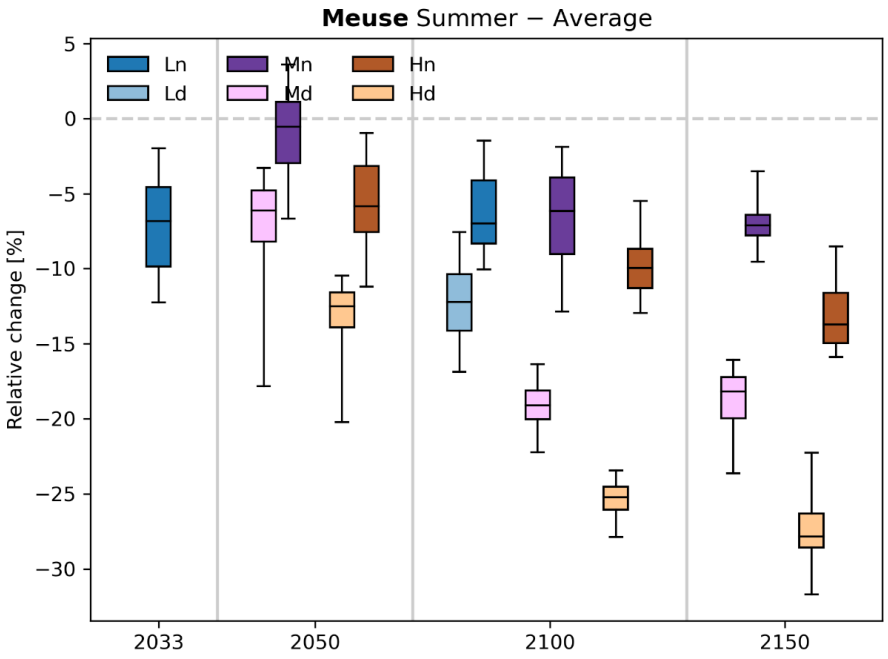

Figure 6-11: Change in average summer discharge of the Meuse at the Dutch border for the current (Ref = grey) and future climate (future time-horizons on the x-axis). Blue boxes present the low climate change scenarios (Ln = wet and Ld = dry), purple boxes present the moderate scenarios (Mn = wet and Md = dry) and brown boxes present the high scenarios (Hn = wet and Hd = dry).

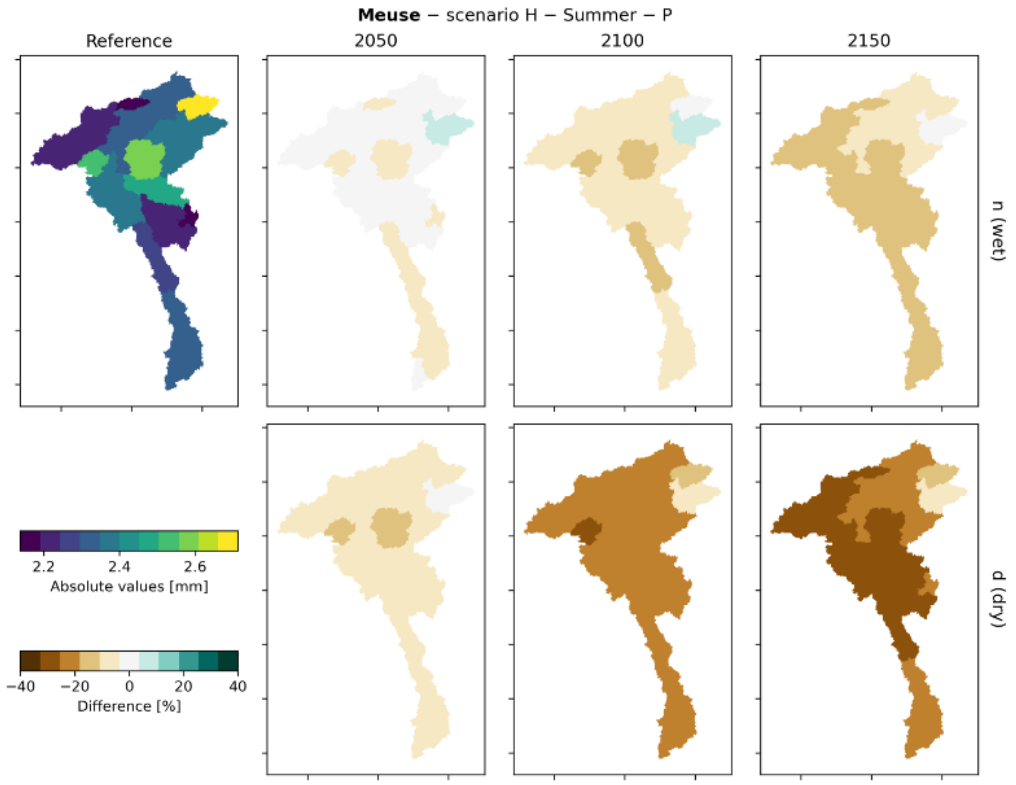

Figure 6-12: Historical average daily summer sub-catchment rainfall (top-left; absolute values) and projected changes in summer rainfall amounts for the Meuse basin for the time-horizons 2050, 2100, 2150 (from left to right) for the wet (top) and dry (bottom) variants of the High scenario.

The direction of change for the winter discharge of the Meuse is very uncertain (Figure 6-13). Although, the wettest scenario does project large increases (up to ~30%).

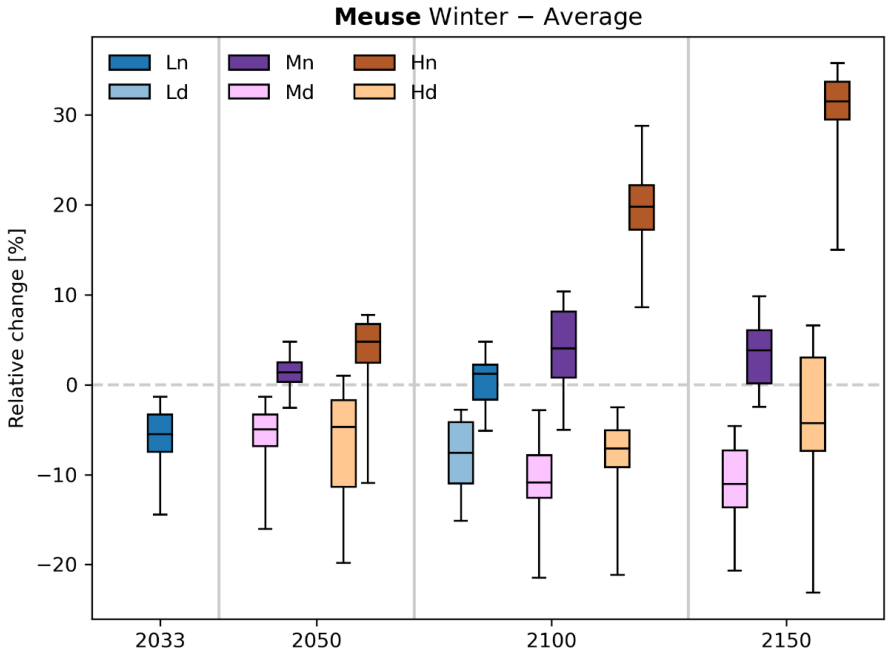

Figure 6-13: Relative change in average winter discharge of the Meuse at the Dutch border for the future climate (future time-horizons on the x-axis). Blue boxes present the low climate change scenarios (Ln = wet and Ld = dry), purple boxes present the moderate scenarios (Mn = wet and Md = dry) and brown boxes present the high scenarios (Hn = wet and Hd = dry).

When we look at *annual maximum discharges* (Figure 6-14) we see that all dry scenarios project decreases up until 2100. By 2150 both the H and M scenarios, except the Md scenario project increases. Changes in winter average discharge can reach up to 30% according to the Hn scenario. This is a result of the large increases in winter precipitation throughout the basin (see Figure 6-9)

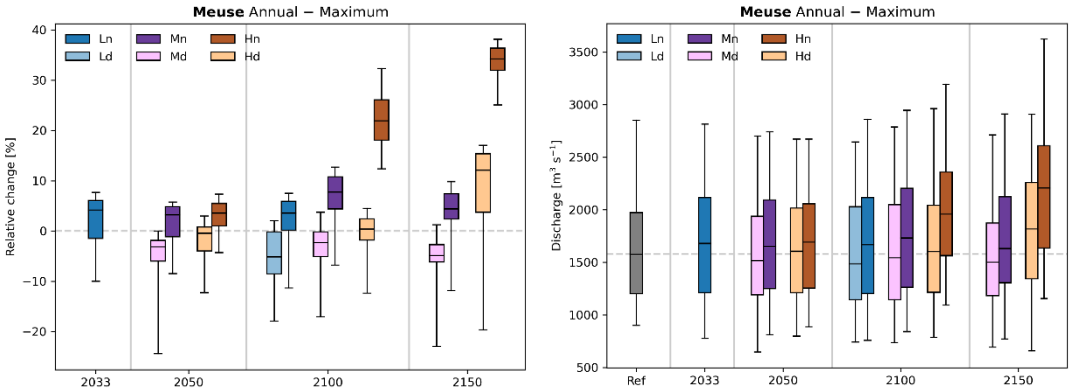

Figure 6-14: Change in annual maximum discharge for the Meuse at Dutch border for the current (Ref = grey) and future climate (future time-horizons on the x-axis). Left panel shows the relative changes, right panel the absolute values. Blue boxes present the low climate change scenarios (Ln = wet and Ld = dry), purple boxes present the moderate scenario (Mn = wet and Md = dry) and brown boxes present the high scenario (Hn = wet and Hd = dry).

A decrease in *7-day minimum discharge* is consistently projected by all scenarios (Figure 6-15). By 2033 decreases may already be -10%, by 2150 decreases can reach up to -30% or even more.

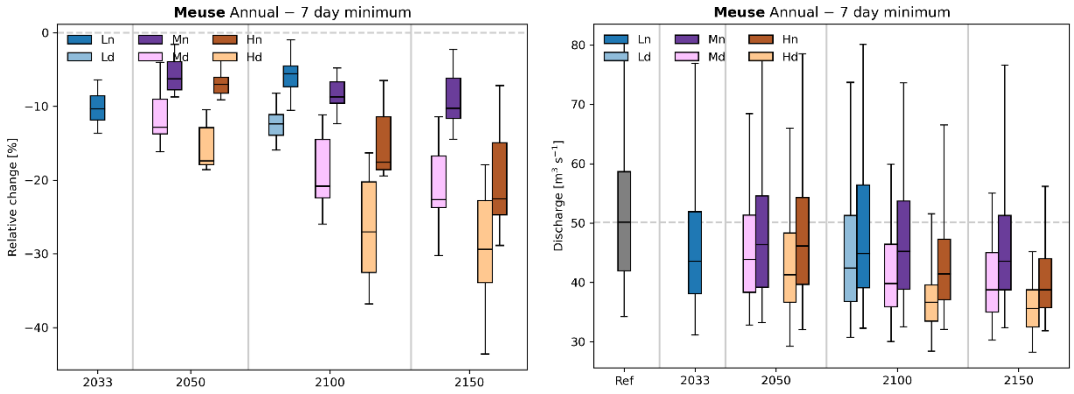

Figure 6-15: Change in annual 7-day minimum discharge for the Meuse at the Dutch border for the current (Ref = grey) and future climate (future time-horizons on the x-axis). Blue boxes present the low climate change scenarios (Ln = wet and Ld = dry), purple boxes present the moderate scenario (Mn = wet and Md = dry) and brown boxes present the high scenario (Hn = wet and Hd = dry).

The impacts of the climate scenarios on the discharge of the Meuse at the Dutch border can be summarized as follows:

- The annual average discharge is projected to decrease according to all scenarios except Mn and Hn. The Mn scenario shows average discharge values that closely resemble the current conditions, while the Hn scenario projects an increase of about 10% in 2100. The projections for the Ld, Md, and Hd are more or less the same.
- Most scenarios project little change in annual maximum discharge (within the ~5% change). Only at 2100, Mn and Hn show an increase of ~5% and ~20%, respectively. The Hn scenario projects an increase of 35% in 2150.
- All scenarios show a decrease for the 7-day minimum discharge. By 2100, the most severe decrease is projected by the Hd scenario, with a decrease of about 25% which increases to 30% in 2150.
- On average, almost all scenarios (with the exception of Md) project an increase of the discharge during the winter period. These are driven by increases in winter precipitation, combined with a reduction in snowfall leading to more direct discharge.
- All scenarios show a decrease of discharge during the summer, which is driven by increases in evaporation

6.2 Rhine

6.2.1 Climate projections

Similar to the Meuse, all scenarios project increases in air temperature for the Rhine basin (see Figure 6-16). According to the Hd scenario, temperature may increase up to nearly 7 degrees Celsius by 2150 compared to the reference scenario that is also based on RACMO data. The more moderate Md/Mn scenarios project increases of around 3 degrees Celsius and after 2100 this scenario projects a slowdown of the increase. The Ld/Ln scenarios project smaller increases of around 1 degree.

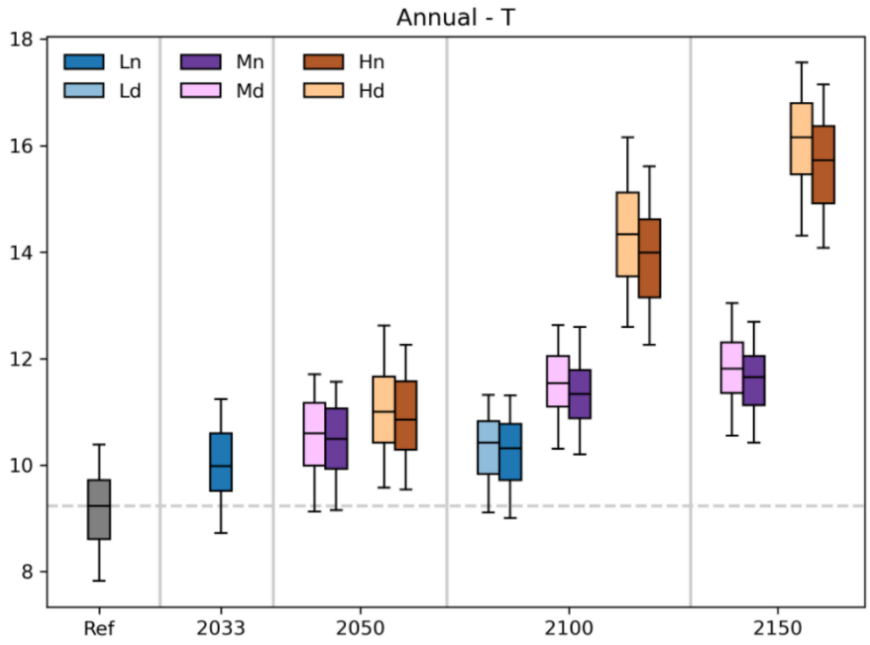

Figure 6-16: Boxplots of the annual average temperature over the Rhine basin up till Lobith (degrees Celsius) for the current (Ref = grey) and future climate (future time-horizons on the x-axis). Blue boxes present the low climate change scenarios (Ln = wet and Ld = dry), purple boxes present the moderate scenarios (Mn = wet and Md = dry) and brown boxes present the high scenarios (Hn = wet and Hd = dry).

As could be expected, increases in temperature will also lead to increases in potential evaporation (EP - see Figure 6-17). Hd and Hn project an annual average increase of approximately 0.4 mm / day which corresponds to an increase of around 150 mm per year. This will likely cause decreases in discharge, especially in (early) summer.

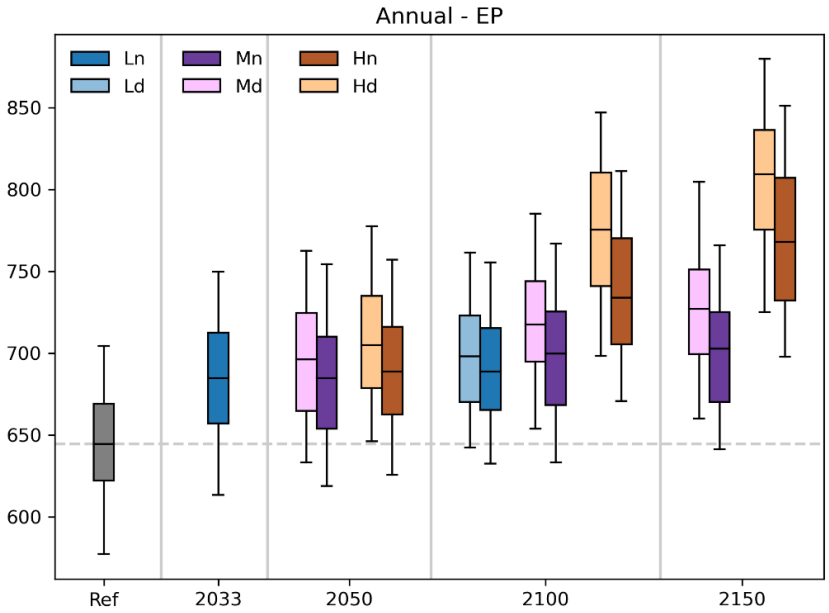

Figure 6-17: Annual average potential evaporation (mm per year) over the Rhine basin up till Lobith for the current (Ref = grey) and future climate (future time-horizons on the x-axis). Blue boxes present the low climate change scenarios (Ln = wet and Ld = dry), purple boxes present the moderate scenarios (Mn = wet and Md = dry) and brown boxes present the high scenarios (Hn = wet and Hd = dry).

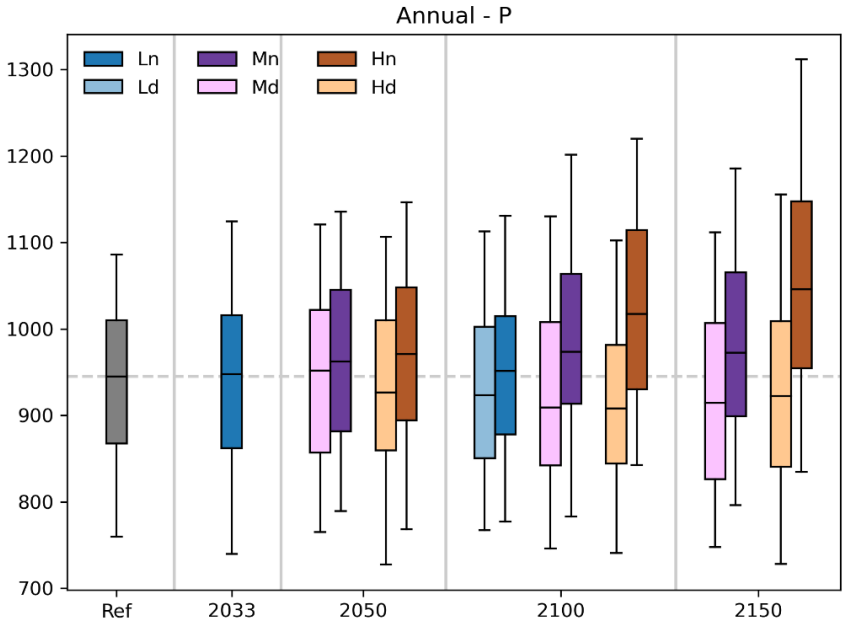

Figure 6-18: Annual average precipitation over the Rhine basin up till Lobith (mm per year) for the current (Ref = grey) and future climate (future time-horizons on the x-axis). Blue boxes present the low climate change scenarios (Ln = wet and Ld = dry), purple boxes present the moderate scenarios (Mn = wet and Md = dry) and brown boxes present the high scenarios (Hn = wet and Hd = dry).

For precipitation (see Figure 6-18) the changes are relatively uncertain and less pronounced. The width of the boxes (25 – 75 percentage uncertainty range) is often larger than the projected changes. The dry scenarios project nearly any change, or very small decreases.

The Mn, Hn and Hd scenarios project precipitation increases of up to ~0.25 mm by 2150. This is an increase of approximately 90 mm per year averaged over the basin.

6.2.2 Discharge projections

The results presented in this section are based on the bias-corrected discharge time-series for Lobith (see section 4.3.5). For the other stations (Maxau, Cochem) uncorrected data are used, because there are no bias-corrected time-series available.

Figure 6-19 displays *the annual discharge regime* for the current climate and Paris scenario (on top) and the other scenarios for 2050, 2100, 2150 (top to bottom). The values in the graph are the long-term average discharge values for the given day-of-the year (DOY) to avoid an irregular pattern caused by short extremes the graphs are smoothened by applying a moving average window of 30 days. In general, the KNMI'23 scenarios lead to increases in winter discharge and decreases in (late) summer discharge. Changes are most pronounced for the high-end scenario. Discharge conditions assuming the moderate Paris scenario (1.5 degrees increase by 2033; blue line) remain nearly the same. For all scenarios the changes are small by 2050, but they become more pronounced towards 2150.

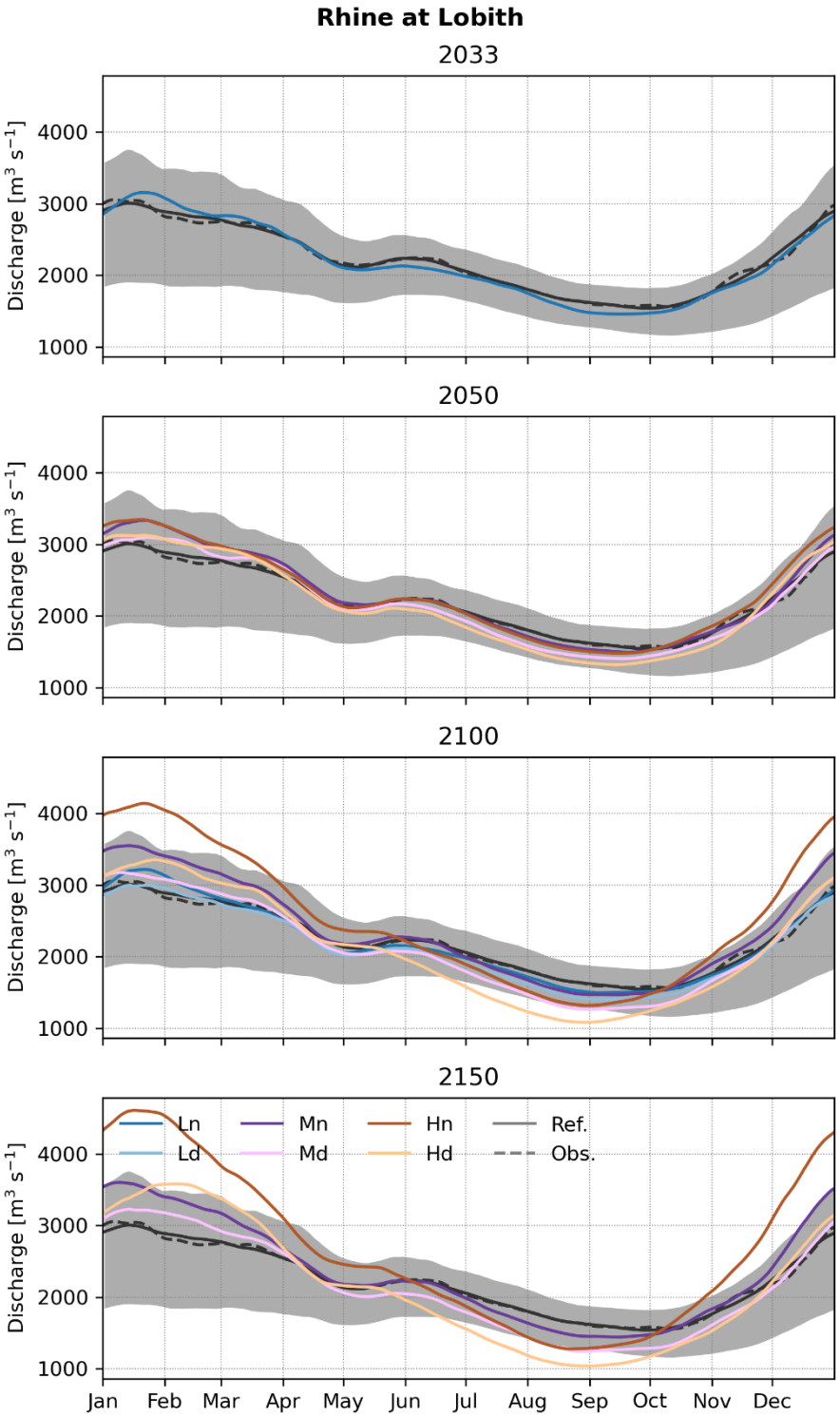

Figure 6-19: Long-term average discharge at Lobith for the given day-of-year derived from the 30-year time windows, considering a moving average window of 30 days. The moving average window is used to reduce the effects of single extreme events influencing the Day-Of-Year (DOY) averages. Blue lines present the low climate change scenarios (Ln = wet and Ld = dry), purple lines present the moderate scenario (Mn = wet and Md = dry) and brown lines present the high scenario (Hn = wet and Hd = dry). The top panel contains the results for the current climate including the interannual variation (grey bands representing the 25% to 75% range), the reference climate simulation (black line) and the Paris scenario (blue line) after that the 3 future time-horizons of interest are displayed: 2050, 2100 and 2150.

Maxau (Figure 6-20) and Cochem (Figure 6-21) have been added to the analysis to explain the changes at Lobith. Only results for 2100 are presented for these gauges. The presented discharges are uncorrected model simulations. For Maxau, we find increases in winter and spring discharge. Due to increased temperatures, less precipitation is accumulated as snow and the runoff during winter increases. As a consequence, spring and early summer discharges decrease. These results are in line with, but smaller, than the tendency of changes we see at Lobith. At Lobith the changes of the full upstream basins are aggregated which explains the difference.

For Cochem, located at the Mosel, the total discharge is projected to increase. The largest increases are projected for the winter months. This contributes to future increase of winter discharge at Lobith as well. The main cause of summer discharge decreases at Lobith is the change in the discharge regime in the mountainous snow influenced part of the Rhine basin. Absolute summer average discharge decreases are smaller for Cochem, but still between 5 and 30% in summer and autumn.

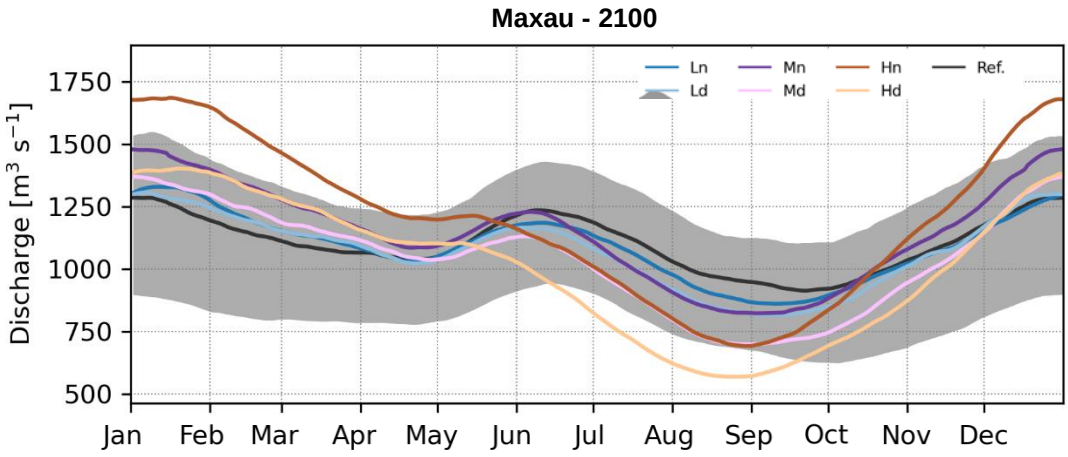

Figure 6-20: Similar to Figure 6-19 panel 3 but than for long-term average discharge at Maxau for the given day-of-year for 2100.

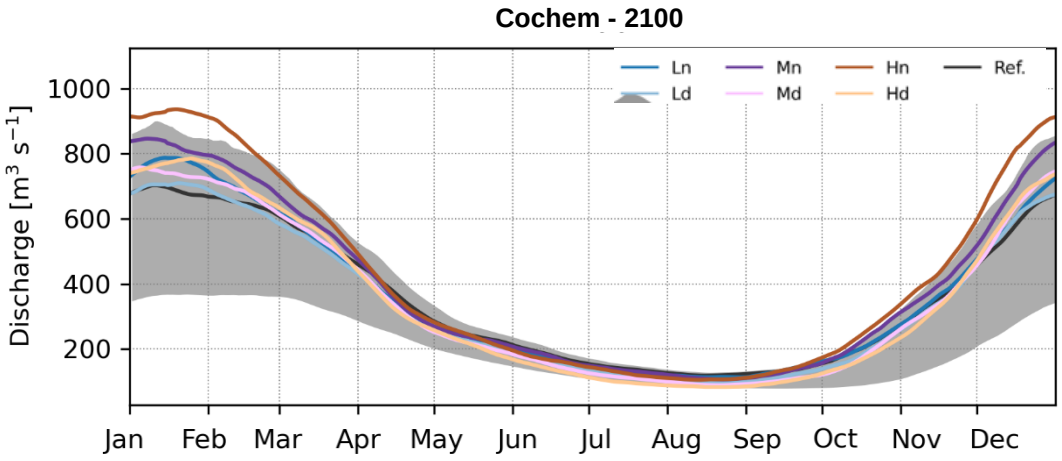

Figure 6-21: Similar to Figure 6-19 but than for long-term average discharge at Cochem for the given day-of-year for 2100.

Actual evaporation

Figure 6-22 shows the increase in actual evapotranspiration (EA) calculated with wflow_sbm. The change in EA is less than potential evaporation (EP – see Figure 6-17) and thus not directly related to temperature increases due to restrictions in soil water availability, which occur especially in summer. The soil is losing water through evaporation, sub-surface runoff and percolation. During periods with little rain the compartments are not refilled. Evapotranspiration occurs from soil, surface water and vegetation. In drier periods, as for example summer, there is less water available in these compartments to evaporate and the reduction from potential to actual evaporation is larger.

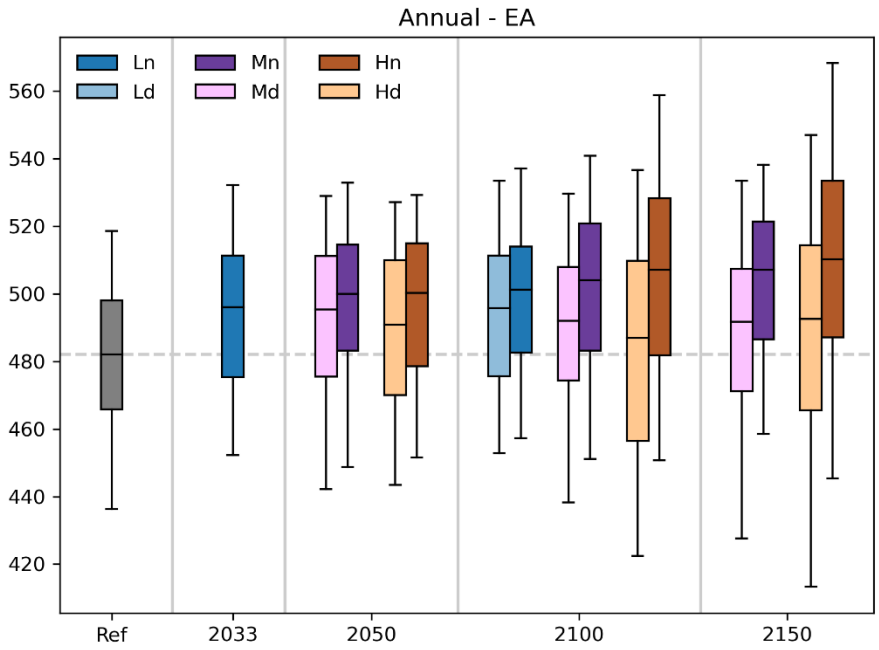

Figure 6-22: Annual average actual evaporation over the Rhine basin up till Lobith (mm per year) for the current (Ref = grey) and future climate (future time-horizons on the x-axis). Blue boxes present the low climate change scenarios (Ln = wet and Ld = dry), purple boxes present the moderate scenarios (Mn = wet and Md = dry) and brown boxes present the high scenarios (Hn = wet and Hd = dry).

Snow

To assess and evaluate the impact of temperature on the accumulation of snow in the Alps Figure 6-23 and Figure 6-24 display the area average snow depth in mm over the Aare basin in Switzerland. These values are obtained by averaging the wflow calculated snow depth over the sub-basin, over the 8 ensembles of 30-years. The snow depth during winter (December-January-February) will decrease during this century. By 2150 the average snow depth may be only ~5 mm. During the summer season (June-July-August) snow will be nearly absent by 2100 and totally absent by 2150 (see Figure 6-22). This is in line with the findings of Stahl et al. (2022). They concluded that all Alpine glaciers will have disappeared by 2100 and snow accumulation will only occur during winter in the Alpine regions and no longer in the lower elevation mountains in Germany.

The decrease in snow accumulation will affect the Rhine discharge in two ways. Peak discharges caused by snow melt in the Alps and especially in the mountains at lower elevation will occur less often. But also, the contribution of snow melt to the overall Rhine discharge will decrease over time which will especially be notable during the summer season.

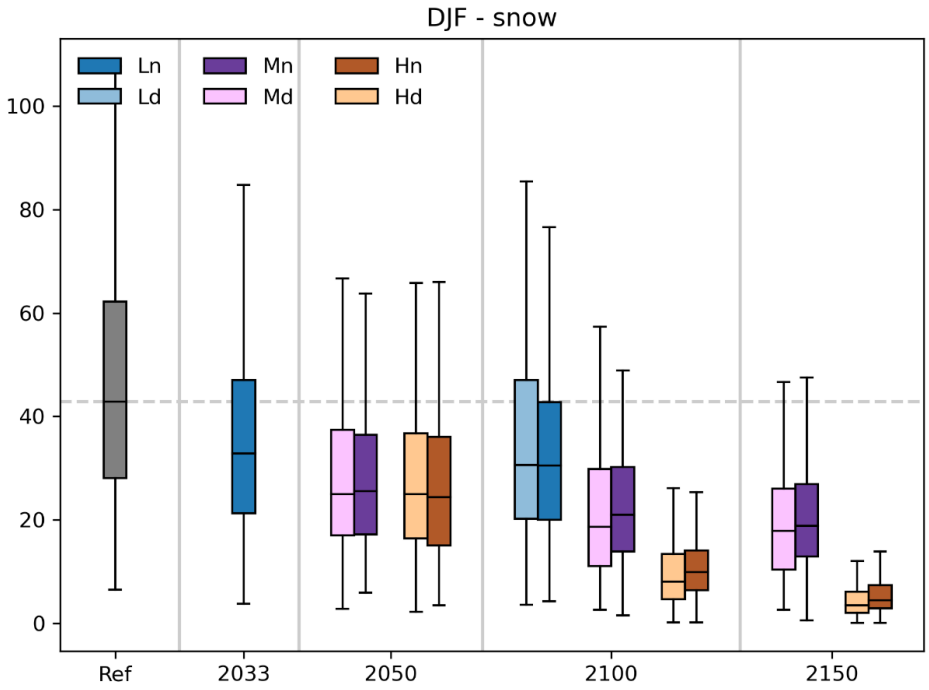

Figure 6-23: Average winter snow depth (mm; December-January-February) in the Aare basin for the current (Ref = grey) and future climate (future time-horizons on the x-axis). Blue boxes present the low climate change scenarios (Ln = wet and Ld = dry), purple boxes present the moderate scenarios (Mn = wet and Md = dry) and brown boxes present the high scenarios (Hn = wet and Hd = dry).

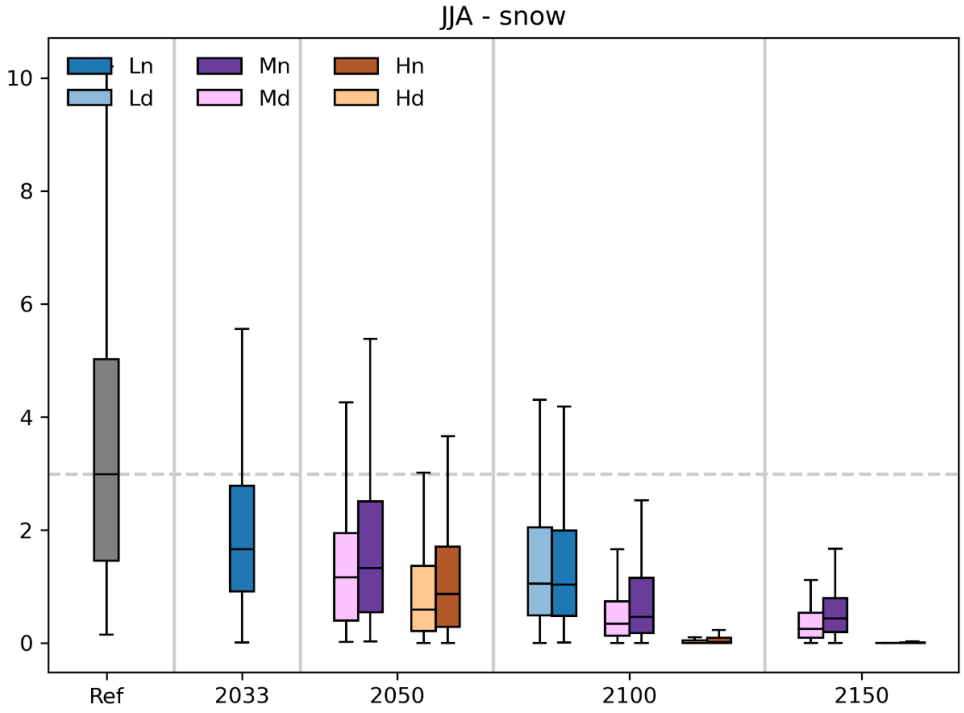

Figure 6-24: Average summer snow depth (mm; June-July-August) in the Aare basin for the current (Ref = grey) and future climate (future time-horizons on the x-axis). Blue boxes present the low climate change scenarios (Ln = wet and Ld = dry), purple boxes present the moderate scenarios (Mn = wet and Md = dry) and brown boxes present the high scenarios (Hn = wet and Hd = dry).

Discharge statistics

In the remainder of this chapter, we look at the changes in the main discharge statistics at Lobith. Figure 6-25 displays the changes in *annual average discharge*. All dry scenarios result in decreasing annual average discharges at Lobith, whereas the wet scenarios result in (larger) increases. There is thus no consistent projection of change in average discharge. The uncertainty in discharge projections is in line with the precipitation projections shown in Figure 6-18, especially the Hn scenario projects large increases in precipitation. For Mn a discharge increase is project for 2050 and 2100, but after that there is no change signal anymore. For precipitation we saw an increase for 2050 and after that also nearly any change. For the Hd scenario the change in discharge is also not consistent over time, again this can also be related to the projected changes in precipitation.

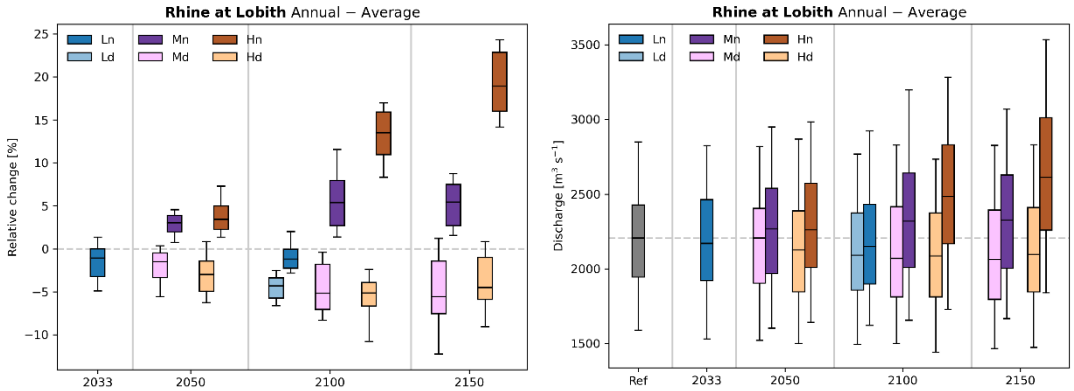

Figure 6-25: Change in annual average discharge at Lobith for the current (Ref = grey) and future climate (future time-horizons on the x-axis). Left panel shows the relative changes, right panel the absolute values. Blue boxes present the low scenarios (Ln = wet and Ld = dry), purple boxes present the moderate scenarios (Mn = wet and Md = dry) and brown boxes present the high scenarios (Hn = wet and Hd = dry).

When we differentiate between average summer discharge (Apr-Sep) and average winter discharge (Oct-Mar), we obtain clearer signals. The summer discharge will very likely decrease (Figure 6-26). Decreases as large as –15 or –20% are not unlikely. This relates back to (1) decrease in snow melt in the Alps, (2) decrease in summer precipitation over the basin (represented by the 60-day minimum rainfall amounts) (see Figure 6-27) and (3) the increase in potential evaporation.

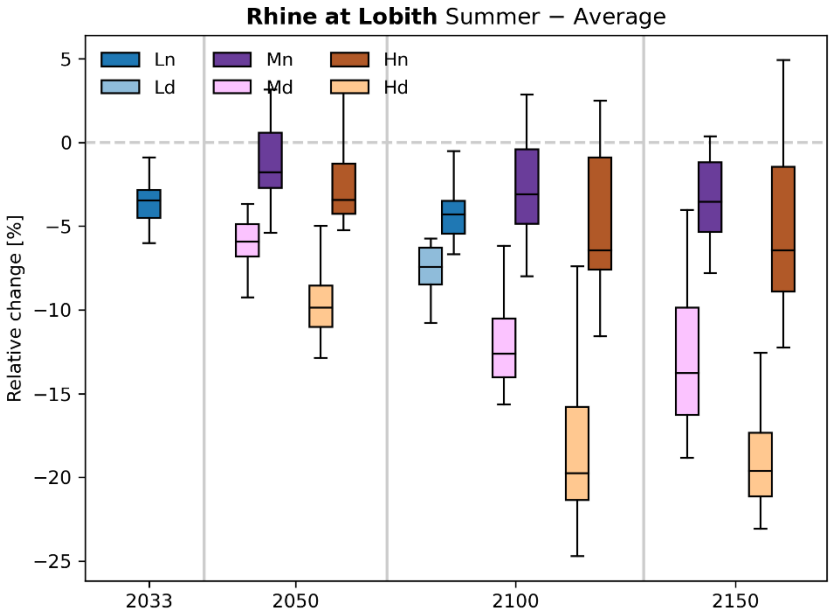

Figure 6-26: Change in average summer discharge at Lobith for the current (Ref = grey) and future climate (future time-horizons on the x-axis). Blue boxes present the low climate change scenarios (Ln = wet and Ld = dry), purple boxes present the moderate scenarios (Mn = wet and Md = dry) and brown boxes present the high scenarios (Hn = wet and Hd = dry).

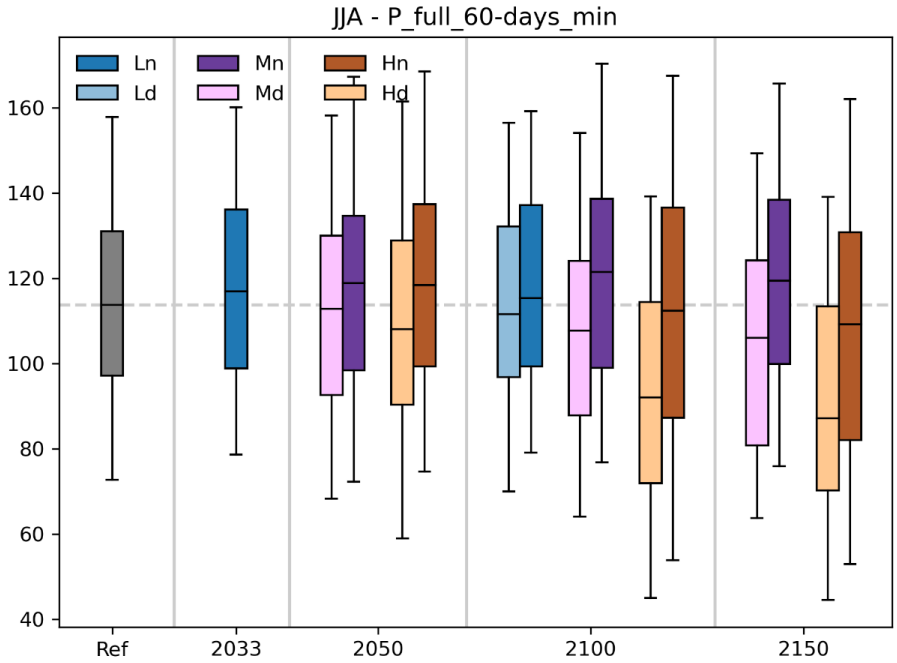

Figure 6-27: Change in minimum 60-day precipitation during the summer months (JJA) over the Rhine basin for the current (Ref = grey) and future climate (future time-horizons on the x-axis). Blue boxes present the low climate change scenarios (Ln = wet and Ld = dry), purple boxes present the moderate scenarios (Mn = wet and Md = dry) and brown boxes present the high scenarios (Hn = wet and Hd = dry).

The winter discharge (Figure 6-28), on the other hand, will likely increase towards the end of the century with increases up to ~40% according to the Hn scenario. By 2050, when the temperature increases are only moderate, changes in average winter discharge are still small.

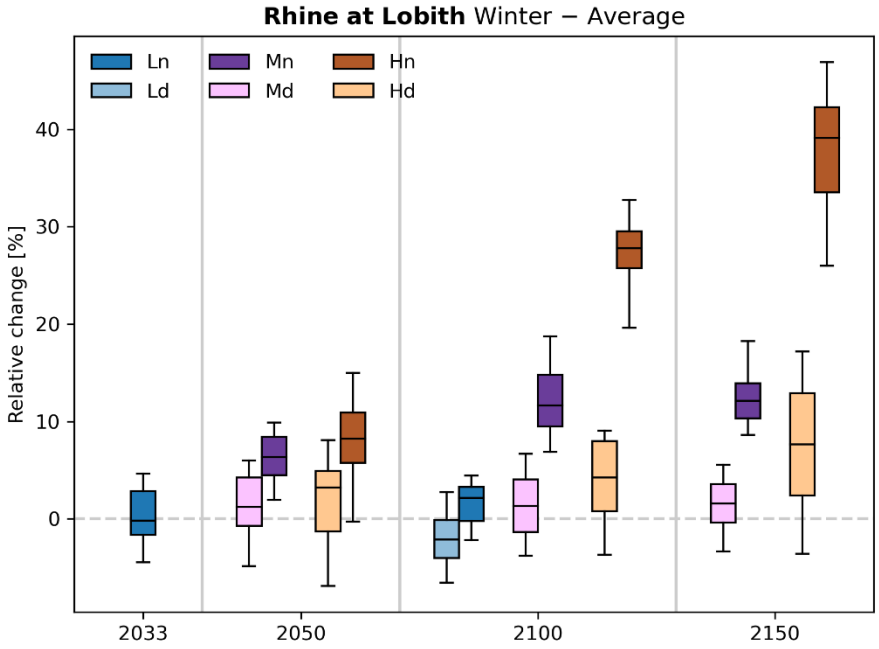

Figure 6-28: Change in average winter discharge at Lobith for the current (Ref = grey) and future climate (future time-horizons on the x-axis). Blue boxes present the low climate change scenarios (Ln = wet and Ld = dry), purple boxes present the moderate scenario (Mn = wet and Md = dry) and brown boxes present the high scenario (Hn = wet and Hd = dry).

The signal for change in *annual maximum discharge* is rather consistently projected (Figure 6-29). Nearly all scenarios, except for the dry variant of the L scenario by 2100, project increases in the long-term average annual maximum discharge. The statistics in discharge extremes will be presented in a second report in 2024.

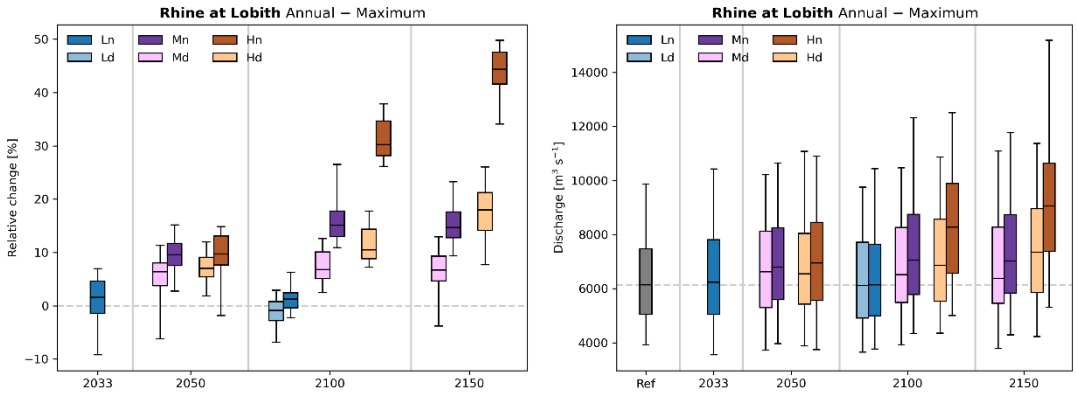

Figure 6-29: Change in annual maximum discharge at Lobith for the current (Ref = grey) and future climate (future time-horizons on the x-axis). Left panel shows the relative changes, right panel the absolute values. Blue boxes present the low climate change scenarios (Ln = wet and Ld = dry), purple boxes present the moderate scenarios (Mn = wet and Md = dry) and brown boxes present the high scenarios (Hn = wet and Hd = dry).

The 10-day winter precipitation sum over the Rhine basin is highly correlated to the annual maximum discharge at Lobith (van Pelt et al., 2012). Figure 6-30 shows that indeed the increase in annual maxima is in line with the increases in 10-day precipitation sums we see throughout the Rhine basin.

By 2150 these increases reach ~15 mm throughout the basin (see Fig. 6-30). For the moderate scenario and Low scenario, the increase in maximum 10-day precipitation sums is much lower and so is the increase in annual maximum discharge (Figure 6-29).

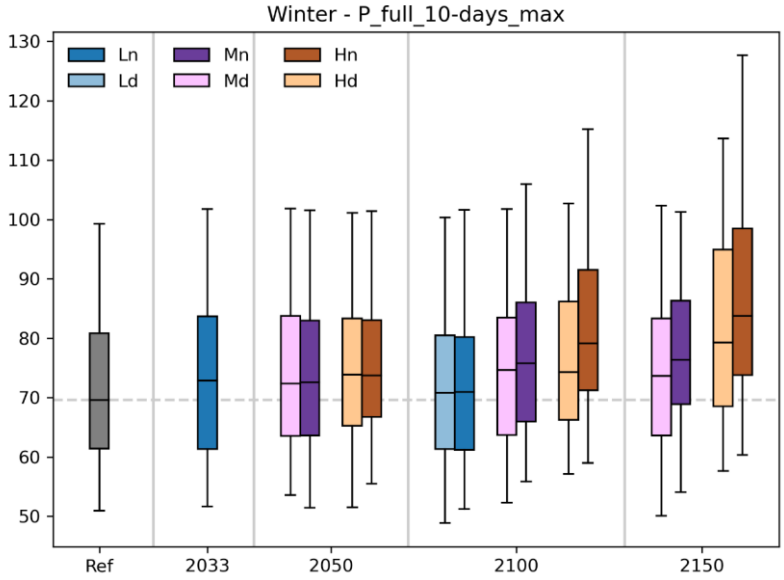

Figure 6-30: Change in maximum 10-day winter precipitation sum over the Rhine basin for the current (Ref = grey) and future climate (future time-horizons on the x-axis). Blue boxes present the low climate change scenarios (Ln = wet and Ld = dry), purple boxes present the moderate scenarios (Mn = wet and Md = dry) and brown boxes present the high scenarios (Hn = wet and Hd = dry).

The *7-day minimum discharge* at Lobith is consistently projected to decrease (see Figure 6-31), with decreases of 20% by 2050 and nearly 35% by 2150 according to Hd. This is in line with the recent study of Stahl et al. (2022) where they concluded that reduced snow accumulation will reduce river discharge in spring and early summer and retreating glaciers will lead to a reduction of late summer discharge of the Rhine.

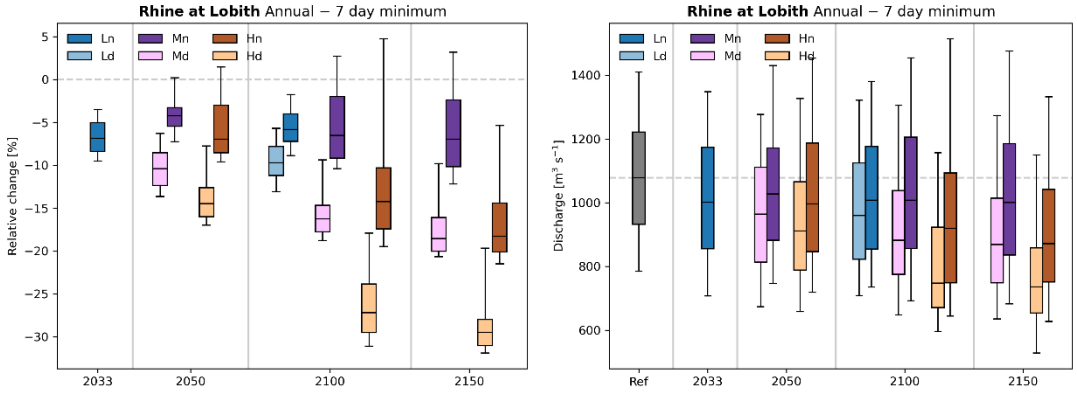

Figure 6-31: Change in annual 7-day minimum discharge at Lobith for the current (Ref = grey) and future climate (future time-horizons on the x-axis). Left panel shows the relative changes, right panel the absolute values. Blue boxes present the low climate change scenarios (Ln = wet and Ld = dry), purple boxes present the moderate scenarios (Mn = wet and Md = dry) and brown boxes present the high scenarios (Hn = wet and Hd = dry).

To summarise, the different climate scenarios project the following impacts for the Rhine basin:

- A decrease in *annual average discharge* according to the majority of scenarios for all time horizons. Only the Mn and Hn scenarios project an increase in average discharge. On average all scenarios except Mn and Hn project a decrease of about 5% (for all time horizons). Scenario Hn projects an increase of ~15% for 2100.

- All scenarios except the low scenarios project an increase in *annual maximum discharge* values at Lobith. For 2100, the changes range from an increase of ~5% (Md) to an increase of 25% (Hn). The three L scenarios project little change.

- The *7-day minimum discharge* is projected to decrease by all scenarios. Even in the low emission scenarios, we see a decrease of almost 10%. The Hd scenario projects the strongest decrease at 2100 of about 30%.

These changes are largely driven by the strong increases in temperature (especially in the 2150Hn scenario, where we see increases up to 5 degrees). This results in substantially less snowfall in the Alpine basins. In the lower elevated regions, snow accumulation will seldomly occur. This effect results in a reduction of snow melt driver discharge peaks. Furthermore, this absence of melt water combined with increases in evaporation, causes late summer discharges to strongly decrease.

7 Results: Comparison KNMI'23 with KNMI'14

This chapter addresses the comparison of the new discharge projections for the Rhine and Meuse derived from the KNMI'23 scenarios with the existing projections based on the KNMI'14 scenarios that were reported in Deltares (2015). The main aim of this comparison is to evaluate whether the KNMI'23 provide new insights in future discharge changes that may also influence choices and strategies for water management.

The data and modelling chains for KNMI'14 and KNMI'23 are not fully consistent. The future time-horizons considered for KNMI'23 differ from those considered for KNMI'14. The KNMI'23 scenarios focus on the future horizons 2050, 2100 and 2150, for KNMI'14 this was 2050 and 2085. Furthermore, the reference periods that represent the historical conditions are not the same. For KNMI'23 this is 1991-2020, whereas for KNMI'14 it used to be 1961-1995. As a result, only the trends in the projections can be compared.

It should be noted that (as also explained in section 4.3) an extra dry scenario (WHdry) was added to the KNMI'14 scenarios set to provide the full spread. This scenario projected quite large decreases in average and minimum discharge (Deltares, 2015; Hegnauer, 2020).

Differences between the KNMI'23 and KNMI'14 projections can originate from any of the components changed in the experiment setup (listed in Table 5-1). Both setups are based on the best available knowledge, models, and methods at the time of writing[1].

7.1 Comparison for the Meuse

The dry scenario variants of the KNMI'23 scenarios consistently project decreases throughout time (Figure 7-1), whereas it used to be only the driest scenario of the KNMI'14 set projecting decreases in average discharge. After 2050, the projected changes in average discharge for the Meuse vary more for the KNMI'23 scenarios than for the KNMI'14 scenarios. Additionally, the spread in average discharge changes is smaller in the KNMI'23 scenarios in 2050.

For the change in maximum discharge (Figure 7-2) all KNMI'14 scenarios projected increases throughout time. For the KNMI'23 scenarios the dry scenarios tend to project decreases and the wet scenarios increases. The maximum projected increase for KNMI'14 for 2085 is similar to the maximum projected increase for KNMI'23 for 2100. By 2150 the KNMI'23 Hn scenario projects a higher increase, up to more than 30%. The bandwidth of changes from the KNMI'23 scenarios for 2150 is larger, because the climate change signal is stronger and by then there is more variation between the emission scenarios.

[1] No sensitivity analysis was performed to assign the differences to specific components.

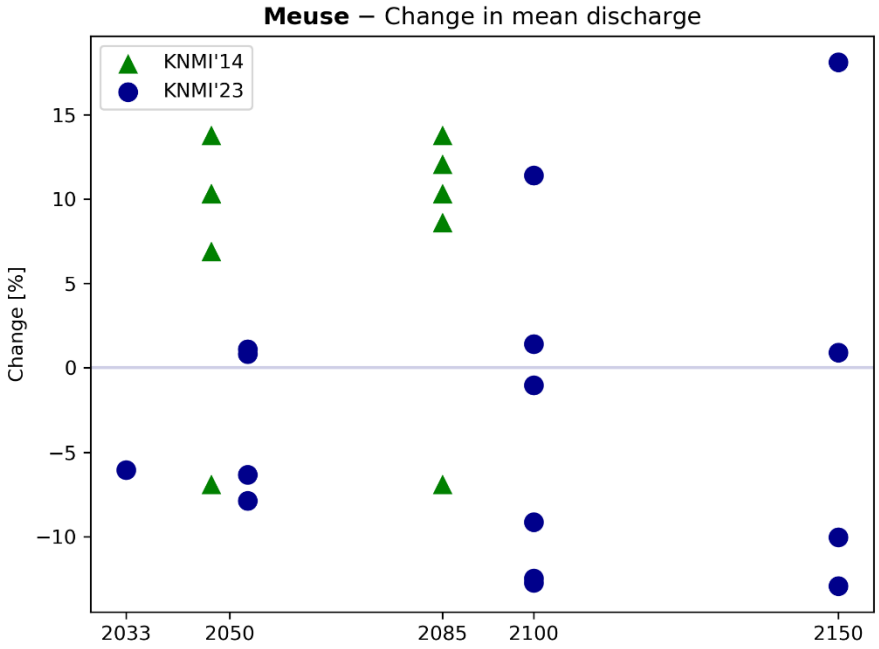

Figure 7-1: Projected changes (%) in average discharge for the Meuse at the Dutch border according to the KNMI'14 scenarios (green) and KNMI'23 scenarios (blue) for the time horizons of interest.

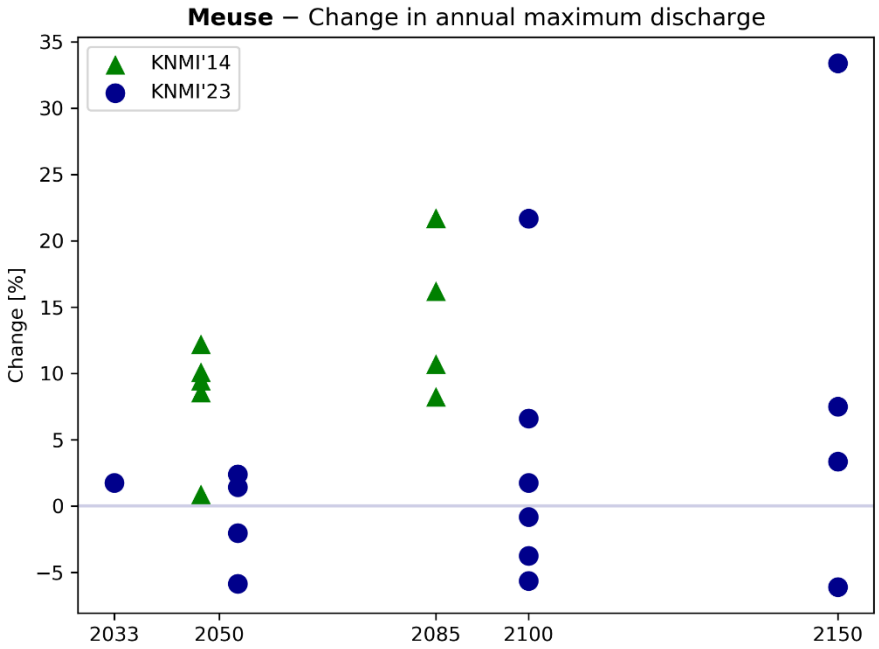

Figure 7-2: Projected changes (%) in annual maximum discharge for the Meuse according to the KNMI'14 scenarios (green) and KNMI'23 scenarios (blue) for the time horizons of interest.

Both the KNMI’14 and the KNMI’23 scenarios project decreases in 7-day minimum discharge (Figure 7-3). According to the driest KNMI’23 scenarios the decrease will not become more than 30%, even by 2150. The KNMI’14 scenarios on the other hand already projected decreases of more than 40% by 2050 and decreases of more than 50% by 2085. The spread between the climate scenarios is smaller for the KNMI’23 projections than for the KNMI’14 projections.

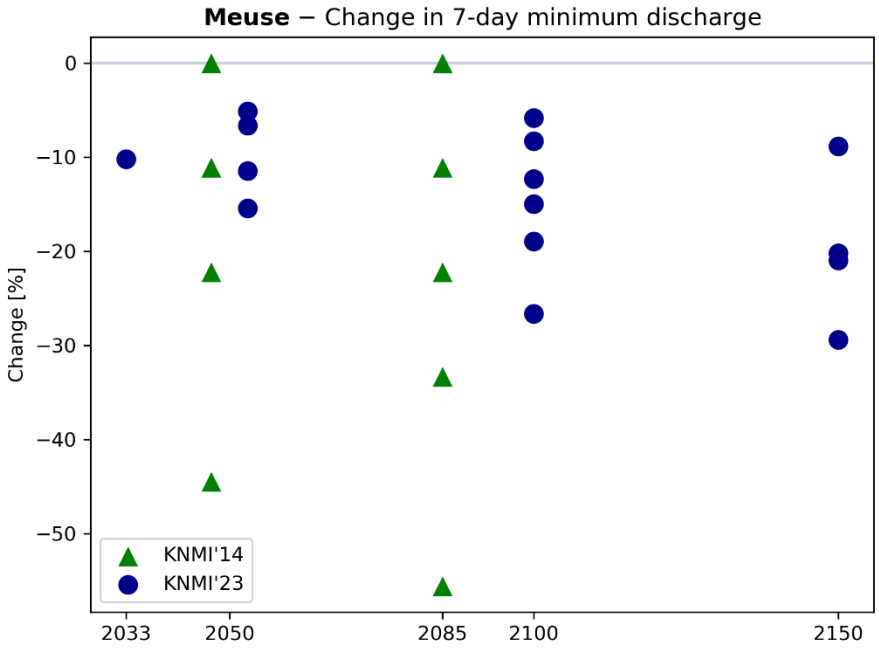

Figure 7-3: Projected changes (%) in 7-day minimum discharge for the Meuse according to the KNMI’14 scenarios (green) and KNMI’23 scenarios (blue) for the time horizons of interest.

See Annex D for the figures containing the same data, but also showing the climate scenario corresponding to each value.

The results of the comparison between the discharge projections based on the KNMI’23 and KNMI’14 scenarios for the Meuse are summarized below:

- The average annual discharge can increase or decrease depending on the climate scenario chosen. The KNMI’23 projects in general larger decreases in annual discharges for the Meuse than the KNMI’14 scenarios.
- According to all KNMI’14 projections the maximum annual discharge will increase. In the KNMI’23 projections there is more variation.
- KNMI’23 projects in general smaller maximum discharge increases for the Meuse than KNMI’14, suggesting that high discharges may increase less in the near future for the Meuse.
- The 7-day minimum annual discharge decreases for all scenarios in the KNMI’23 and KNMI’14 projections. KNMI’23, however, projects smaller decreases. Future droughts for the Meuse may thus be less severe according to the new scenarios than they were according to the KNMI’14 scenarios.
- The projected increase of annual maximum discharge for the Meuse by 2150 is substantially higher (+33%) than the projections of the KNMI’14 scenarios for 2085 (+22%) indicating a continuous increase.

7.2 Comparison for the Rhine

Figure 7-4 displays the comparison of the projections for annual average discharge for the Rhine for the KNMI'14 and KNMI'23 scenario sets. The projections presented in the graph are the median of the projected changes for a given scenario for a specific time-horizon. The figure shows that by 2050 the spreading between the different scenarios was bigger for the KNMI'14 scenarios. Also, the wettest KNMI'14 scenarios suggested a larger increase. When the projections for 2085 and 2100 are compared we see a similar range of projections for KNMI'14 and KNMI'23, although the wet scenarios of the KNMI'14 set projects the largest increases up to nearly 20%. The range of projected changes obtained for the KNMI'23 scenarios for 2150 are rather comparable to the KNMI'14 range of projections for 2085, although they are projected for a further time horizon.

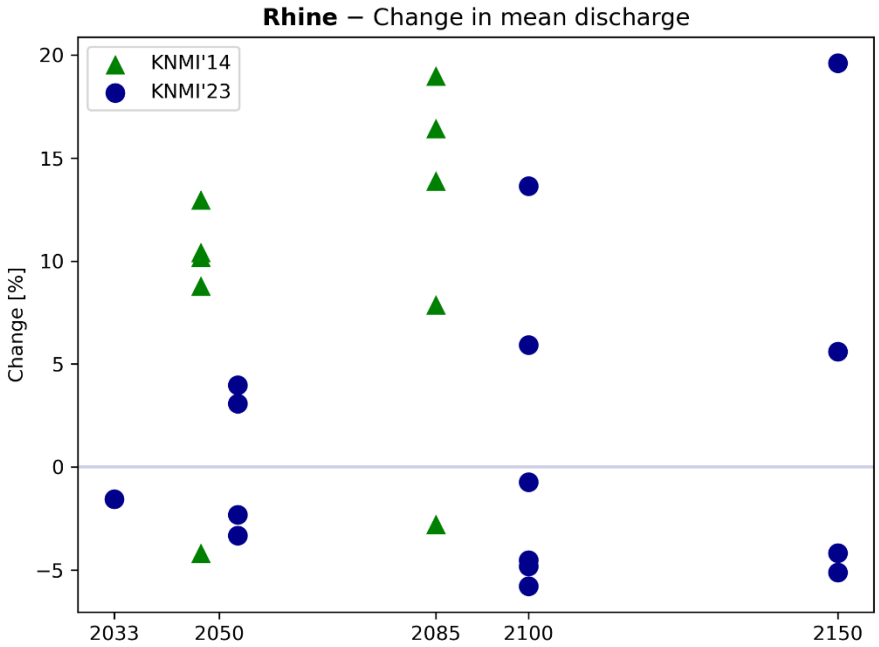

Figure 7-4: Projected changes (%) in annual average discharge for the Rhine at Lobith according to the KNMI'14 scenarios (green) and KNMI'23 scenarios (blue) for the time horizons of interest.

Figure 7-5 presents the projections for average annual maximum discharge. Again, the maximum projections of the KNMI'14 scenarios by 2085 are comparable with the maximum KNMI'23 scenarios by 2150. The KNMI'23 projections for 2100 are lower. Large increases seem to be reached later for the KNMI'23 projections, suggesting possibly more time for climate adaptation but this is to be further explored in follow-up impact assessments.

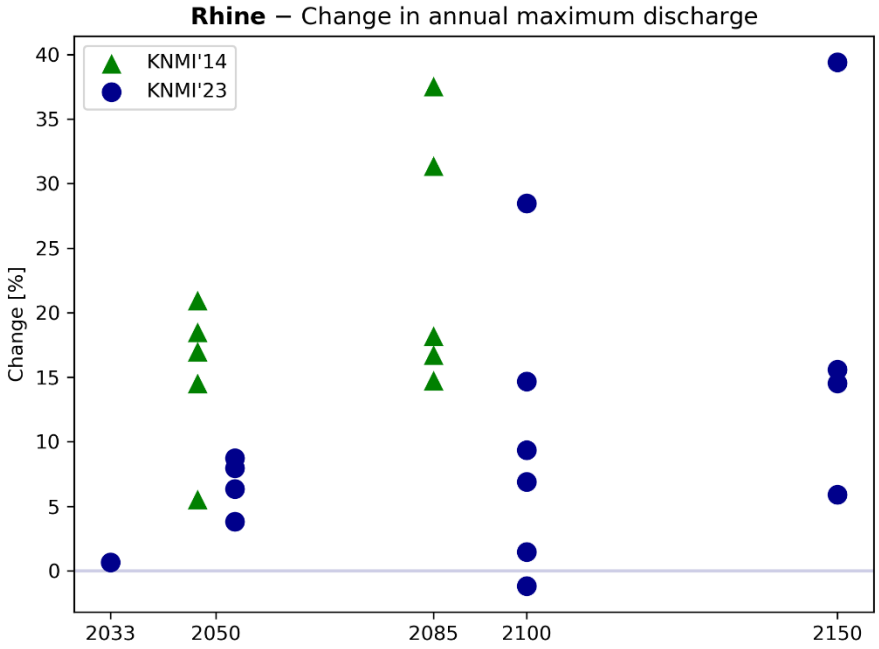

Figure 7-5: Projected changes (%) in annual maximum discharge for the Rhine at Lobith according to the KNMI'14 scenarios (green) and KNMI'23 scenarios (blue) for the time horizons of interest.

The main difference between the KNMI'14 and KNMI'23 projections for 7-day minimum discharge is that a few KNMI'14 scenarios projected increases whereas all KNMI'23 scenarios project decreases (Figure 7-6). We can be more confident that low discharges will become even lower in the future.

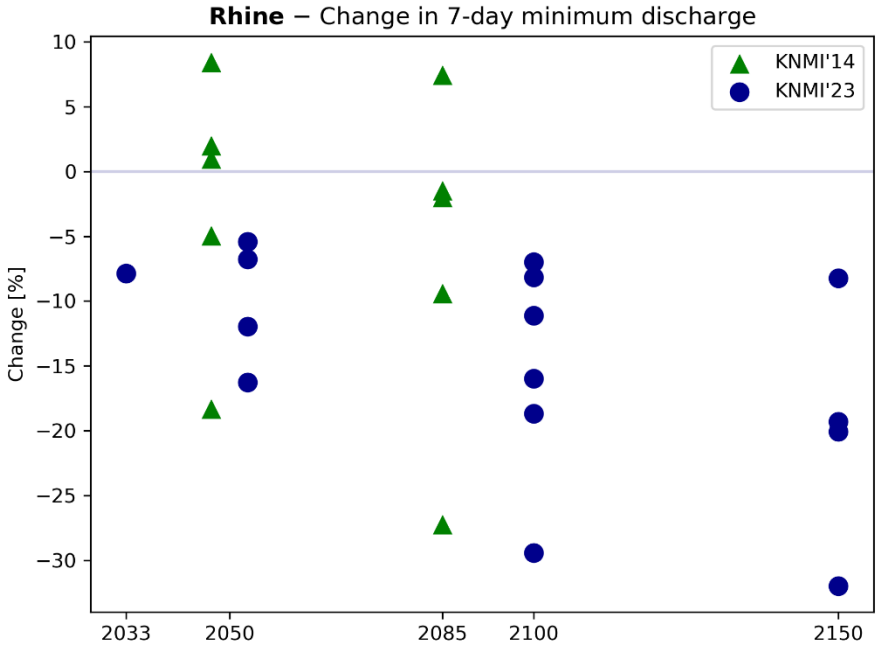

Figure 7-6: Projected changes (%) in minimum 7-day discharge for the Rhine at Lobith according to the KNMI'14 scenarios (green) and KNMI'23 scenarios (blue) for the time horizons of interest.

The comparison between the discharge projections based on the KNMI'23 and KNMI'14 scenarios for the Rhine shows in summary the following:

- For both the KNMI'14 and KNMI'23 scenarios there is no clear change signal in *annual average discharge* for the Rhine.

- The *maximum annual discharge* increases in the KNMI'14 and KNMI'23 projections. The KNMI'23 projections show an increase in maximum discharge for 2150 similar to the KNMI'14 projections for 2085. The KNMI'23 scenarios, therefore, suggest that there is more time for adaptation for high discharges in the Rhine than projected in KNMI'14.

- The *7-day minimum annual discharge* decreases for all scenarios in the KNMI'23 projections in contrast to the KNMI'14 projections. The largest decrease in 7-day minimum annual discharge is additionally larger for KNMI'23 than for the KNMI'14 projections for all projected years. These results suggest that the Rhine will experience more droughts in the near future according to the KNMI'23 projections in comparison to the KNMI'14 projections.

8 Conclusions

In this study we assessed the implications of the KNMI'23 scenarios for the discharges of the river Rhine at Lobith and Meuse the Meuse at the Dutch border. Fifteen new discharge projections have been created by use of the wflow_sbm hydrological model.

Scenario discharge time-series
An ensemble of 8 time-series of 30 years was created for the reference period (1991-2020) and for each future climate scenario. The discharge projections have been analyzed and compared with the existing projections based on the KNMI'14 scenarios.

For the reference period the simulated discharges for the Rhine deviate substantially from observed discharges for average and low flow conditions. Therefore, the simulated discharge time-series for the Rhine have been bias-corrected. For the Meuse, the difference between simulated and observed discharge was much smaller and no correction was required here. Therefore, we only provide the uncorrected time-series for the Meuse.

Overall, future discharges of the rivers Rhine and Meuse will likely increase in winter and spring and decrease in (late) summer. This is in line with the results of existing climate impact studies for the Rhine and the Meuse. Although, especially for the later time-horizons, the spread between the scenarios has decreased.

Additionally, the comparison of the discharge projections based on KNMI'23 scenarios with those based on KNMI'14 scenarios, shows that the direction of projected changes in general remain similar, however the magnitudes change. In the next sections we summarize the main results for the two rivers.

User instructions for the discharge time-series

For additional analysis related to water management and climate adaptation *in the Netherlands* we recommend the user to use the bias-corrected time-series. The bias-corrected time-series are only provided for Lobith, because the bias is relatively large here and because applying the bias-correction for multiple locations along the Rhine introduces deviations in the water balance of the river.

For users with an interest *in the full Rhine basin* we recommend using the uncorrected time-series. Also, depending on the research interest, for research purposes the uncorrected time-series may be preferred. Especially when there is mainly an interest in relative changes.

8.1 Meuse

Discharge projections based on the KNMI'23 scenarios

- The *annual average discharge* of the Meuse is projected to decrease according to 4 out of 6 scenarios. The Mn scenario shows average discharge values that closely resemble the current conditions, while the Hn scenario projects an increase of about 10% by 2100.

- Most scenarios (4 out of 6) show little change in annual maximum. Only by 2100, Mn and Hn show an increase up to ~20%. After that the Hn scenario projects a further increase to 35% by 2150.

- All scenarios project a decrease of the 7-day minimum discharge. By 2100 and 2150, the most severe decrease is projected by the Hd scenario (~-30%).

- The direction of change for the winter discharge of the Meuse is very uncertain. Although, the 2 wettest scenarios, project large increases (up to ~30%).
- Additionally, all scenarios show a decrease of discharge during the summer, which is driven by increases in evaporation.

Comparison KNMI'14 vs KNMI'23

- For the Meuse the largest projected reduction in *minimum 7-day discharge* is smaller in the KNMI'23 scenarios than what was envisaged by the KNMI'14 scenarios (-30% vs -50%). Future droughts for the Meuse may thus be less severe according to the new scenarios than they were according to the KNMI'14 scenarios.

- For the Meuse most dry scenario variants of the KNMI'23 scenarios project decreases in *annual maximum discharge,* whereas the KNMI'14 scenarios projected only increases.

- The projected increase of *annual maximum discharge* for the Meuse by 2150 is substantially higher (+33%) than the projections of the KNMI'14 scenarios for 2085 (+22%) indicating a further increase over time.

8.2 Rhine

Discharge projections based on the KNMI'23 scenarios

- For *annual average discharge* no substantial change is projected. On average all scenarios, except Mn and Hn, project a decrease of about 5% (for all time horizons).

- 4 out of 6 scenarios project an increase in *annual maximum discharge* values at Lobith. For 2100, the changes range from an increase of ~5% (Md) to an increase of 25% (Hn). The three L scenarios project little change.

- The *7-day minimum discharge* is projected to decrease by all scenarios. Even in the low scenarios, we see a decrease of almost 10% in 2100. The Hd scenario projects the strongest decrease in 2100 of about 30%.

These changes are largely driven by the strong increases in temperature (especially in the 2150Hn scenario, where we see increases up to 5 degrees), driving snow and evaporation. According to the hydrological model, this results in substantially less snowfall and accumulation in the Alpine basins. In the lower elevated regions, snow accumulation will seldomly occur. This effect results in a reduction of snow melt driver discharge peaks. Furthermore, this absence of melt water combined with increases in evaporation, causes strong reduction of late summer discharges.

Comparison KNMI'14 vs KNMI'23

- The KNMI'23 scenarios for 2150 for the Rhine are rather similar to the KNMI'14 projections for the Rhine for 2085 for *annual average discharge*. In both scenarios sets the direction of change is uncertain.

- KNMI'14 and KNMI'23 project increases for *annual maximum discharge*. Again, the KNMI'14 projections for 2085 are quite similar to the projections based on the KNMI'23 scenarios for 2150.

- For 2100 the KNMI'23 projected changes in annual maximum discharge are smaller than the KNMI'14 projected changes for 2085, which suggests that there may be more time for adaptation to high discharges in the Rhine than projected by KNMI'14.

- Finally, there is even more confidence in the projected decreases of low flows with the KNMI'23 scenarios. All KNMI'23 scenarios project decreases in the *7-day minimum discharge*, whereas for the KNMI'14 scenarios there were still a few scenarios suggesting increases in 7-day minimum discharge.

9 References

Bergström, S. (1992) The HBV-Model—Its Structure and Applications. SMHI Reports RH No. 4, Norrköping.

Bouaziz, L.J.E. (2021) Internal processes in hydrological models: A glance at the Meuse basin from space. PhD Thesis TU Delft.

Cannon, A.J., Sobie, S.R. and Murdock, T.Q., 2015. Bias correction of GCM precipitation by quantile mapping: how well do methods preserve changes in quantiles and extremes? Journal of Climate, 28(17), pp.6938-6959.

de Boer-Euser, T. (2017). Added value of distribution in rainfall-runoff models for the Meuse basin. Dissertation Delft University of Technology

Deltares (2015). Implications of the KNMI'14 climate scenarios for the discharge of the Rhine and Meuse; comparison with earlier scenario studies. Authors: F. Sperna Weiland, M. Hegnauer, L. Bouaziz, J.J. Beersma.

Deltares (2020). Evaluation of hydrological models of the Meuse river basin, 11205237-002-ZWS-0009, 30 November 2020, author: L. Bouaziz.

Deltares (2021). Developments 2021 Wflow Julia Meuse and Rhine basins, 11205237, November 2021, author: Laurene Bouaziz.

Deltares (2022). Developments of the wflow Meuse and Rhine hydrological models in 2022, 11208037, December 2022, authors: L. Bouaziz and J. Buitink

Deltares (2023). Memo: Kennisontwikkeling Hydrologische modellen Rijn en Maas. Floodplain 1d, 11209265, March 2023, authors: J. Buitink and L. Bouaziz

Döscher, R. et al. (2022). The EC-Earth3 Earth system model for the Coupled Model Intercomparison Project 6, Geoscientific Model Development 15.7, pp. 2973–3020. doi:

10.5194/gmd-15-2973-2022

Eilander, D., Boisgontier, H., van Verseveld, W., Bouaziz, L., and Hegnauer, M.: hydroMT-wflow (v0.1.4), Zenodo, https://doi.org/10.5281/zenodo.6221375, 2022.

Eilander, D., and Boisgontier, H.: hydroMT (v0.4.5), Zenodo, https://doi.org/10.5281/zenodo.610766, 2022

Eyring, V., Bony, S., Meehl, G. A., Senior, C. A., Stevens, B., Stouffer, R. J., and Taylor, K. E.: Overview of the Coupled Model Intercomparison Project Phase 6 (CMIP6) experimental design and organization, Geosci. Model Dev., 9, 1937-1958, doi:10.5194/gmd-9-1937-2016, 2016.

Gupta, H.V., Kling, H., Yilmaz, K.K. and G.F. Martinez (2009). Decomposition of the mean squared error and nse performance criteria: implications for improving hydrological modelling. J. Hydrol., 377 (1) (2009), pp. 80-91, 10.1016/j.jhydrol.2009.08.003

Heganuer, M. (2020). Statistiek extreme hoogwaters Rijn en Maas op basis van geschaalde KNMI'14 scenario's, Deltares report, 11205237-003-ZWS-0014.

Hersbach, H, Bell, B, Berrisford, P, et al. The ERA5 global reanalysis. Q J R Meteorol Soc. 2020; 146: 1999–2049. https://doi.org/10.1002/qj.3803

ICPR (2001), Atlas of flood danger and potential damage due to extreme floods of the Rhine, International Commission on the Protection of the Rhine, Koblenz, Germany, available at: http: //www.iksr.org/.

Keywan et al. (2017). "The Shared Socioeconomic Pathways and their energy, land use, and greenhouse gas emissions implications: An overview". Global Environmental Change. 42: 153–168.

KNMI (2023). KNMI National Climate Scenarios 2023 for the Netherlands R. van Dorland, J. Beersma, J. Bessembinder, N. Bloemendaal, H. van den Brink M. Brotons Blanes, S. Drijfhout, R. Groenland, R. Haarsma, C. Homan, I. Keizer, F. Krikken, D. Le Bars, G. Lenderink, E. van Meijgaard, J. F. Meirink, B. Overbeek, T. Reerink, F. Selten, C. Severijns, P. Siegmund, A. Sterl, C. de Valk, P. van Velthoven, H. de Vries, M. van Weele, B. Wichers Schreur, K. van der Wiel, Scientific report; WR-23-02.

Kwadijk, J.C.J. and J. Rotmans (1995). The impact of climate change on the river Rhine: a scenario study, Climatic Change, 30(4), 397-425.

Meijgaard, E. van et al. (2012). Refinement and application of a regional atmospheric model for climate scenario calculations of Western Europe. KvR 054/12, ISBN/EAN 978-90-8815-046-8435 3. also available at http://climexp.knmi.nl/publications/FinalReport KvR-CS06.pdf. Climate changes Spatial Planning.

Pinter, N., Van der Ploeg, R.R., Schweigert, P. and G. Hoefer (2006). Flood magnification on the river Rhine, Hydrol. Processes, 20, 147–164.

Razafimaharo, C., Krähenmann, S., Höpp, S. et al. New high-resolution gridded dataset of daily mean, minimum, and maximum temperature and relative humidity for Central Europe (HYRAS). Theor Appl Climatol 142, 1531–1553 (2020). https://doi.org/10.1007/s00704-020-03388-w

Ruiter, A. (2012) Delta-change approach for CMIP5 GCMs. De Bilt, 2012 | Trainee report,

Sperna Weiland, F.C., Visser, R.D., Greve, P., Bisselink, B., Brunner, L., and Weerts, A.H.: Estimating Regionalized Hydrological Impacts of Climate Change Over Europe by Performance-Based Weighting of CORDEX Projections, Frontiers of Water, 10.3389/frwa.2021.713537, 1035 2021

Stahl, K., Weiler, M., van Tiel, M., Kohn, I., Hänsler, A., Freudiger, D., Seibert, J., Gerlinger, K., Moretti, G. (2022): Impact of climate change on the rain, snow and glacier melt components of streamdischarge of the river Rhine and its tributaries. CHR report no. I 28. International Commission for the Hydrology of the Rhine basin (CHR), Lelystad.

Te Linde, A. H., Bubeck, P., Dekkers, J. E. C., de Moel, H., and Aerts, J. C. J. H. (2011). Future flood risk estimates along the river Rhine, Nat. Hazards Earth Syst. Sci., 11, 459-473, doi:10.5194/nhess-11-459-2011.

H. Van den Brink, Bepaling van de optimale referentie en de optimale subsets voor

de KNMI'23 klimaatscenario's, KNMI memo, Juli 2023.

E van Meijgaard, LH van Ulft, WJ van de Berg, FC Bosveld, BJJM van den Hurk, G Lenderink, AP Siebesma. The KNMI regional atmospheric climate model RACMO, version 2.1. KNMI number: TR-302, Year: 2008, Pages: 43

van Osnabrugge, B. (2020). Interpolate, simulate, assimilate: operational aspects of improving hydrological forecasts in the Rhine basin. Wageningen University. https://doi.org/10.18174/513157

van Pelt, S. C., Beersma, J. J., Buishand, T. A., van den Hurk, B. J. J. M., and Kabat, P.: Future changes in extreme precipitation in the Rhine basin based on global and regional climate model simulations, Hydrol. Earth Syst. Sci., 16, 4517–4530, https://doi.org/10.5194/hess-16-4517-2012, 2012.

Ward, P. J., Renssen, H., Aerts, J. C. J. H., van Balen, R. T., and Vandenberghe, J.: Strong increases in flood frequency and discharge of the River Meuse over the late Holocene: impacts of long-term anthropogenic land use change and climate variability, Hydrol. Earth Syst. Sci., 12, 159–175, https://doi.org/10.5194/hess-12-159-2008, 2008.

Zhao, T., Bennett, J.C., Wang, Q.J., Schepen, A., Wood, A.W., Robertson, D.E. and Ramos, M.H., 2017. How suitable is quantile mapping for postprocessing GCM precipitation forecasts?. Journal of Climate, 30(9), pp.3185-3196.

A Comparison between wflow_sbm and HBV

This Annex presents a comparison of main discharge statistics for the Rhine and Meuse calculated by the hydrological HBV and wflow_sbm models. Note: the figures are taken from existing reports that focused on the comparison of wflow_sbm with HBV for the Rhine and Meuse river basins. More details can be found in the reports from Deltares (2022, 2023). In these studies, several routing schemes were compared. The 1d floodplain routing (fld1d) performed best and the remainder of this Annex focusses on the comparison between “fld1d” and “HBV”, see Figure A-1.

For the Rhine, only the discharge series at Lobith and Kaub are considered, as they are the two most relevant stations where the comparison between HBV and wflow_sbm was performed.

For the Meuse, the results for the Dutch border, Chooz, and Chaudfontaine are shown.

A.1 Rhine

The annual discharge regime derived from the wflow_sbm simulations is closer to the observed regime than the HBV based discharge regime (see Figure A1). Discharges simulated with HBV are overall too low. Although, it should be noted that both the HBV and wflow_sbm models are not performing really well for the Rhine.

The performance for annual maxima values is comparable between HBV and wflow_sbm.

The exceedance probability curves obtained from wfow_sbm are closer to the observed curves than the once based on HBV simulations. This is especially the case for logQ which can be considered a better representation of low flows.

The wflow_sbm model slightly outperforms HBV when evaluating the 7-day minimum discharge values. HBV tends to underestimate the low discharges especially for higher return periods.

Highest values for the performance measures NSE, NSElog and KGE are obtained with wflow_sbm. For Kaub the differences in performances are even more pronounced than for Lobith (Figure A-2).

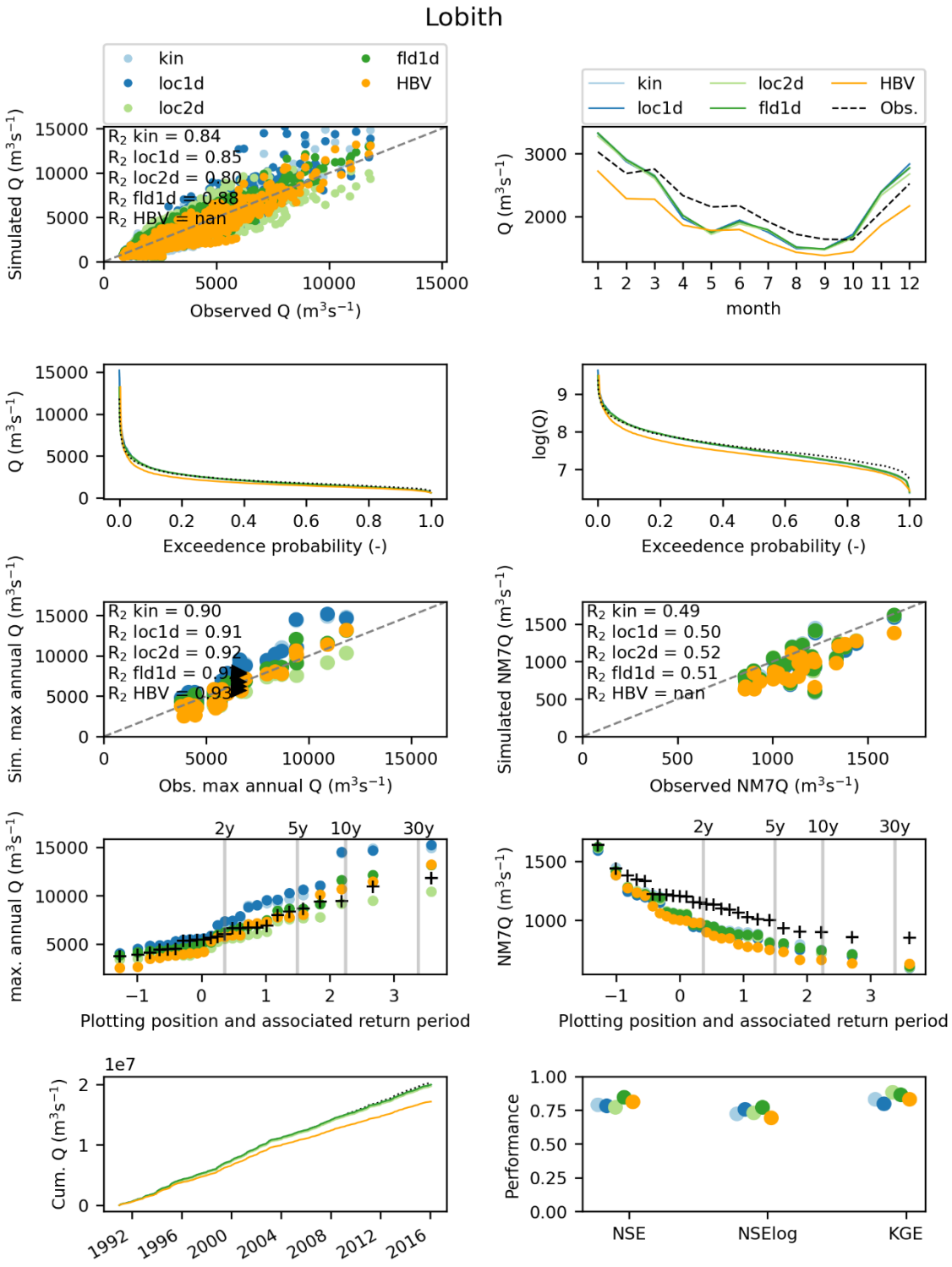

Figure A-1: Hydrological signatures for the Rhine at Lobith. Several different versions of wflow_sbm are compared with HBV (orange); the "fld1d" version (dark green) matches with the version used in this report. The other runs are there for comparison and can be ignored.

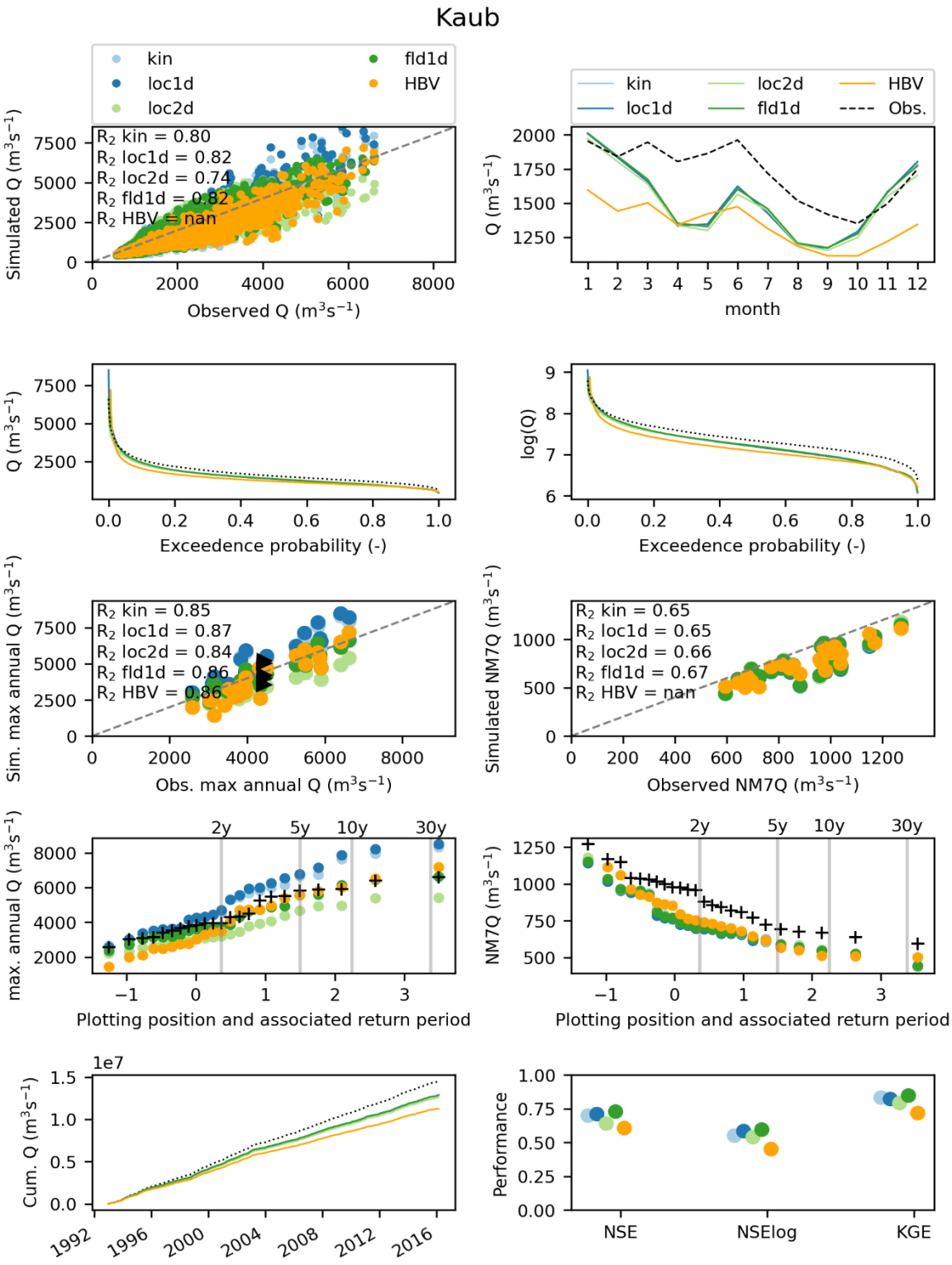

Figure A 2: Hydrological signatures for the Rhine at Kaub. Several different versions of wflow_sbm are compared with HBV (orange); the "fld1d" version (dark green) matches with the version used in this report. The other runs are there for comparison and can be ignored.

A.2 Meuse

The annual discharge regime for the Meuse derived from the wflow_sbm is comparably close to the observed regime as the HBV based discharge regime at the Dutch border (Figure A-3).

The performance for annual maxima values is comparable between HBV and wflow_sbm.

The wflow_sbm model mainly outperforms the HBV model for the simulation of low flows and low flow statistics (NSElogQ, logQ and 7-day minimum). Low flows are underestimated by HBV. At Chooz this is even more clear. In addition, for Chooz all performance measures are higher for wflow_sbm than for HBV (Figure A-4).

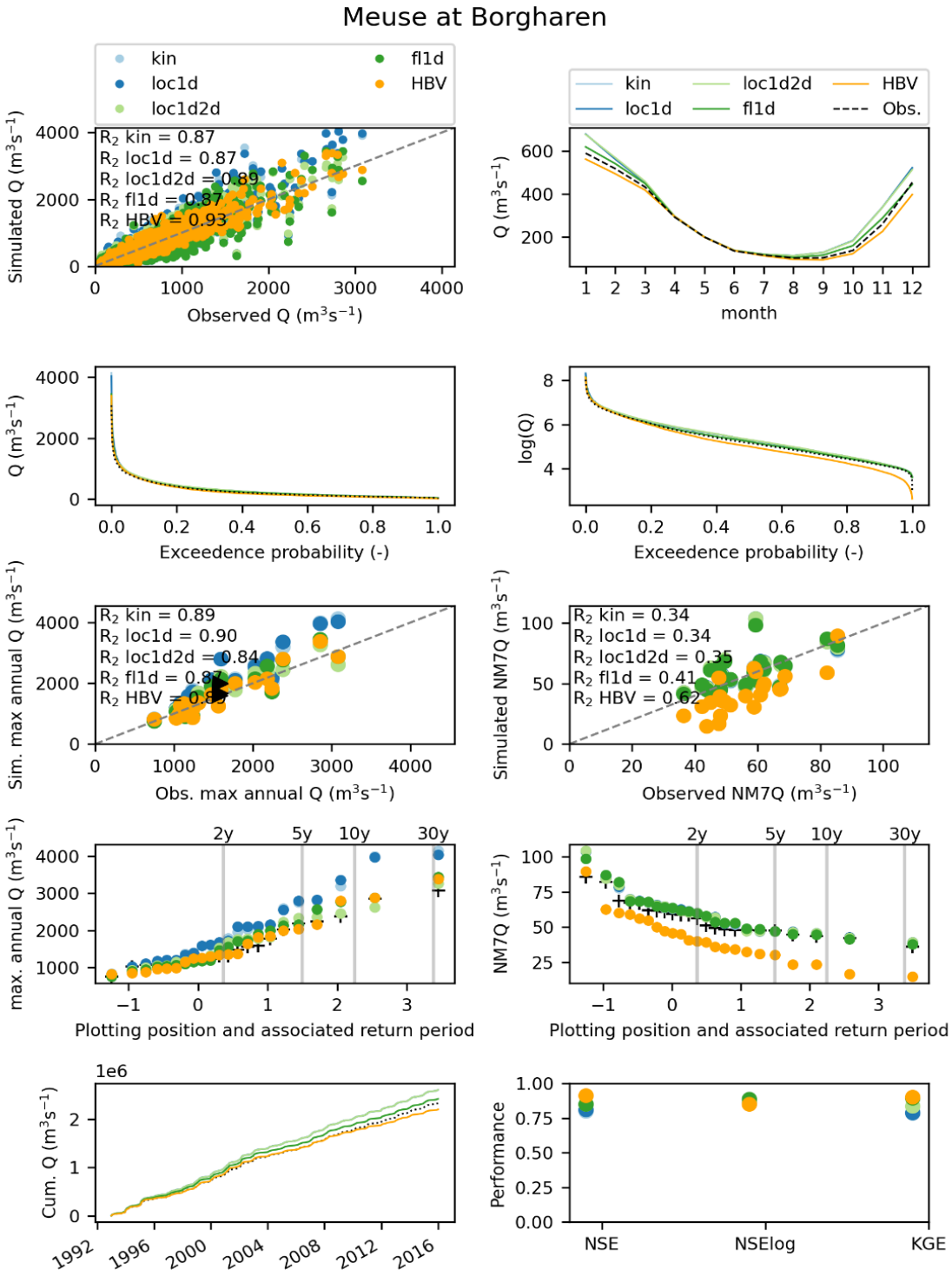

Figure A 3: Hydrological signatures for the Meuse at the Dutch border. Several different versions of wflow_sbm are compared with HBV (orange); the "fld1d" version (dark green) matches with the version used in this report. The other runs are there for comparison and can be ignored.

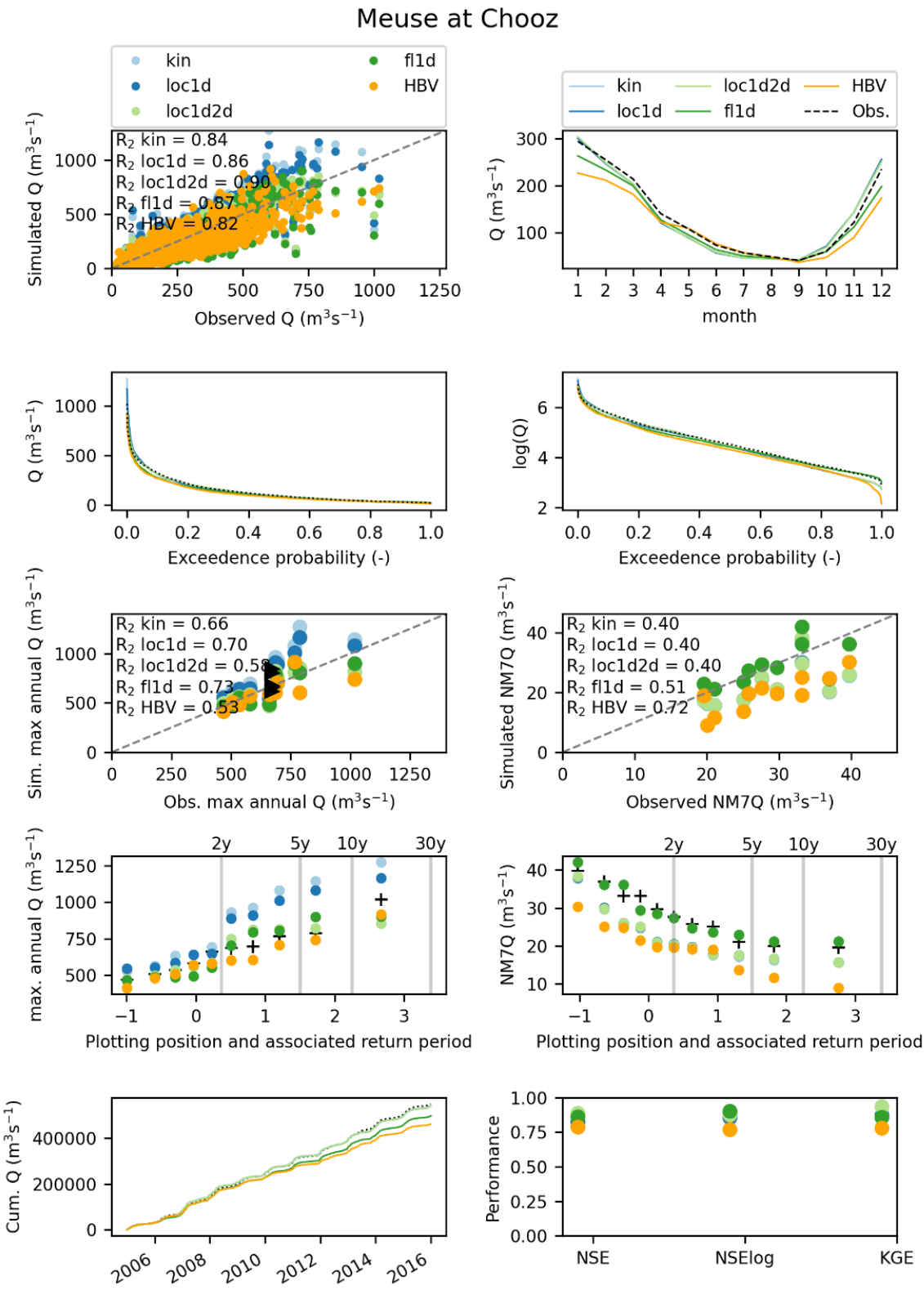

Figure A 4: Hydrological signatures for the Meuse at Chooz. Several different versions of wflow_sbm are compared with HBV (orange); the "fld1d" version (dark green) matches with the version used in this report. The other runs are there for comparison and can be ignored.

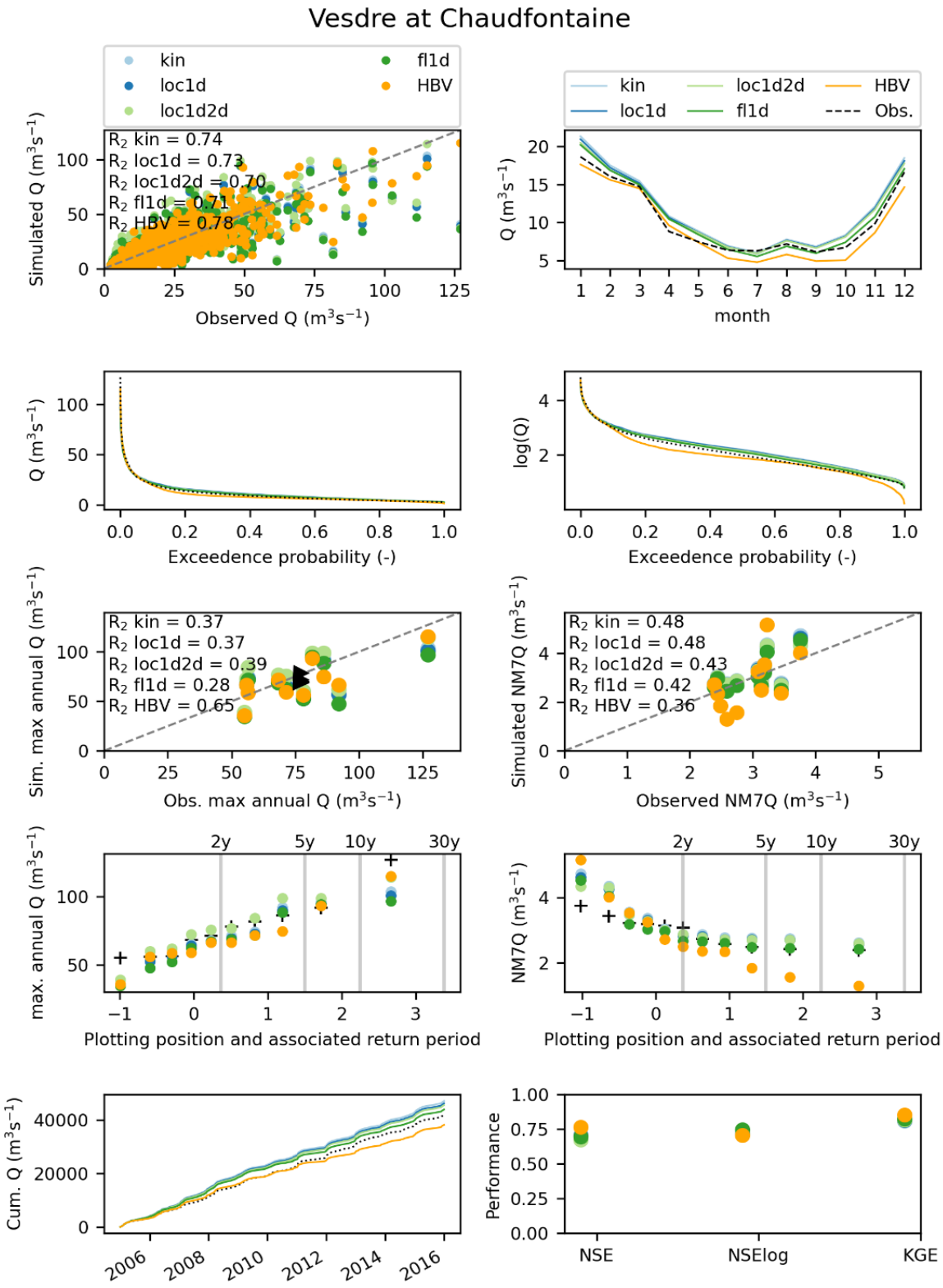

Figure A 5: Hydrological signatures for the Vesdre at Chaudfontaine. Several different versions of wflow_sbm are compared with HBV (orange); the "fld1d" version (dark green) matches with the version used in this report. The other runs are there for comparison and can be ignored.

B Evaluation the need for discharge bias-correction for the Meuse

The statistics of the simulated discharge using the reference climate scenario closely matches the observed discharge values, as can be seen in Figure B1. For the Meuse there are also less reasons to expect biases. The wflow_sbm model for the Meuse has been calibrated with potential evaporation calculated with the Makkink's equation the same equation that is used for the climate datasets by KNMI. Moreover, in the Meuse catchment biases in precipitation are much smaller than the precipitation biases over the Alps.

To confirm that bias-correction is not needed for the Meuse, we also performed the discharge bias-correction here but obtained only minor gains in accuracy. While at the same time the correction introduces noise. The difference in 7-day minimum discharge around 40 m^3/s is notable. Here we see the discharge bias-correction switching from increasing the discharge values to decreasing the discharge values. This causes an additional signal in the simulated discharge values that is unwanted. Therefore, it was decided not to perform a discharge bias-correction for the Meuse.

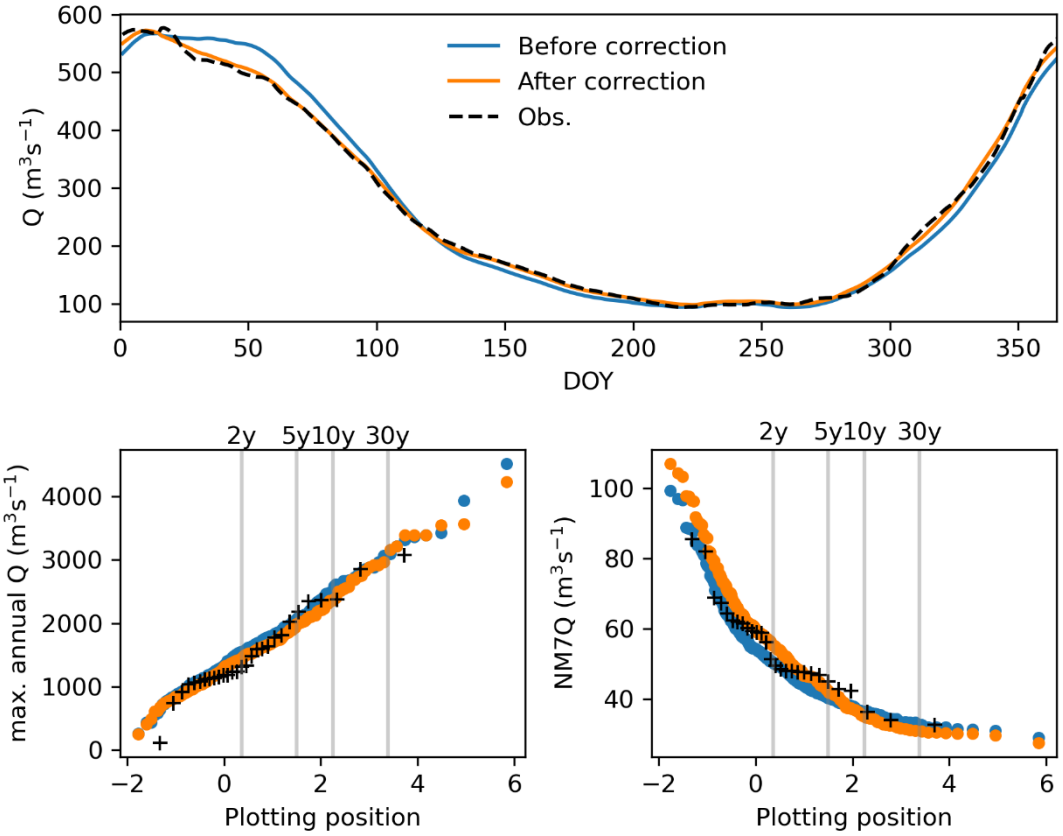

Figure B 1: Comparing the simulated discharge of the reference climate with the observed values (black) for the Meuse at the Dutch border, including the return periods of the annual maxima and the 7-day minima discharges for the non-corrected (blue) and corrected (orange) simulations.

C The influence of bias-correction on the climate change signal and time-series

C.1 The influence of bias-correction on the climate change signal

In this Annex the influence of the bias-correction of the climate simulations on the climate change signal is evaluated. Cannon et al. (2015) reported that quantile mapping can affect trends in extreme quantiles differently than trends in the average. As a consequence, the correction introduces a different shift in simulated discharges for the current and future climate. This will also lead to a slightly altered change signal which will be most notable in the tails of the distribution, i.e., the high and low discharge values. In the figures below we compare the climate change signal derived from the non-corrected and corrected discharges. Each set of two boxplots displays the change signal for the non-corrected (left) and corrected (right) time-series.

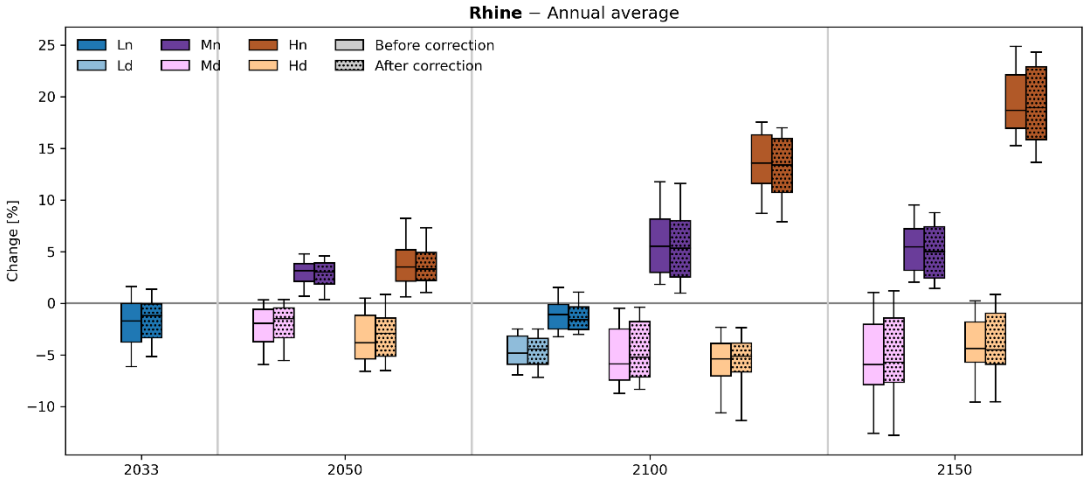

Figure C-1: Change in annual average discharge of the Rhine at Lobith for all scenarios calculated from the uncorrected (left boxplot) and corrected (right boxplot) discharge simulations.

Figure C-1 shows that for the change in average discharge at Lobith the bias-correction hardly influences the change signal. For annual maximum discharge (Figure C-2) the differences are already a bit larger.

Differences are largest for the change signal in the 7-day minimum discharge, see FigureC-3. However, the direction of the change signal remains the same and the magnitude of change is still in the same order of magnitude.

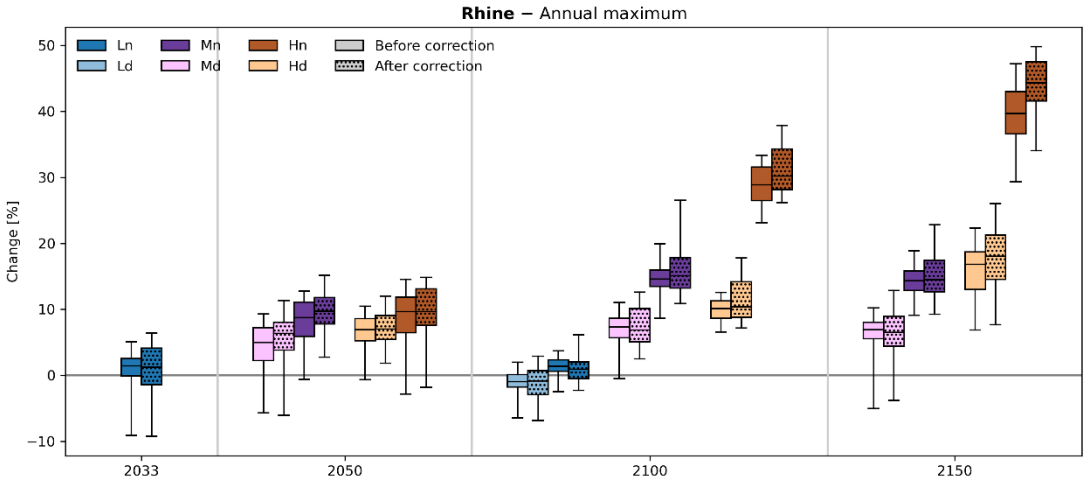

Figure C-2: Change in annual max discharge of the Rhine at Lobith for all scenarios (x-axis) calculated from the uncorrected (left boxplot) and corrected (right boxplot) discharge simulations.

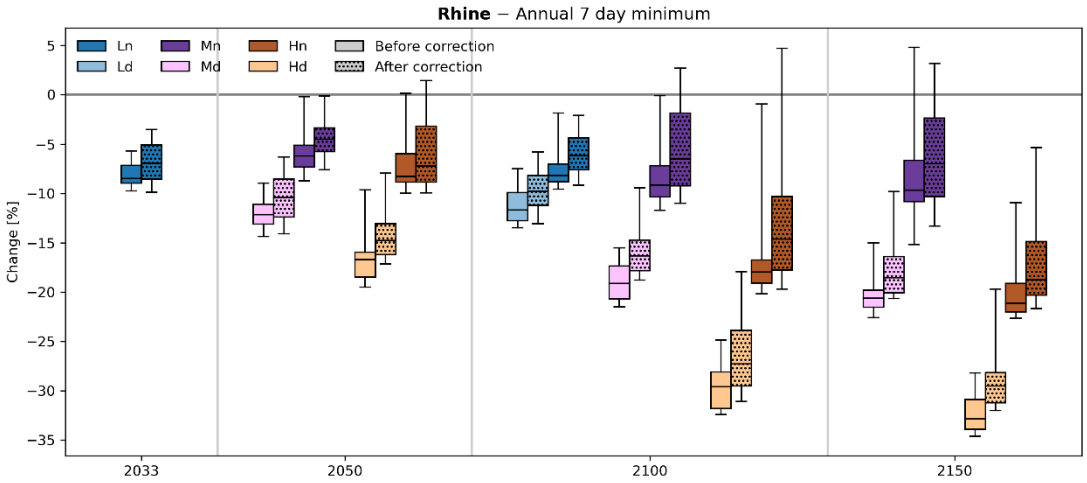

Figure C-3: Change in 7-day minimum discharge of the Rhine at Lobith for all scenarios (x-axis) calculated from the uncorrected (left boxplot) and corrected (right boxplot) discharge simulations.

C.2 The influence of bias-correction on the climate time-series

In this section we evaluate the influence of the bias-correction on the simulated discharge time-series. For this evaluation a comparison with observations is required. The climate models only provide a possible realization of the historic climate, the individual years do not match the observed inter-annual variability. Therefore, we ran wflow_sbm with the historical meteorological HYRAS dataset and made a comparison with the observed discharge time-series at Lobith.

As can be seen overall the bias-correction brings the simulated time-series closer to the observations. This is in line with our expectation. There is no perfect match after bias-correction. This is because only the monthly percentile statistics of the time-series are corrected. In this way also the future climate timeseries can be corrected.

The bias-correction method increases the low discharges in late summer. Values after correction are closer to the observations. For the very dry year 2003, some improvement is achieved but for these specific conditions the final time-series are still not perfect. Peak discharges are also improved or remain more or less the same see for example the discharge peaks in November / December 1996.

From this visual presentation of the time-series we can also see that the bias-correction does not introduce any unexpected noise or bumps.

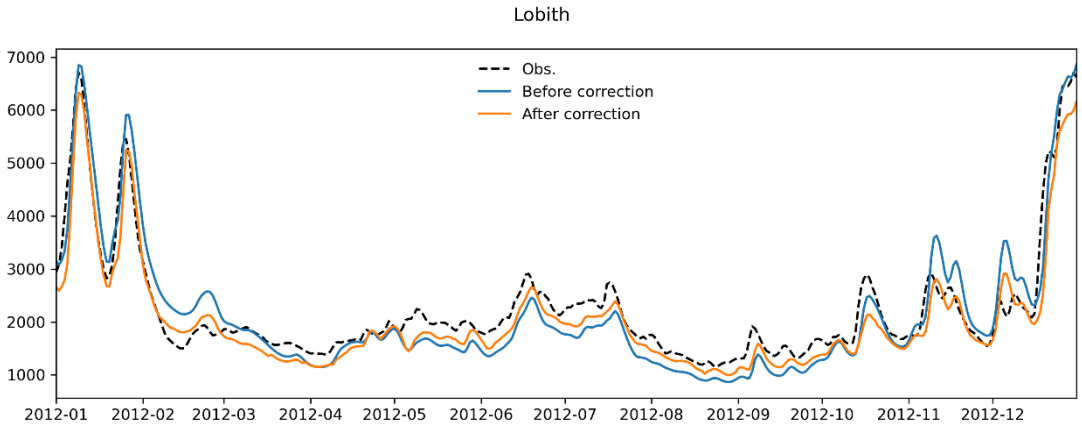

Figure C-7: Comparing the corrected (orange) and uncorrected (blue) simulated discharge of the reference climate with the observed values (black dashes) for Lobith for 2012.

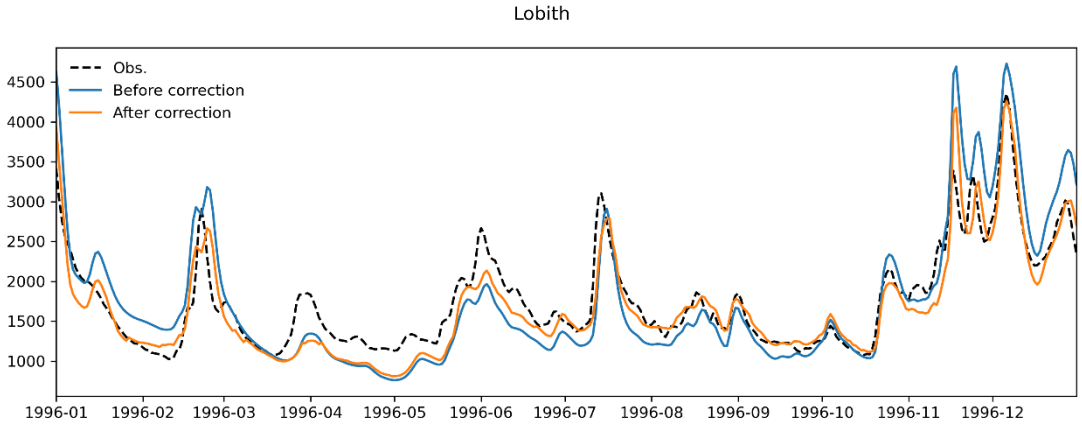

Figure C-8: Comparing the corrected (orange) and uncorrected (blue) simulated discharge of the reference climate with the observed values (black dashes) for Lobith for 1996.

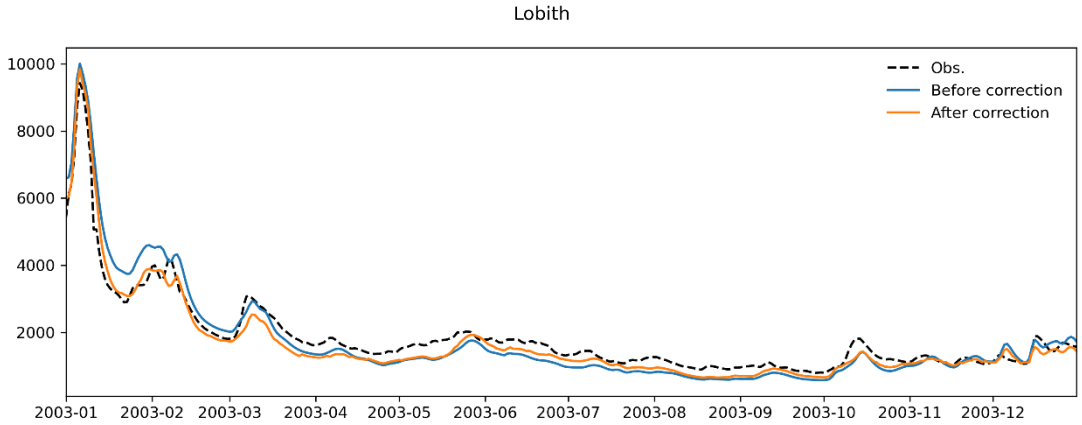

Figure C-9: Comparing the corrected (orange) and uncorrected (blue) simulated discharge of the reference climate with the observed values (black dashes) for Lobith for 2003.

D Comparison KNMI'23 vs KNMI'14 with labels

This Annex shows the results of the comparison between KNMI'14 and KNMI'23. These results are equal to the results presented in Chapter 7, but these figures show where the different scenarios are positioned.

D.1 Rhine

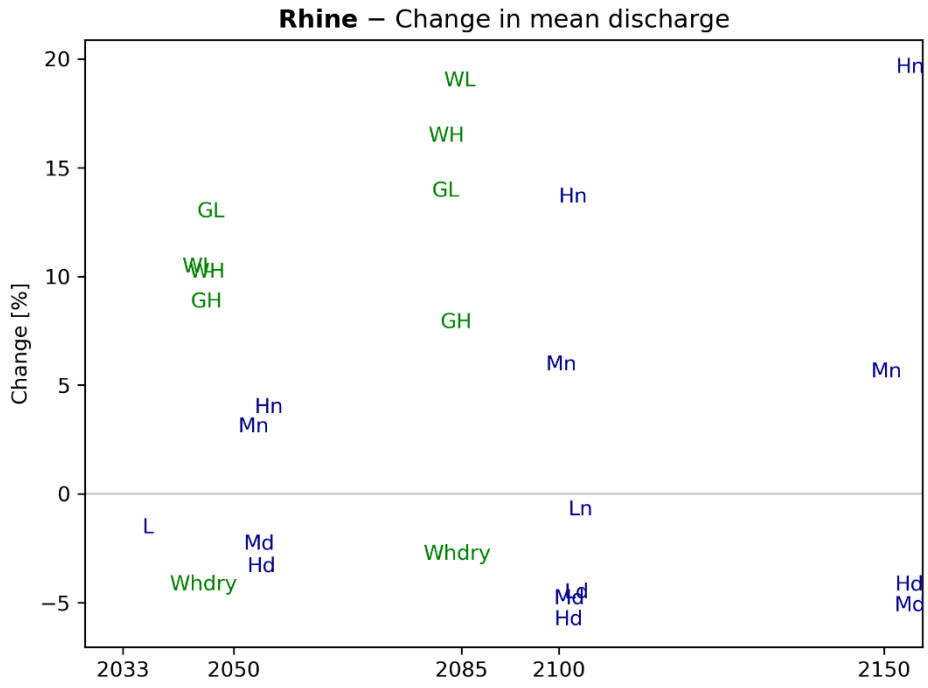

Figure D-1: Projected changes (%) in annual average discharge for the Rhine at Lobith according to the KNMI'14 scenarios (green) and KNMI'23 scenarios (blue) for the time horizons of interest.

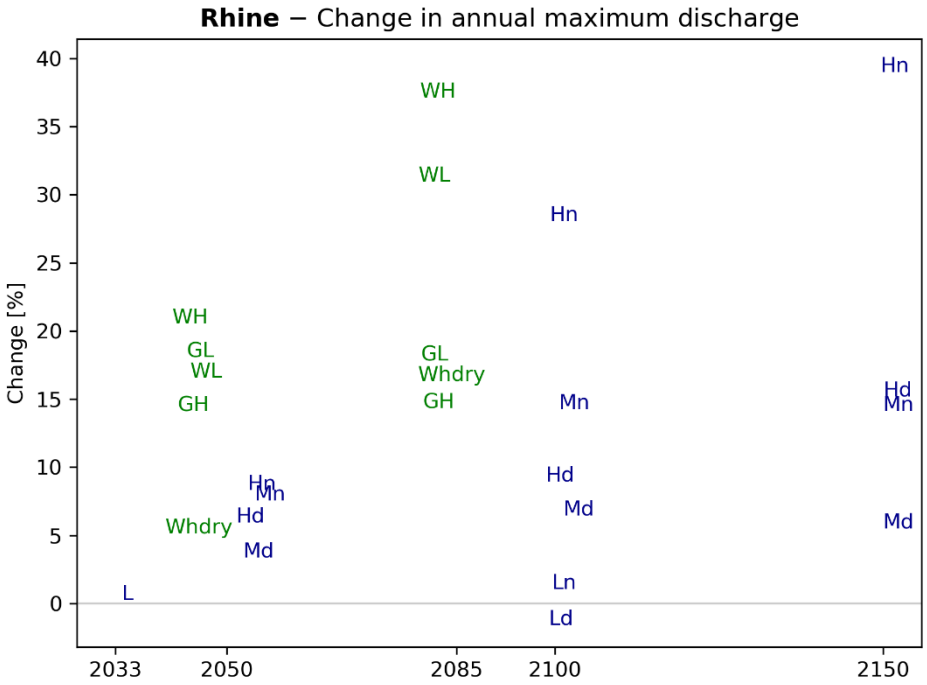

Figure D-2: Projected changes (%) in annual maximum discharge for the Rhine at Lobith according to the KNMI'14 scenarios (green) and KNMI'23 scenarios (blue) for the time horizons of interest.

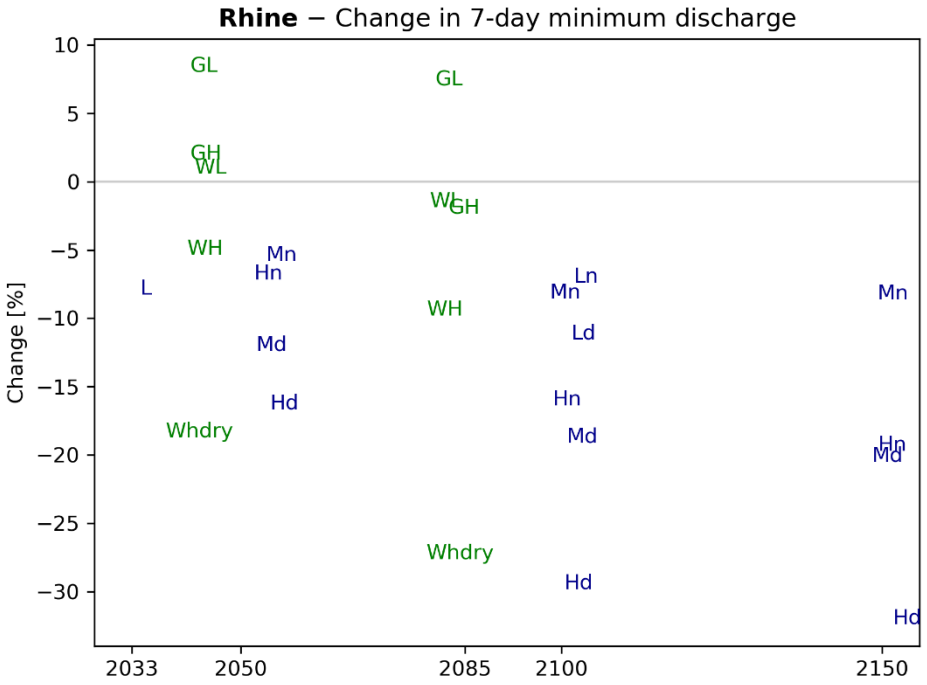

Figure D-3: Projected changes (%) in minimum 7-day discharge for the Rhine at Lobith according to the KNMI'14 scenarios (green) and KNMI'23 scenarios (blue) for the time horizons of interest.

D.2 Meuse

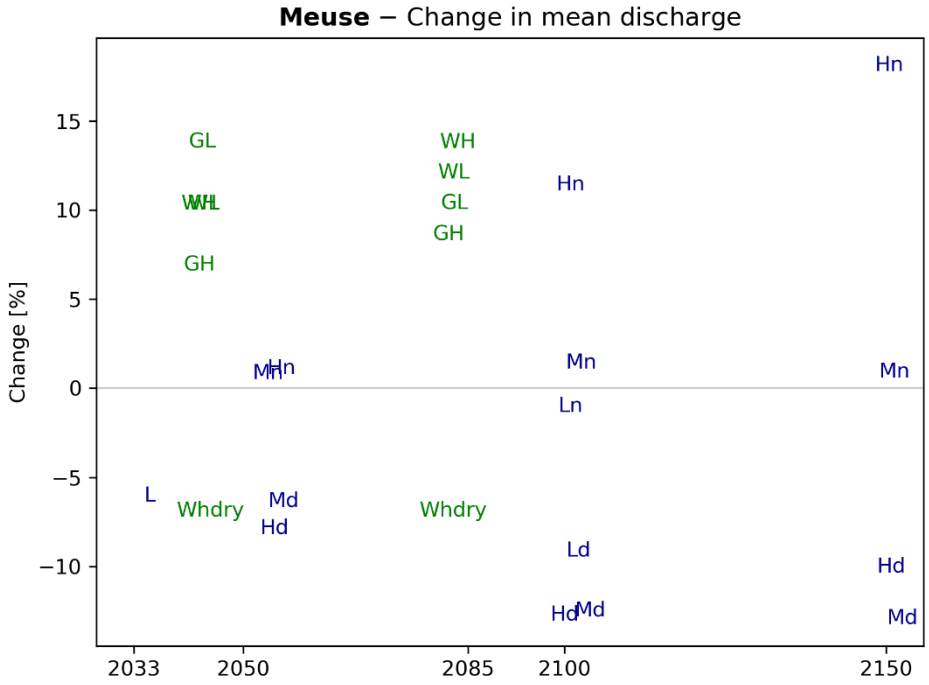

Figure D-4: Projected changes (%) in average discharge for the Meuse according to the KNMI'14 scenarios (green) and KNMI'23 scenarios (blue) for the time horizons of interest.

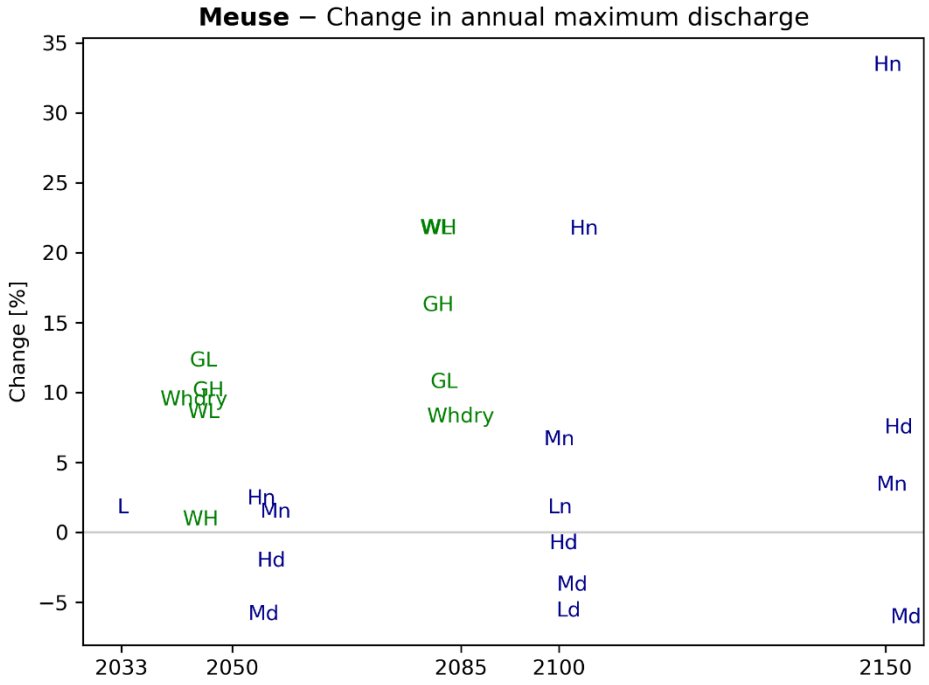

Figure D-5: Projected changes (%) in annual maximum discharge for the Meuse according to the KNMI'14 scenarios (green) and KNMI'23 scenarios (blue) for the time horizons of interest.

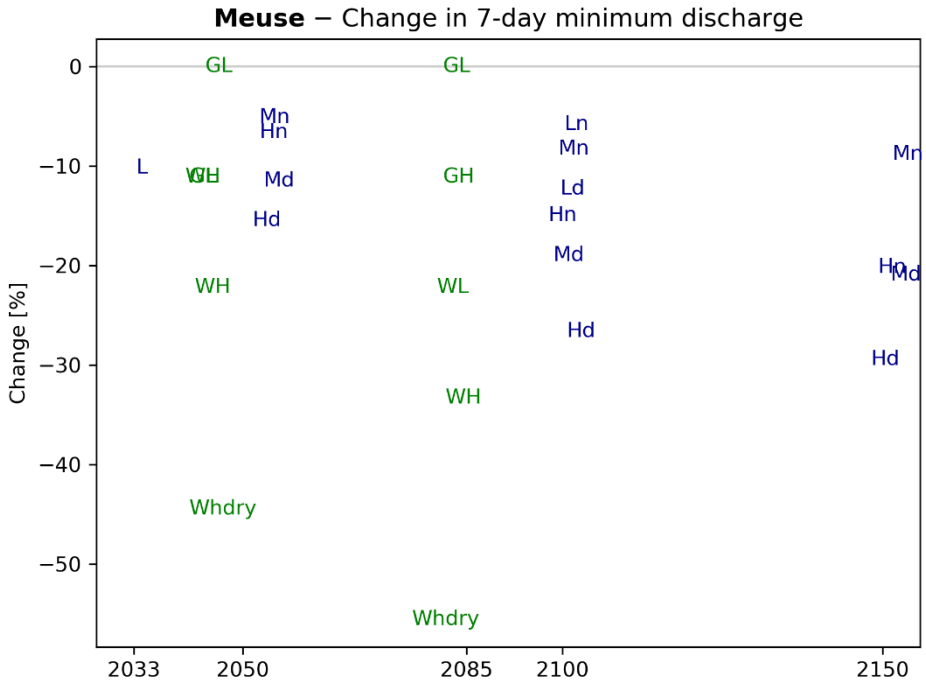

Figure D-6: Projected changes (%) in 7-day minimum discharge for the Meuse according to the KNMI'14 scenarios (green) and KNMI'23 scenarios (blue) for the time horizons of interest.

E Bias-correction vs time-series transformation

To correct the discharge values a quantile-mapping correction was implemented (Cannon et al., 2015). This method is similar to the approach followed by KNMI for the climate data. This method (explained in Section 4.3.5) has several benefits over another common method: time-series transformation. With time-series transformation the observed discharge time-series form the reference climate dataset. These time-series are transformed into future discharge time-series by adding the climate change signal derived from climate models.

An overview of pros and cons is provided in Table E-7 below. The pros and cons have been identified in a joined meeting and memo with Rijkswaterstaat, Deltares, KNMI and the end-users. In principle these are pros and cons for the correction of the climate datasets, the criteria that are also valid for discharge corrections have been included in this table.

The most important advantages and disadvantages have been color-coded. Especially, the ability to capture the change in prolonged / multi-year droughts was considered extremely relevant by Deltaprogramma Zoetwater. In recent years, we have seen that longer periods of drought can negatively impact the groundwater conditions for the upcoming season and this has long-lasting consequences for the lower parts of the Rhine sub-basins. Similarly, snow conditions in the Alps influence the water availability downstream in the basin in the upcoming year. By a simple transformation of the observed time-series changes in drought frequency and duration cannot be captured. Given these advantages, it was decided to use make use of the quantile-mapping approach, also called the bias-correction method.

Table E-1: Overview of advantages and disadvantages of the time-series transformation and bias-correction methods to improve simulated discharges.

	Advantages	**Disadvantages**
Bias-Correction	***Changes in persistency of droughts can be captured well***	The bias-correction method may influence the climate change signal
	The length of the time-series can be increased by using multiple ensemble members	The climate time-series form the basis and representative years (2003, 2018) are not available in these time-series
	By using 30-year periods of multiple ensemble members there is no trend in the data	***The underlying water balance and hydrological processes are not respected by the bias-correction method***
	The approach is consistent with the method followed for the improvement of the climate time-series by KNMI	
Time-series transformation	***Specific dry / wet years are recognizable in the time-series (2003, 2018)***	Change in persistency's in drought occurrence, for example multi-year droughts, cannot be captured
	The same approach is applied for KNMI'14	***To construct a time-series of ~100 years, as required by Deltaprogramma Zoetwater additional extrapolation is required***
	For the historical period observed data can be used, which are by definition unbiased	***There is always a trend in an observed ~100 year time-series***

Deltares is an independent institute for applied research in the field of water and subsurface. Throughout the world, we work on smart solutions for people, environment and society.

Deltares

www.deltares.nl